PROBING THE RELATIONSHIP OF CYANOBACTERIAL TOXINS AND REACTIVE OXYGEN SPECIES WITHIN THE NATURAL WORLD

by

Meagan Lachelle Smith

Bachelor of Arts
Washington and Jefferson College, 2014

Submitted in Partial Fulfillment of the Requirements

For the Degree of Doctor of Philosophy in

Chemistry

College of Arts and Sciences

University of South Carolina

2019

Accepted by:

John Ferry, Major Professor

Susan Richardson, Chair, Examining Committee

Thomas Makris, Committee Member

Geoffrey Scott, Committee Member

Cheryl L. Addy, Vice Provost and Dean of the Graduate School

DEDICATION

To my father, who believed in me more than I believed in myself. For reminding me to stay strong in our most vulnerable points in life and that it's okay to show emotion. I love you and I miss you. To my mother, for showing me how to be independent and for always being there for me. I love you. To my sister Abigail, I will never stop striving to support you in all that you do. To Jesse, my partner throughout this entire process. Thank you for your patience, love, support, and for keeping me sane.

ACKNOWLEDGEMENTS

I want to thank my advisor, Dr. John Ferry whose guidance and support is what drove the completion of this degree. Thank you for having faith in me and guiding me when I wanted to give up. I'd like to acknowledge current and former group members, who answered my endless questions and allowed for endless distractions. I'd also like to thank Dr. Susan Richardson, who is responsible for much of my mass spec knowledge. I'd also like to extend special thanks to my committee, Dr. Thomas Makris, and Dr. Geoff Scott. I am deeply thankful to Sam Putnam, Benson Solomon, Alyssa Abraham, and Dayla Rich for enabling my weekly trivia habit. Finally, I'd like to thank Allyse Corbin, my best friend. She has provided me with infinite encouragement. Thank you for being the brightest positive light in my life and always listening to me. You are my sunshine in this world.

ABSTRACT

The occurrence of harmful algal blooms (HABs) and their impacts on human health and the economy are only expected to worsen in the coming years, mainly due to climate change related factors. In Lake Wateree, SC, a HAB of the species *Lyngbya wollei*, has been persistent for more than 10 years and is estimated to occupy 60 - 90 km of shoreline. This natural laboratory provided and continues to provide a unique window into the chemistry and microbial ecology of HABs. Work in this dissertation was directed at answering a critical question: are biomass-to-toxin ratios constant in HABs? Initial work focused on analytical method development to identify and quantify the toxins produced by the *Lyngbya wollei* bloom in Lake Wateree. A series of method development steps was designed to refine the understanding of how algal-derived samples interact with analytical procedures. A method was established to increase method response and limit matrix-derived suppression interactions. Toxins produced by *Lyngbya wollei* include *Lyngbya wollei* toxins 1-6. The toxin production in three locations was monitored over 8 months, during the growing and following dormant season. Toxin production was normalized against total carbon, and the inorganic content of the *Lyngbya wollei* samples was recorded. Consideration of how biomass in grab samples correlates to the biomass of *Lyngbya wollei* and its toxins is presented.

The second half of this manuscript demonstrates the importance of autoxidation processes on the rate and yield of hydrogen peroxide in natural waters. ROS are ubiquitous in natural waters; however, their concentrations are low (micromolar – attomolar concentrations) and their source in these waters is poorly understood. In the absence of photons, gallic acid was used as a source of hydrogen peroxide over a pH range of 5-9 and in natural waters collected from around South Carolina. The autoxidation of gallic acid was initiated by the reaction between gallic acid and dioxygen and propagated by superoxide through a free radical chain process. The addition of natural organic matter increased the rates of hydrogen peroxide production and gallic acid degradation. Results of this study suggest that 90% of hydrogen peroxide in natural waters may be tied to the autoxidation of natural organic matter.

TABLE OF CONTENTS

Dedication iii

Acknowledgements iv

Abstract v

List of Tables viii

List of Figures ix

List of Abbreviations xii

Chapter 1 Interactions Between Cyanobacteria Harmful Algal Blooms and Reactive Oxygen Species 1

Chapter 2 Emerging *Lyngbya wollei* Toxins: A New High Resolution Mass Spectrometry Method to Elucidate a Potential Environmental Threat 31

Chapter 3 Inventory of Lyngbya wollei Toxins in Lake Wateree, South Carolina 53

Chapter 4 Autoxidation Provokes Synergistic Reactive Oxygen Species Formation in Natural Water 73

Appendix A Chapter 1 Supplemental Material 111

Appendix B Chapter 2 Supplemental Material 114

Appendix C Chapter 3 Supplemental Material 127

Appendix D Chapter 4 Supplemental Material 131

LIST OF TABLES

Table 1.1 Literature review of cyanobacteria genera and whether their cells react with ROS and if they produce ROS 28

Table 1.1. Toxins produced by associated cyanobacteria genera and their potential to react with ROS..... 29

Table 2.1 High Resolution fragmentation data for A: LWT1, B: LWT4, C: LWT5, and D: LWT6 (ESI+)..... 48

Table 3.1 Slope and R2 from best fit line of each toxin's peak area vs. date from Cove 1, Cove 2, and Cove 3 71

Table 4.1 Redox active metal and dissolved organic carbon content in the water at the four sites 101

Table A.1 Literature results from June 30, 2019 for "cyanobacteria" followed by "ROS" 112

Table A.2 Literature results from June 30, 2019 for "toxins" followed by "ROS" 113

Table B.1 LC-TQ source parameters for detection of LWTs 116

Table B.2 Fragmentation ions, losses, and ppm mass error for STX on the UHPL-QTOF 123

Table B.3 Fragmentation ions, losses, and ppm mass error for LWT2/3 on the UHPLC-QTOF..... 125

Table D.1 UPLC-MS source parameters for gallic acid detection 132

Table D.2 ICP-MS results of raw and filtered river waters from the four natural water samples collected 137

LIST OF FIGURES

Figure 1.3 Structure A, saxitoxin is reacted with hydrogen peroxide and oxidized to form the fluorescent product, B. 30

Figure 2.1 LC-MS chromatogram for LWT1, LWT4, LWT5, and LWT6 47

Figure 2.2 Normalized MS peak area vs. mass of lyophilized *L. wollei*..... 49

Figure 2.3 Calibration curve of a model LWT, saxitoxin, in 0.1M acetic acid and in algal extract 50

Figure 2.4 Normalized MS peak area of LWTs and saxitoxin in the algal matrix as a function of (Log10) dilution factor. Inset: Calibration curve of saxitoxin in diluted algae extract 51

Figure 2.5 Normalized MS peak area vs. mass of lyophilized *L. wollei* 52

Figure 3.1 Map of Lake Wateree, recorded occurrence of Lyngbya wollei, and quantity of samples per each location 69

Figure 3.2 LWTX/$LWTX_{min}$ for LWT1, LWT4, LWT5, and LWT6 for Cove 1 from June 2018 thru February 2019 70

Figure 3.3 Total average LWT amount for Cove 1, Cove 2, and Cove 3 72

Figure 4.1 Sources of reactive oxygen species in the water column..... 102

Figure 4.2 Rate of gallic acid loss over the pH range of 5 – 10..... 103

Figure 4.3 Proposed set of equations in the free radical chain reaction initiated by the direct oxidation of gallic acid by dioxygen 104

Figure 4.4 Rate of hydrogen peroxide production over the pH range of 5 - 10..... 105

Figure 4.5 Ratio of the concentration of hydrogen peroxide to nominal gallic acid concentration over time 106

Figure 4.6 Gallic acid concentration loss over time in the presence and absence of superoxide dismutase 107

Figure 4.7 Concentration of GA and hydrogen peroxide over time in natural water 108

Figure 4.8 Production of hydrogen peroxide from Site 2, Old Bates River, during GA oxidation 109

Figure 4.9 Fraction of superoxide reacting with NOM at three pHs 110

Figure B.1 Molecular structures of the Lyngbya wollei toxins 1-6 (free base). 115

Figure B.2 Peak area vs. cone voltage for LWT1, LWT4, LWT5, and LWT6 117

Figure B.3 High resolution spectra obtained from the UHPLC-QTOF for Saxitoxin at 6.38 mins 118

Figure B.4 High resolution spectra obtained from the UHPLC-QTOF for LWT1 at 3.87 mins 119

Figure B.5 High resolution spectra obtained from the UHPLC-QTOF for LWT4 at 6.13 mins 120

Figure B.6 High resolution spectra obtained from the UHPLC-QTOF for LWT5 at 5.84 mins 121

Figure B.7 High resolution spectra obtained from the UHPLC-QTOF for LWT6 at 4.96 mins 122

Figure B.8 High resolution spectra obtained from the UHPLC-QTOF for LWT2/3 at 3.94 mins 124

Figure B.9 Normalized MS peak area of LWTs as a function of Log10(dilution factor) in different extraction solvent. 126

Figure C.1 Percent total carbon and percent inorganic content for Cove 1, Cove 2, and Cove 3 over the sampled season 128

Figure C.2 LWTX/$LWTX_{min}$ for LWT1, LWT4, LWT5, and LWT6 for Cove 2 from June 2018 to February 2019 129

Figure C.3 LWTX/$LWTX_{min}$ for LWT1, LWT4, LWT5, and LWT6 for Cove 3 from June 2018 to February 2019 130

Figure D.1 MRM chromatogram for gallic acid which eluted at 0.49 mins during the gradient flow 133

Figure D.2 Full MS spectra of GA, eluted at 0.49 mins under the instrument conditions 134

Figure D.3 The locations of the four sampling locations in South Carolina 135

Figure D.4 Background hydrogen peroxide over three hours in the four locations where water was collected 136

Figure D.5 Oxidation of GA over the pH range of 4-10 over three hours. 138

Figure D.6 Production of hydrogen peroxide over the pH range of 4-10 over three hours 139

Figure D.7 The ration of the rate of gallic acid oxidation and hydrogen peroxide production over the pH range 5-10. 140

Figure D.8 Production of hydrogen peroxide during the oxidation of 10 μM and 20 μM gallic acid. 141

Figure D.9 Concentration of hydrogen peroxide from GA oxidation during an added 5 μm spike of hydrogen peroxide 142

Figure D.10 Hydrogen peroxide stability in the four, natural water samples, unfiltered and filtered..... 143

Figure D.11 Oxidation of GA and production of hydrogen peroxide in the four natural water samples..... 144

Figure D.12 Hydrogen peroxide production from the autoxidation of gallic acid in the presence and absence of 50 μM Fe(III) 145

Figure D.13 The calculation for superoxide in our system derived from the superoxide steady state in aqueous solutions 146

LIST OF ABBREVIATIONS

2-MIB 2-Methylisoborneol

ANA ..... Anatoxin-a

BMAA ..... beta-Methylamino-L-Alanine

cHAB ..... Cyanobacteria Harmful Algal Bloom

CYL ..... Cylindospermopsin

DOC ..... Dissolved Organ Carbon

DOM ..... Dissolved Organic Matter

ESI ..... Electrospray Ionization

GA ..... Gallic Acid

HAB ..... Harmful Algal Bloom

HO ..... Hydroxyl Radical

LC-FL ..... Liquid Chromatography Fluorescence

LWT1 ..... Lyngbya wollei Toxin 1

LWT2/3 ..... Lyngbya wollei Toxin 2/3

LWT4 ..... Lyngbya wollei Toxin 4

LWT5 ..... Lyngbya wollei Toxin 5

LWT6 ..... Lyngbya wollei Toxin 6

MC ..... Microcystin

NOM ..... Natural Organic Matter

PST ..... Paralytic Shellfish Toxin

Q-TOF ..... Quadrupole Time-of-Flight

ROS.....Reactive Oxygen Species

STX.....Saxitoxin

SCP.....Sodium Carbonate Peroxyhydrate

TQ.....Triple Quadrupole

UPLC.....Ultra-Performance Liquid Chromatograph

UV.....Ultra-Violet

UHPLC..... Ultrahigh Performance Liquid Chromatograph

CHAPTER 1

INTERACTIONS BETWEEN CYANOBACTERIA HARMFUL ALGAL BLOOMS AND REACTIVE OXYGEN SPECIES

1.1 ABSTRACT

Cyanobacterial harmful algal blooms (cHABs) are increasingly becoming widespread and have the potential to influence human health and the economy. Climate change is cited as one of the largest causes for their increased occurrence and the impacts of these HABs are only expected to worsen. Current remediation technologies often involve heavy metals and/or analytes that can be harmful to non-target species. Recently, the use of reactive oxygen species (ROS), such as hydrogen peroxide, ozone, and hydroxyl radical, as well as algicides whose active ingredient is hydrogen peroxide have been implemented as alternatives for remediation. Due to their short lifetime in water and effectiveness, these technologies are promising. Understanding the role of ROS within the HAB community can be challenging, as several species are known to produce extracellular ROS. The role of extracellular ROS in HAB and non-HAB species has been linked to metal acquisition and growth. Furthermore, many species of HABs produce toxic secondary metabolites, or toxins, and current methodologies for the detection of these toxins use hydrogen peroxide for oxidation followed by fluorescence. It is no surprise that hydrogen peroxide may react with these toxins in the water column: however, studies regarding hydrogen peroxide and toxins for remediation purposes are largely unpublished. Remediation technologies using ROS, and ROS algicides, will be discussed as well as the role extracellular ROS may have in HAB development. Finally, analytical technologies using ROS oxidation of HAB toxins will be discussed, drawing parallels between the analytical methods literature and the ROS remediation literature.

1.2 INTRODUCTION

The occurrence of large algal blooms is becoming increasingly common in freshwater and marine water environments, causing physical and chemical problems with the waters they inhabit.[1, 2] Also known as harmful algal blooms (HABs), their occurrence and emergent human health risk is only expected to worsen with climate change, as climate related outcomes are one of the largest factors for HAB growth. HABs develop when aquatic conditions, such as changes in nutrient loading, water temperature, salinity, and many others combine to cause the proliferation of the algae and its secondary metabolites into the ecosystem.[1] Adverse effects from HABs include the release of toxins into the water column causing animal and human poisonings,[3, 4] fish kills, oxygen depletion, and a decrease in overall water quality due to taste and odor compounds,[5-7] especially for drinking water.[8] They are associated with acute morbidity and mortality in many species of animals[9, 10] and have been linked to development of non-alcoholic fatty liver disease in humans.[11]

The presence of HABs affects more than the ecosystem, leading to economic impacts through ecological and human health costs.[12, 13] In 1991, a toxic bloom in the Darling River, Central Australia led to a loss of $1.5 million in tourism.[14] In that same year, a non-toxic bloom in Hawkesbury Nepean River, New South Wales, Australia garnered enough negative press that tourism estimated a $6.7 million loss in revenue.[15] A HAB in Lake Erie during the summer of 2014 resulted in a “Do Not Drink” advisory for Toledo, Ohio, leaving 500,000 residents without water for three days. The resulting economic impact is estimated to have cost over $65 million.[16] Most recently in 2018, Florida

experienced two species of toxic HABs, affecting both marine and freshwater ecosystems. Along the coast, a persistent bloom lasting over a year has led to numerous fish kills, dolphin, and manatee deaths as well as a decline in tourism to beaches.[17]

With increased nutrient loading, extreme climatic events, and invasive species, the occurrence of HABs are only expected to expand.[18] Prevention of HABs through nutrient restriction will lead to long-term positive outcomes, but is costly, time-consuming, and can be nearly impossible due to economic limitations.[2] Therefore, short-term control, such as removal of HABs and their secondary metabolites through growth inhibition or changes in nutrient concentrations, can be effective and manageable. The use of hydrogen peroxide, ozone, and hydrogen peroxide based algicides has proven useful in controlling and managing HABs (Table 1.1). Collectively, these removal techniques are useful because they are non-persistent and often more efficient than previous techniques that include heavy metal active sites and ecotoxic active ingredients. Remediation of HABs often results in the lysing of cells and the proliferation of secondary metabolites into the water column. Since many HABs produce toxic secondary metabolites, control of these compounds is necessary to mitigate the risk of contaminating the water and affecting the ecosystem. Removal of these secondary metabolites has also been studied using similar ROS technologies (Table 1.2).

Several species of ichthyotoxic microalgae and cyanobacteria have been shown to produce extracellular hydrogen peroxide, superoxide, and hydroxyl radical (collectively, ROS).[19] ROS occur naturally in the environment as a result of abiotic and biotic chemical reactions but are present at low concentrations (10^{-6} – 10^{-18} molar). The production of

ROS by oxygen-metabolizing organisms is well established; however, recently, research shows biological ROS production can promote growth and survival. For HABs, the production of extracellular ROS has been linked to toxicity, growth, and iron acquisition.

The use of hydrogen peroxide for remediation is promising, however studies on the remediation of HAB secondary metabolites are largely unpublished. Currently, hydrogen peroxide and hydrogen peroxide oxidation are used for the detection of HAB secondary metabolites. The use of these methods is ideal for a family of toxins known as saxitoxins, comprised of over 50 structural analogues.[20] Although this family of toxins is large, these methods have only been used on a fraction of the known compounds. It's interesting to note that little overlap exists between studies regarding oxidation of these toxins for fluorescence detection and remediation by hydrogen peroxide. Here we will discuss the relationship between HABs and ROS, demonstrating its use for control and management practices, as well as its association with fish kills and HAB growth and use for detection methods of toxic secondary metabolites.

1.3 REACTIVE OXYGEN SPECIE REMEDIATION TECHNOLOGIES

1.3.1 HYDROGEN PEROXIDE

The use of hydrogen peroxide to cause growth inhibition and/or nutrient loss in the management of HABS has been studied for a variety of species, however its use for large-scale control is limited, most likely due to the potential toxicity observed in fish and invertebrates and how quickly it degrades.[2] Hydrogen peroxide may be more effective towards prokaryotic cyanobacteria than eukaryotic alga, making hydrogen peroxide a potential ideal and selective way to remove and prevent cyanobacteria.[21] When properly

dosed, hydrogen peroxide can be effective in controlling HABs, while limiting its potential toxic effect to the ecosystem. Unfortunately, in many of the studies performed in natural water systems, HABs returned shortly (days to weeks) after hydrogen peroxide dosing.[22-24] Repeated applications are suggested as means for long-term control, but literature on the toxicity to zooplankton and other eukaryotic phytoplankton is limited.

In Lake Koetshuis, Netherlands, Matthijs et al. were able to remove 99% of *Planktothrix agardhii* cell numbers with 2 mg/L of hydrogen peroxide. At this concentration, only a mild negative impact was observed on the eukaryotic phytoplankton, zooplankton, and macrofauna.[23] Similarly, 90% inhibition of *Aphanizomenon* occurred between 0.80 and 0.98 mg/L hydrogen peroxide[25] and 90% of proteins were destroyed for *Oscillatoria rubescens* at 1.75 ppm hydrogen peroxide.[26] Treatment of *Pseudoanabaena* with 3 mg/L – 20 mg/L resulted in complete inactivation of live cells after 48 hours as well as cell proliferation and release of odor compounds into the water.[27] Higher concentrations (4mg/L, 8 mg/L, and 12 mg/L) of hydrogen peroxide were required for only 50% removal of *Microcystis aeruginosa* after 11 days.[28] *Synechococcus lividus*, on the other hand, was more resistant to treatment by hydrogen peroxide, requiring millimolar levels of hydrogen peroxide and cell lysis did not occur until 13 days.[29]

Published studies on the use of hydrogen peroxide for HAB management focus on removal of cell density and cell counts, however removal of HAB toxins cannot be overlooked. The most studied HAB toxins to date are the microcystins (MC), with over 90 variants and congeners varying in toxicity.[30, 31] MC are hepatotoxins and can accumulate

in the water column. The concentration of intracellular and extracellular MC was studied in laboratory experiments in water obtained from Lake Karla, Greece[31] and in waste stabilization ponds.[32] In both studies a decrease in intracellular MC was observed after dosing and an immediate increase of extracellular MC was observed, likely due to the lysing of cells and the subsequent release of intracellular toxins into the water. Over time, the concentration of extracellular MC decreased, and in the waste stabilization ponds 100% removal was observed up to 25 days.[32] While hydrogen peroxide is effective in removal of MC, literature relating to the removal of other HAB toxins, such as nodularin (NOD), anatoxin (ANA), cylindospermopsin (CYL), and saxitoxin (STX) by hydrogen peroxide is unpublished.

1.3.2 UV / HYDROGEN PEROXIDE

Literature using a combination of UV and hydrogen peroxide is primarily limited to the removal of HAB toxins. The use of UV/hydrogen peroxide for control of HABs, monitoring cell counts, and cell death is unpublished; however, the use of UV/hydrogen peroxide for the degradation of HAB toxins is well established for multiple classes of toxins. The mode of action for the degradation of HAB toxins by UV/hydrogen peroxide is primarily through reactions of hydroxyl radical (HO). Because of this, concentration of hydrogen peroxide, pH, and the presence of dissolved organic matter (DOM) can drastically affect the efficiency of the technique.[1, 33] As hydrogen peroxide concentration is increased, increased production of hydroxyl radical is observed, but increased rates of degradation are not. HO will react unselectively, therefore additional amounts of

hydrogen peroxide, or DOM, will preferentially react with HO before reacting with the HAB toxins.

The use of UV irradiation without hydrogen peroxide has the potential to remove MC,[34-36] ANA,[37] and CYL,[38] however addition of hydrogen peroxide increased the efficacy of degradation.[34, 37, 39, 40] MC was degraded 8 times more in the presence of both UV and hydrogen peroxide, while ANA required a medium pressure UV lamp (which can be costly and inefficient) for only 50-80% removal.[37] Similarly, CYL degraded 7 times faster in the presence of UV and hydrogen peroxide compared to UV irradiation alone, but also required added photosensitizers (such as TiO2) to increase hydroxyl radical formation. [1, 41-43] Although the use of this system is effective for removal of HAB toxins, effectiveness for the prevention of the HAB by this technology is unknown. Literature relating to the removal of other HAB toxins, such as nodularin (NOD) and saxitoxin (STX) by UV/hydrogen peroxide is largely unpublished.

1.3.3 OZONE

The use of ozone is a well-known and studied method for disinfection and has the potential to be used for cyanotoxin degradation. Like the UV/hydrogen peroxide system discussed, ozone's primary mode of action is through the generation of hydroxyl radicals. Since ozone is not persistent in the water column, ozonation of large bodies of water for HAB and cyanotoxin removal is difficult Ozonation of *Microcystis aeruginosa* resulted in 99% cell lysis in 10 mins at 0.5 – 2.0 mg/L ozone[44] and complete cell and cyanotoxin removal in the presence of 8 mg/L DOC within 12 mins during ozone dosing of 2.4 mg

/min.[45] *Pseudoanabaena* sp. was completely inactivated by the addition of 0.5 mg/L ozone.

Ozonation of HABs often results in cell wall damage, releasing toxins, taste and odor compounds, and other secondary metabolites into the water.[8, 46-48] In the ozonation of *Pseudoanabaena* sp., 2-methylisoborneol (2-MIB, a taste and odor compound) was released upon cell inactivation. However, additional dosing of ozone effectively removed 2-MIB. Similar release of HAB toxins was observed in the ozonation of *Microcystis aeruginosa*, *Lyngbya* sp. and *Oscillatoria tenuisa*.[49, 50] Ozonation of *Aphanizomenon gracile* resulted in increased assimilable carbon content in the water, likely due to cell proliferation and cell content release and oxidation of non-assimilable carbon.[51] Oxidation of *Cylindrospermopsis raciborskii* exhibited complete inactivation after one minute and no build-up of CYL, over 130 minutes at 1 mg/ L min dose.[47]

Ozone reacts with MC, ANA, CYL, NOD, and poorly with STX,[52] resulting in toxin alteration instead of removal.[1] Since these toxins are altered, toxicity studies of residual solutions after ozonation are required to determine the efficacy of treatment. Since the mode of action for ozonation treatments is through hydroxyl radical, pH and the concentration of DOM can significantly change cyanotoxin removal efficiency. MC is effectively removed at near neutral-acidic pHs, whereas ANA removal was improved with increasing pH.[53-55] In order to ensure complete removal of toxin, even in the presence of high DOM, a residual of 0.05 mg/L of ozone is suggested for MC.[52, 56]

So far, the discussion regarding ozone and HABs has been limited to freshwater species. In seawater, ozone's mode of action is altered slightly due to high concentrations

of bromide. Ozonation of bromide results in a weak, stable disinfectant that has been used for the removal of dinoflagellates, particularly *Karenia brevis*, *Prorocentrum triestinum*, *Scrippsiella trochoidea*, *Karenia digitale*, and *Amphidinium sp*.[57] Toxins released upon cell lysis of *Karenia brevis* were significantly reduced (94% removal) after 10 mins of ozonation at a rate of 0.51 mg / L min ozone.[58] The use of ozone in freshwater and marine environments is promising for HAB removal and has been recently recommended for use in ballast water tanks of ships, which is a significant cause of the introduction of HAB species into new water systems but has not been studied extensively in regards to cyanobacteria.[59]

The combination of UV and photosensitizers increased hydrogen peroxide's efficacy in HAB and cyanotoxin removal. Similarly, ozone/hydrogen peroxide and ozone/iron systems were shown to enhance the transformation of MC and ANA. Combinations of ozone with other disinfectants have not been studied extensively. Future research on ozone and ozone enhanced degradation of HABs and HAB toxins in marine and freshwater systems is needed.

1.3.4 HYDROGEN PEROXIDE ALGICIDES

Reactive oxygen species have been established as potential inhibitors of HAB cell growth as well as removers of their associated secondary metabolites, HAB toxins. Several companies have taken advantage of this and developed algicides whose mode of action is primarily through hydrogen peroxide. These aquatic algicides are made by mixing hydrogen peroxide and sodium carbonate to form sodium carbonate peroxyhydrate (SCP).[60] SCP can be applied from a powder, which allows for easy application and limits

exposure to applicators. SCP will break down to form sodium carbonate and hydrogen peroxide, allowing hydrogen peroxide to react or decompose into water and oxygen according to Equations 1 and 2. SCP algicides are commercially available under the trade

[1] $2Na_2CO_3 \bullet 3H_2O_2 \rightarrow 2Na_2CO_3 + 3H_2O$

[2] $3H_2O \rightarrow 1.5\ O_2 + \text{Heat}$

names PAK 27, GreenClean, TerrCyte Pro, and Phycomycin. Granular powders are 85% active ingredient, SCP, which is equivalent to 27.6% hydrogen peroxide.

Control of *Microcystis aeruginosa* by PAK 27 was effective (90%) at suppressing the concentrations of cells for two weeks. GreenClean, which yielded approximately 3 mg/L hydrogen peroxide was applied to a bloom of *Planktothrix rubescens*. Within 1-3 days surface cells and MC from the bloom decreased, and over the course of several months no algae filaments were observed. The use of GreenClean was effective in the control of *Lyngbya wollei* in laboratory studies, however these experiments were done in combination with multiple non-ROS based algicides. Phycomycin was effective against filamentous *Lyngbya wollei*, but only upon subsequent addition of copper based algicides.[61] The effect of Phycomycin on its target specie, *Microcystis aeruginosa* (cyanobacteria), and non-target species, *Pseudokirchneriella subcapitata* (chlorophyte), *Ceriodaphnia dubia* (microcrustacean), *Hyalella Azteca* (benthic amphipod), and *Pimephales promelas* (fathead minnow) was studied by Geer et al. The target specie *M. aeruginosa* was the most sensitive to Phycomycin (96 hr EC50 = 0.9-10.9 mg/L hydrogen

peroxide), followed by *Pseudokirchneriella subcapitata* (7-day EC50 = 5.2-9.2 mg/L hydrogen peroxide).[62] They also compared the effectiveness of SCP to copper-based algicides, endothall, and diquat dibromide, and found that SCP was just as potent against the target specie, *M. aeruginosa*, but has lower potency towards the non-target species, *H. Azteca* and *C. dubia.* Lower potency towards non-target species allows for enhanced margins of safety while selectively removing toxic cyanobacteria.

Other ROS based algicides, under trade names such as ZeroTol and Phyton X3, use hydrogen dioxide or a liquid combination of peroxyacetic acid and hydrogen peroxide. According to ZeroTol, the addition of peroxyacetic acid increases the oxidation strength of the algicide by 10-12 times compared to hydrogen peroxide alone.[63] ZeroTol claims to be non-phototoxic. ZeroTol has been studied for use in control of *Oscillatoria porornata*, *Pseudoanabaena* sp., *Oscillatoria agardhii*, and *Selenastrum capricornutum* (green algae) with IC50 values of 0.4, 1.7, 1.4, 3.4 as mg/L of active ingredient, respectively.[64, 65]

Using hydrogen peroxide as an active ingredient to decrease cell count and control HABs is established; however, the potential for the release of HAB toxins after cell lysis and their fate in the presence of these algicides has not been studied. Research is needed on the effect stabilizers and surfactants used in the commercial formulations may have on the target and non-target species. To date, no published studies exist on the environmental fate of these algicides. Hydrogen peroxide will not persist in the environment, but long-term control studies on cyanobacteria have not been done. The published literature relating to algicides and cyanobacteria has taken place in laboratory

settings; studies in natural water matrices are needed to investigate the potential for synergistic or non-targeted reactions occurring.

1.4 EXTRACELLULAR PRODUCTION OF REACTIVE OXYGEN SPECIES BY CHABS

Hydrogen peroxide has been demonstrated as an effective algicide in multiple forms against cyanobacteria. However, this isn't the only role hydrogen peroxide has within the cyanobacteria community. A broad diversity of phytoplankton produce hydrogen peroxide, superoxide, and even hydroxyl radical.[19] Many of the ROS producing species are eukaryotic phytoplankton, such as dinoflagellates,[66-70] diatoms,[71-74] and raphidophytes,[75-78] however four cyanobacteria species have been cited for production of extracellular ROS.[79-81] In general, HAB-forming species generate more extracellular ROS, and ROS production may be related to the tendency of these species to form HABs.[19, 82] HAB toxicity of raphidophytes and dinoflagellates (non-cyanobacteria HABs) to other organisms may be related to ROS production and not toxic secondary metabolites. Production of extracellular ROS is thought to indirectly or synergistically interact with other toxins, causing fish kills by suffocation.[83] Several studies have pointed out that ROS alone cannot be responsible for the harmful effects observed, therefore more research is needed to determine what the mode of action is for these fish kills.

Lyngbya majuscula and *Microcystis aeruginosa* (two HAB forming species) had rates of ROS extracellular superoxide of 155 nmol/g/hr[79] and 0.4-0.2 amol/cell/hr,[81] respectively. Differences in production rate may be attributed to growth phase, cell lysis, inter-strain differences, sunlight, water temperature, salinity, and iron availability.[19] Production of superoxide during growth regulation can act as an autocrine growth

promoter for microbial species such as *Saccharomyces cerevisiae*, *Escherichia coli*, and *Salmonella typhimurium*. A positive relationship between superoxide and growth has been established for several non-cyanobacteria species.[84-86] An inverse relationship with cell density and cell-normalized ROS was observed for the non-HAB forming cyanobacterium *Trichodesmium* spp.,[87] indicating a potential signaling role for ROS.

Indirectly, extracellular ROS production may influence growth via metal nutrient acquisition. The reaction of superoxide and iron allows for iron to be reduced from iron(III) to iron(II); extracellular superoxide can increase the bioavailability of iron, as mechanistically detailed by Rose et al. Extracellular superoxide has been proposed as a strategy for iron acquisition for the harmful cyanobacteria *Lyngbya majuscule*[79] and *Microcystis aeruginosa*,[81] non-harmful cyanobacteria *Trichodesmium erythraeum*,[88] and harmful marine raphidophyte *Chattonella marina.*[89] Bioavailability of iron will largely depend on the concentration of iron species near the cell's uptake sites, concentration of ligands that result in less liable forms, the presence of other oxidants that may affect iron speciation, transport processes, and biological uptake of iron species. Despite these factors, under some environmental conditions, extracellular superoxide still has the potential to significantly increase iron bioavailability.

1.5 HYDROGEN PEROXIDE OXIDATION OF SECONDARY METABOLITES

Secondary metabolites produced by HABs are susceptible to reactions with hydrogen peroxide, as discussed earlier. However, hydrogen peroxide is also used as an analytical technique to measure the concentration of paralytic shellfish toxins (PSTs). PSTs are naturally occurring secondary metabolites produced by several HAB-forming genera.

Saxitoxins are an important family of PSTs, made up of over 50 structural analogues. Saxitoxin and its analogues react with hydrogen peroxide under alkaline conditions to form fluorescent products. This method has been developed for use in shellfish tissues and used as a pre-column oxidation protocol followed by liquid chromatography fluorescence (LC-FL). Since 2006, the LC-FL method has been the standard method for monitoring saxitoxin and analogues in the UK for regulatory testing of live bivalve mollusks.

The derivatization of saxitoxin was first established in 1975 by Bates et al. where pure saxitoxin dihydrochloride, isolated from *Saxidomus giganteus,* was reacted with 10% hydrogen peroxide under basic conditions, Figure 1.1. The fluorescence method coupled with liquid chromatography was developed into a pre-column oxidation protocol using hydrogen peroxide and sodium periodate as the oxidants, and more than 15 saxitoxin analogues were successfully analyzed.[90-93] Oxidation of saxitoxin and its analogues resulted in similar products, all cleaving at the same position, Figure 1.3. Multiple oxidation products were observed and because chirality is lost during cleavage, several toxins formed identical fluorescent products.[94-96] Literature relating to hydrogen peroxide and saxitoxin fluorescence has focused mostly on the method and method optimization. Toxicity and stability of the resulting oxidation products is unpublished.

1.6 CONCLUSIONS

HABs are widespread, and their occurrence and impacts on human health and the economy are only expected to worsen with climate change. Removal techniques for HABs have been largely unsuccessful; however, the use of hydrogen peroxide, hydrogen

peroxide/UV, and ozone methods is promising as they provide short-term removal and control options while also being eco-friendly (non-persistent in the water column). A couple HAB species have been noted as superoxide producers; although the exact ecophysiological role is unknown, literature suggests it may involve indirect uptake of nutrients. Finally, hydrogen peroxide has been widely used as a detection method for saxitoxin and its analogues (secondary HAB metabolites) in environmental samples and in regulatory sampling.

Although hydrogen peroxide's role in the HAB community has been broadly studied, further research is required to address significant gaps in the state of knowledge. For example, there is a need for research on the fate of HAB toxins in the presence of ROS control methods, including algicides. Understanding the mechanism of how ROS interact with HABs and HAB toxins will aid in understanding the potential impacts these techniques have on removal and control. Production of ROS by HAB species has been studied extensively for non-cyanobacteria species and the role of extracellular ROS is still under investigation. While the use of hydrogen peroxide for the detection of saxitoxin and its analogues has been studied significantly, the potential for hydrogen peroxide to react with these compounds in the natural environment has not been studied. Literature surrounding hydrogen peroxide as a removal and control method and hydrogen peroxide as an analytical method seem to be mutually exclusive. Toxicity of the fluorescent saxitoxin products is unknown but may be a connection in understanding the fate of hydrogen peroxide control methods and cyanotoxin removal in environmental settings.

1.7 REFERENCES

1. Merel, S.; Walker, D.; Chicana, R.; Snyder, S.; Baures, E.; Thomas, O., State of knowledge and concerns on cyanobacterial blooms and cyanotoxins. *Environment International* **2013,** *59*, 303-327.

2. Jancula, D.; Marsalek, B., Critical review of actually available chemical compounds for prevention and management of cyanobacterial blooms. *Chemosphere* **2011,** *85*, (9), 1415-1422.

3. Briand, J. F.; Jacquet, S.; Bernard, C.; Humbert, J. F., Health hazards for terrestrial vertebrates from toxic cyanobacteria in surface water ecosystems. *Veterinary Research* **2003,** *34*, (4), 361-377.

4. Kuiper-Goodman, T.; Falconer, I.; Fitzgerald, J., Human health aspects. In *Toxic cyanobacteria in water: A guide to their public health consequences, monitoring and mangement*, Chorus, I.; Bartram, J., Eds. Taylor & Francis: London, U.K., 1999; pp 113-153.

5. Griffiths, D. J.; Saker, M. L., The palm island mystery disease 20 years on: A review of research on the cyanotoxin cylindrospermopsin. *Environmental Toxicology* **2003,** *18*, (2), 78-93.

6. Pouria, S.; de Andrade, A.; Barbosa, J.; Cavalcanti, R. L.; Barreto, V. T. S.; Ward, C. J.; Preiser, W.; Poon, G. K.; Neild, G. H.; Codd, G. A., Fatal microcystin intoxication in haemodialysis unit in caruaru, brazil. *Lancet* **1998,** *352*, (9121), 21-26.

7. Carmichael, W. W.; Boyer, G. L., Health impacts from cyanobacteria harmful algae blooms: Implications for the north american great lakes. *Harmful Algae* **2016,** *54*, 194-212.

8. Westrick, J. A.; Szlag, D. C.; Southwell, B. J.; Sinclair, J., A review of cyanobacteria and cyanotoxins removal/inactivation in drinking water treatment. *Analytical and Bioanalytical Chemistry* **2010,** *397*, (5), 1705-1714.

9. Landsberg, J. H., The effects of harmful algal blooms on aquatic organisms. *Reviews in Fisheries Science* **2002,** *10*, (2), 113-390.

10. Van Dolah, F. M., Effects of harmful algal blooms. *Marine Mammal Research: Conservation Beyond Crisis* **2005**, 85-99.

11. Zhang, F.; Lee, J.; Liang, S.; Shum, C. K., Cyanobacteria blooms and non-alcoholic liver disease: Evidence from a county level ecological study in the united states. *Environmental Health* **2015,** *14*.

12. Hoagland, P.; Anderson, D. M.; Kaoru, Y.; White, A. W., The economic effects of harmful algal blooms in the united states: Estimates, assessment issues, and information needs. *Estuaries* **2002,** *25*, (4B), 819-837.

13. Anderson, D. M.; Hoagland, P.; Kaoru, Y.; White, A. W., Estimated annual economic impacts from harmful algal blooms (habs) in the united states. In Institution, W. H. O., Ed. 2000.

14. Wales, E. Y. N. S., The assessment of the socio-economic impacts of murray river blue-green algae blooms: Stage one. In Office of Water: Sydney, 2010.

15. Steffensen, D. A., Economic cost of cyanobacterial blooms. In *Cyanobacterial harmful algal blooms: State of the science and reserach needs. Advances in experimental medicine and biology*, Hudnell, H. K., Ed. Springer: New York NY, 2008; Vol. 619.

16. Harmful algal blooms (habs) in the great lakes. In Commerce, U. S. D. o., Ed. National Oceanic and Atmospheric Administraction, Great Lakes Environmental Reserach Laboratory, Cooperative Institute for Great Lakes Reserach: 2016.

17. Wei-Haas, M. Red tide is devastating florida's sea life. Are humans to blame? https://www.nationalgeographic.com/environment/2018/08/news-longest-red-tide-wildlife-deaths-marine-life-toxins/ (06/03),

18. Ho, J. C.; Michalak, A. M., Challenges in tracking harmful algal blooms: A synthesis of evidence from lake erie. *Journal of Great Lakes Research* **2015,** *41*, (2), 317-325.

19. Diaz, J. M.; Plummer, S., Production of extracellular reactive oxygen species by phytoplankton: Past and future directions. *Journal of Plankton Research* **2018,** *40*, (6), 655-666.

20. Wiese, M.; D'Agostino, P. M.; Mihali, T. K.; Moffitt, M. C.; Neilan, B. A., Neurotoxic alkaloids: Saxitoxin and its analogs. *Marine Drugs* **2010,** *8*, (7), 2185-2211.

21. Drabkova, M.; Matthijs, H. C. P.; Admiraal, W.; Marsalek, B., Selective effects of h2o2 on cyanobacterial photosynthesis. *Photosynthetica* **2007,** *45*, (3), 363-369.

22. Jia, Y. H.; Yang, Z.; Su, W.; Johnson, D.; Kong, F. X., Controlling of cyanobacteria bloom during bottleneck stages of algal cycling in shallow lake taihu (china). *Journal of Freshwater Ecology* **2014,** *29*, (1), 129-140.

23. Matthijs, H. C. P.; Visser, P. M.; Reeze, B.; Meeuse, J.; Slot, P. C.; Wijn, G.; Talens, R.; Huisman, J., Selective suppression of harmful cyanobacteria in an entire lake with hydrogen peroxide. *Water Research* **2012,** *46*, (5), 1460-1472.

24. Visser, P. M.; Reeze, B.; Talens, R.; Matthijs, H. C. P. In *A new promising way to remove cyanobacteria from lakes: Addition of hydrogen peroxide in low concentration.*, The 8th International Conference on Toxic Cyanobacteria (ICTC8), Istanbul, Turkey, August 29th - September 4th 2010; Istanbul, Turkey, 2010.

25. Peterson, H. G.; Hrudey, S. E.; Cantin, I. A.; Perley, T. R.; Kenefick, S. L., Physiological toxicity, cell-membrane damage and the release of dissolved organic-carbon and geosmin by aaphanizomenon flos-aquae after exposure to water-treatment chemicals. *Water Research* **1995,** *29*, (6), 1515-1523.

26. Barroin, G.; Feuillade, M., Hydrogen-peroxide as a potential algicide for oscillatoria-rubescens dc. *Water Research* **1986,** *20*, (5), 619-623.

27. Li, L.; Zhu, C. W.; Xie, C. Q.; Shao, C.; Yu, S. L.; Zhao, L. C.; Gao, N. Y., Kinetics and mechanism of pseudoanabaena cell inactivation, 2-mib release and degradation under exposure of ozone, chlorine and permanganate. *Water Research* **2018,** *147*, 422-428.

28. Lin, L.; Shan, K.; Xiong, Q.; Li, L.; Gan, N.; Song, L., The ecological risks of hydrogen peroxide as a cyanocide: Its effect on the community structure of bacterioplankton. *Journal of Oceanology and Limnology* **2018,** *36*, (6), 2231-2242.

29. Dupouy, D.; Conter, A.; Croute, F.; Murat, M.; Planel, H., Sensitivity of synechococcus-lividus to hydrogen-peroxide. *Environ. Exp. Bot.* **1985,** *25*, (4), 339-347.

30. Puerto, M.; Pichardo, S.; Jos, A.; Camean, A. M., Comparison of the toxicity induced by microcystin-rr and microcystin-yr in differentiated and undifferentiated caco-2 cells. *Toxicon* **2009,** *54*, (2), 161-169.

31. Papadimitriou, T.; Kormas, K.; Dionysiou, D. D.; Laspidou, C., Using h2o2 treatments for the degradation of cyanobacteria and microcystins in a shallow hypertrophic reservoir. *Environmental Science and Pollution Research* **2016,** *23*, (21), 21523-21535.

32. Barrington, D. J.; Ghadouani, A.; Ivey, G. N., Cyanobacterial and microcystins dynamics following the application of hydrogen peroxide to waste stabilisation ponds. *Hydrology and Earth System Sciences* **2013,** *17*, (6), 2097-2105.

33. Stumm, W.; Morgan, J., *Aquatic chemistry*. 2nd ed.; John Wiley & sons: New York, 1981.

34. He, X. X.; Pelaez, M.; Westrick, J. A.; O'Shea, K. E.; Hiskia, A.; Triantis, T.; Kaloudis, T.; Stefan, M. I.; de la Cruz, A. A.; Dionysiou, D. D., Efficient removal of microcystin-lr by uv-c/h2o2 in synthetic and natural water samples. *Water Research* **2012,** *46*, (5), 1501-1510.

35. Kaya, K.; Sano, T., A photodetoxification mechanism of the cyanobacterial hepatotoxin microcystin-lr by ultraviolet irradiation. *Chemical Research in Toxicology* **1998,** *11*, (3), 159-163.

36. Tsuji, K.; Watanuki, T.; Kondo, F.; Watanabe, M. F.; Suzuki, S.; Nakazawa, H.; Suzuki, M.; Uchida, H.; Harada, K., Stability of microcystins from cyanobacteria .2. Effect of uv light on decomposition and isomerization. *Toxicon* **1995,** *33*, (12), 1619-1631.

37. Afzal, A.; Oppenlaender, T.; Bolton, J. R.; El-Din, M. G., Anatoxin-a degradation by advanced oxidation processes: Vacuum-uv at 172 nm, photolysis using medium pressure uv and uv/h2o2. *Water Research* **2010,** *44*, (1), 278-286.

38. Senogles, P.-J.; Scott, J. A.; Shaw, G., Efficiency of uv treatment with and without the photocatalyst titanium dioxide for the degradation of the cyanotoxin cylindrospermopsin. *Resource and Environmental Biotechnology* **2000,** *3*, (2-3), 111-125.

39. Qiao, R. P.; Li, N.; Qi, X. H.; Wang, Q. S.; Zhuang, Y. Y., Degradation of microcystin-rr by uv radiation in the presence of hydrogen peroxide. *Toxicon* **2005,** *45*, (6), 745-752.

40. Shephard, G. S.; Stockenstroem, S.; De Villiers, D.; Engelbrecht, W. J.; Sydenham, E. W.; Wessels, G. F. S., Photocatalytic degradation of cyanobacterial microcystin toxins in water. *toxicon* **1998,** *36*, 1895-1901.

41. Senogles, P. J.; Scott, J. A.; Shaw, G.; Stratton, H., Photocatalytic degradation of the cyanotoxin cylindrospermopsin, using titanium dioxide and uv irradiation. *Water Research* **2001,** *35*, (5), 1245-1255.

42. Lawton, L. A.; Robertson, P. K. J., Physico-chemical treatment methods for the removal of microcystins (cyanobacterial hepatotoxins) from potable waters. *Chemical Society Reviews* **1999,** *28*, (4), 217-224.

43. Liu, I.; Lawton, L. A.; Bahnemann, D. W.; Robertson, P. K. J., The photocatalytic destruction of the cyanotoxin, nodularin using tio2. *Applied Catalysis B-Environmental* **2005,** *60*, (3-4), 245-252.

44. Xie, P.; Ma, J.; Fang, J.; Guan, Y.; Yue, S.; Li, X.; Chen, L., Comparison of permanganate preoxidation and preozonation on algae containing water: Cell integrity, characteristics, and chlorinated disinfection byproduct formation. *Environmental Science & Technology* **2013,** *47*, (24), 14051-14061.

45. Rositano, J.; Nicholson, B. C.; Pieronne, P., Destruction of cyanobacterial toxins by ozone. *Ozone-Sci. Eng.* **1998,** *20*, (3), 223-238.

46. Huang, W.-J.; Cheng, Y.-L.; Cheng, B.-L., Ozonation byproducts and determination of extracellular release in freshwater algae and cyanobacteria. *Environmental Engineering Science* **2008,** *25*, (2), 139-151.

47. Cheng, X.; Shi, H.; Adams, C. D.; Timmons, T.; Ma, Y., Effects of oxidative and physical treatments on inactivation of cylindrospermopsis raciborskii and removal of cylindrospermopsin. *Water Science and Technology* **2009,** *60*, (3), 689-697.

48. Ho, L.; Tanis-Plant, P.; Kayal, N.; Slyman, N.; Newcombe, G., Optimising water treatment practices for the removal of anabaena circinalis and its associated metabolites, geosmin and saxitoxins. *Journal of Water and Health* **2009,** *7*, (4), 544-556.

49. Wert, E. C.; Korak, J. A.; Trenholm, R. A.; Rosario-Ortiz, F. L., Effect of oxidant exposure on the release of intracellular microcystin, mib, and geosmin from three cyanobacteria species. *Water Research* **2014,** *52*, 251-259.

50. Yuan, B. L.; Xu, D. M.; Li, F.; Fu, M. L., Removal efficiency and possible pathway of odor compounds (2-methylisoborneol and geosmin) by ozonation. *Separation and Purification Technology* **2013,** *117*, 53-58.

51. Ramseier, M. K.; Peter, A.; Traber, J.; von Gunten, U., Formation of assimilable organic carbon during oxidation of natural waters with ozone, chlorine dioxide, chlorine, permanganate, and ferrate. *Water Research* **2011,** *45*, (5), 2002-2010.

52. Newcombe, G.; Nicholson, B., Water treatment options for dissolved cyanotoxins. *Journal of Water Supply Research and Technology-Aqua* **2004,** *53*, (4), 227-239.

53. Al Momani, F. A.; Jarrah, N., Treatment and kinetic study of cyanobacterial toxin by ozone. *Journal of Environmental Science and Health Part a-Toxic/Hazardous Substances & Environmental Engineering* **2010,** *45*, (6), 719-731.

54. Al Momani, F.; Smith, D. W.; El-Din, M. G., Degradation of cyanobacteria toxin by advanced oxidation processes. *Journal of Hazardous Materials* **2008,** *150*, (2), 238-249.

55. Shawwa, A. R.; Smith, D. W., Kinetics of microcystin-lr oxidation by ozone. *Ozone-Sci. Eng.* **2001,** *23*, (2), 161-170.

56. Brooke, S.; Newcombe, G.; Nicholson, B.; Klass, G., Decrease in toxicity of microcystins la and lr in drinking water by ozonation. *Toxicon* **2006,** *48*, (8), 1054-1059.

57. Gallardo-Rodríguez, J. J.; Astuya-Villalón, A.; Llanos-Rivera, A.; Avello-Fontalba, V.; Ulloa-Jofré, V., A critical review on control methods for harmful algal blooms. *Reviews in Aquaculture 0*, (0).

58. Schneider, K. R.; Pierce, R. H.; Rodrick, G. E., The degradation of karenia brevis toxins utilizing ozonated seawater. *Harmful Algae* **2003,** *2*, (2), 101-107.

59. Anderson, D. M.; Boerlage, S. F. E.; Dixon, M. B., Harmful algal blooms (habs) and desalination: A guide to impacts, monitoring and management. In Commission, I. O., Ed. United Nations Educational, Scientific, and Cultural Organization: 2017; Vol. 78.

60. (USEPA), U. S. e. P. A., Registration eligibility decision (red). Paktm 27. Human and ecological risk assessment for section 3 registration of the end-use product paktm 27 for application to lakes, ponds, and drinking reservoirs. Epa registration no. 68660-9-68690. In Office of Pesticide programs, b. a. p. p. d., Ed. Washington, DC, 2004.

61. Calomeni, A. J.; Iwinski, K. J.; Kinley, C. M.; McQueen, A.; Rodgers, J. H., Responses of lyngbya wollei to algaecide exposures and a risk characterization associated with their use. *Ecotoxicology and Environmental Safety* **2015,** *116*, 90-98.

62. Geer, T. D.; Kinley, C. M.; Iwinski, K. J.; Calomeni, A. J.; Rodgers, J. H., Jr., Comparative toxicity of sodium carbonate peroxyhydrate to freshwater organisms. *Ecotoxicology and Environmental Safety* **2016,** *132*, 202-211.

63. Copes, W. In *Efficacy of disinfectants applied to plant production surfaces*, SNA Reserach Conference Atlanta, GA, 2003; Southern Nursery Association, Inc: Atlanta, GA, 2003; pp 212-214.

64. Schrader, K. K., Evaluation of several commercial algicides for control of odor-producing cyanobacteria. *Journal of Aquatic Plant Management* **2005,** *43*, 100-102.

65. Schrader, K. K.; DeRegt, M. Q.; Tucker, C. S.; Duke, S. O., A rapid bioassay for selective algicides. *Weed Technology* **1997,** *11*, (4), 767-774.

66. Saragosti, E.; Katsir, A.; Tchernov, D.; Shaked, Y., Extracellular production and degradation of superoxide in the coral stylophora pistillata and cultured symbiodinium. *Figshare* **2010**.

67. Zhang, T.; Diaz, J. M.; Brighi, C.; Parsons, R. J.; McNally, S.; Apprill, A.; Hansel, C. M., Dark production of extracellular superoxide by the coral porites astreoides and representative symbionts. *Frontiers in Marine Science* **2016,** *3*.

68. Dorantes-Aranda, J. J.; Seger, A.; Mardones, J. I.; Nichols, P. D.; Hallegraeff, G. M., Progress in understanding algal bloom-mediated fish kills: The role of superoxide radicals, phycotoxins and fatty acids. *Plos One* **2015,** *10*, (7).

69. Mardones, J. I.; Dorantes-Aranda, J. J.; Nichols, P. D.; Hallegraeff, G. M., Fish gill damage by the dinoflagellate alexandrium catenella from chilean fjords: Synergistic action of ros and pufa. *Harmful Algae* **2015,** *49*, 40-49.

70. Mooney, B. D.; Dorantes-Aranda, J. J.; Place, A. R.; Hallegraeff, G. M., Ichthyotoxicity of gymnodinioid dinoflagellates: Pufa and superoxide effects in sheepshead minnow larvae and rainbow trout gill cells. *Mar Ecol Prog Ser* **2011,** *426*, 213-224.

71. Rose, A. L.; Webb, E. A.; Waite, T. D.; Moffett, J. W., Measurement and implications of nonphotochemically generated superoxide in the equatorial pacific ocean. *Environmental Science & Technology* **2008,** *42*, (7), 2387-2393.

72. Milne, A.; Davey, M. S.; Worsfold, P. J.; Achterberg, E. P.; Taylor, A. R., Real-time detection of reactive oxygen species generation by marine phytoplankton using flow injection-chemiluminescence. *Limnology and Oceanography-Methods* **2009,** *7*, 706-715.

73. Waring, J.; Klenell, M.; Bechtold, U.; Underwood, G. J. C.; Baker, N. R., Light-induced responses of oxygen photoreduction, reactive oxygen species production and scavenging in two diatom species. *Journal of Phycology* **2010,** *46*, (6), 1206-1217.

74. Schneider, R. J.; Roe, K. L.; Hansel, C. M.; Voelker, B. M., Species-level variability in extracellular production rates of reactive oxygen species by diatoms. *Frontiers in Chemistry* **2016,** *4*.

75. Oda, T.; Nakamura, A.; Shikayama, M.; Kawano, I.; Ishimatsu, A.; Muramatsu, T., Generation of reactive oxygen species by raphidophycean phytoplankton. *Bioscience Biotechnology and Biochemistry* **1997,** *61*, (10), 1658-1662.

76. Marshall, J. A.; de Salas, M.; Oda, T.; Hallegraeff, G., Superoxide production by marine microalgae. *Marine Biology* **2005,** *147*, (2), 533-540.

77. Handy, S. M.; Coyne, K. J.; Portune, K. J.; Demir, E.; Doblin, M. A.; Hare, C. E.; Cary, S. C.; Hutchins, D. A., Evaluating vertical migration behavior of harmful

raphidophytes in the delaware inland bays utilizing quantitative real-time pcr. *Aquatic Microbial Ecology* **2005,** *40*, (2), 121-132.

78. Yang, C. Z.; Albright, L. J.; Yousif, A. N., Oxygen-radical-mediated effects of the toxic phytoplankter *heterosigma-carterae* on juvenile rainbox-trout *oncorhynchus-mykiss*. *Diseases of Aquatic Organisms* **1995,** *23*, (2), 101-108.

79. Rose, A. L.; Salmon, T. P.; Lukondeh, T.; Neilan, B. A.; Waite, T. D., Use of superoxide as an electron shuttle for iron acquisition by the marine cyanobacterium lyngbya majuscula. *Environmental Science & Technology* **2005,** *39*, (10), 3708-3715.

80. Godrant, A.; Rose, A. L.; Sarthou, G.; Waite, T. D., New method for the determination of extracellular production of superoxide by marine phytoplankton using the chemiluminescence probes mcla and red-cla. *Limnology and Oceanography-Methods* **2009,** *7*, 682-692.

81. Fujii, M.; Dang, T. C.; Rose, A. L.; Omura, T.; Waite, T. D., Effect of light on iron uptake by the freshwater cyanobacterium microcystis aeruginosa. *Environmental Science & Technology* **2011,** *45*, (4), 1391-1398.

82. Kustka, A. B.; Shaked, Y.; Milligan, A. J.; King, D. W.; Morel, F. M. M., Extracellular production of superoxide by marine diatoms: Contrasting effects on iron redox chemistry and bioavailability. *Limnol Oceanogr* **2005,** *50*, (4), 1172-1180.

83. Kim, D.; Oda, T., Possible factors responsible for the fish-killing mechanisms of the red-tide phytoplankton, chattonella marina and cochlodinium polkrikoides. In *Coastal environmental and ecosystem issues of the east china sea*, Ishimatsu, A.; Lie, H. J., Eds. TERRAPUB and Nagasaki University: Tokyo, Japan, 2010; pp 245-268.

84. Portune, K. J.; Cary, S. C.; Warner, M. E., Antioxxidant enzyme response and reactive oxygen species production in marine raphidophytes. *Journal of Phycology* **2010,** *46*, (6), 1161-1171.

85. Kim, C. S.; Lee, S. G.; Lee, C. K.; Kim, H. G.; Jung, J., Reactive oxygen species as causative agents in the ichthyotoxicity of the red tide dinoflagellate cochlodinium polykrikoides. *Journal of Plankton Research* **1999,** *21*, (11), 2105-2115.

86. Skeen, A. R.; Tomas, C. R.; Cooper, W. J., The production of hydrogen peroxide by *heterosigma akashiwo* under varying n:P ratios. In *Harmful algae 2002*, Steidinger, K. A.;Landsberg, J. H.;Tomas, C. R.; Vargo, G. A., Eds. Florida Fish and Wildlife Conservation Commission, Floride Institute of Oceanography, and Intergovernmental Oceanographic commission of UNESCO: St. Petersburg, Florida, 2004; pp 77-79.

87. Hansel, C. M.; Buchwald, C.; Diaz, J. M.; Ossolinski, J. E.; Dyhrman, S. T.; Van Mooy, B. A. S.; Polyviou, D., Dynamics of extracellular superoxide production by trichodesmium colonies from the sargasso sea. *Limnol Oceanogr* **2016,** *61*, (4), 1188-1200.

88. Roe, K. L.; Barbeau, K. A., Uptake mechanisms for inorganic iron and ferric citrate in trichodesmium erythraeum ims101. *Metallomics* **2014,** *6*, (11), 2042-2051.

89. Garg, S.; Rose, A. L.; Godrant, A.; Waite, T. D., Iron uptake by the ichthyotoxic chattonella marina (raphidophyceae): Impact of superoxide generation. *Journal of Phycology* **2007,** *43*, (5), 978-991.

90. Lawrence, J. F.; Menard, C., Liquid-chromatographic determination of paralytic shellfish poisons in shellfish after prechromatographic oxidation. *Journal of the Association of Official Analytical Chemists* **1991,** *74*, (6), 1006-1012.

91. Lawrence, J. F.; Menard, C.; Charbonneau, C. F.; Hall, S., A study of 10-toxins associated with paralytic shellfish poison using prechromatographic oxidation and liquid-chromatography with fluorescence detection. *Journal of the Association of Official Analytical Chemists* **1991,** *74*, (2), 404-409.

92. Quilliam, M. A.; Janecek, M.; Lawrence, J. F., Characterization of the oxidation products of paralytic shellfish poisoning toxins by liquid chromatography mass spectrometry. *Rapid Communications in Mass Spectrometry* **1993,** *7*, (6), 482-487.

93. Lawrence, J. F.; Wong, B.; Menard, C., Determination of decarbamoyl saxitoxin and its analogues in shellfish by prechromatographic oxidation and liquid chromatography with fluorescence detection. *Journal of Aoac International* **1996,** *79*, (5), 1111-1115.

94. Dell'Aversano, C.; Tattaglione, L.; Polito, G.; Dean, K.; Giacobbe, M.; Casabianca, S.; Capellacci, S.; Penna, A.; Turner, A. D., First detection of tetrodotoxin and high levels

of paralytic shellfish poisoning toxins in shellfish from sicily (italy) by three different analytical methods. *Chemosphere* **2019,** *215*, 881-892.

95. Turner, A. D.; Lewis, A. M.; Rourke, W. A.; Higman, W. A., Inter laboratory comparison of two aoac liquid chromatographic fluorescence detection methods for paralytic shellfish toxin analysis through characterization of an oyster reference material. *Journal of Aoac International* **2014,** *97*, (2), 380-390.

96. DeGrasse, S. L.; van de Riet, J.; Hatfield, R.; Turner, A., Pre- versus post-column oxidation liquid chromatography fluorescence detection of paralytic shellfish toxins. *Toxicon* **2011,** *57*, (4), 619-624.

Table 1.1. Literature review of cyanobacteria genera and whether their cells react with ROS and if they produce ROS.

Genera	Inactive / react with cells?			Produces extracellular ROS?
	Hydrogen Peroxide	Ozone	Algicides	
Anabaena			—	—
Aphanizomenon	yes	yes	—	—
Cylindrospermopsis	—	Yes	—	—
Lyngbya	—	Yes	Yes	Yes
Microcystis	Yes	Yes	Yes	Yes
Nodularia	—	—	—	—
Nostoc	—	—	—	—
Oscillatoria	Yes	Yes	Yes	—
Phormidium	—	—	—	—
Planktothrix	Yes	–	Yes	—
Pseudoanabaena	Yes	Yes	—	—
Raphidiopsis	—	—	—	—
Synechococcus	Yes	—	—	—
Trichodesmium	—	—	—	Yes

Table 1.2. Toxins produced by associated cyanobacteria genera and their potential to react with ROS.

Toxin	Genera associated with toxin production	React with toxin?		
		Hydrogen Peroxide	Ozone	Algicides
Anatoxin-a	*Anabaena, Aphanizomenon, Oscillatoria, Phormidium*	—	Yes	—
BMAA	*Anabaena*	—	—	—
Cylindrospermopsin	*Aphanizomenon, Cylindrospermopsis, Oscillatoria*	—	Yes	—
Microcystin	*Anabaena, Microcystis, Nostoc, Oscillatoria, Phormidium, Planktothrix*	Yes	Yes	—
Nodularin	*Nodularia*	—	Yes	—
Paralytic shellfish toxins	*Aphanizomenon, Cylindrospermopsis, Lyngbya, Raphidiopsis*	—*	Yes	—

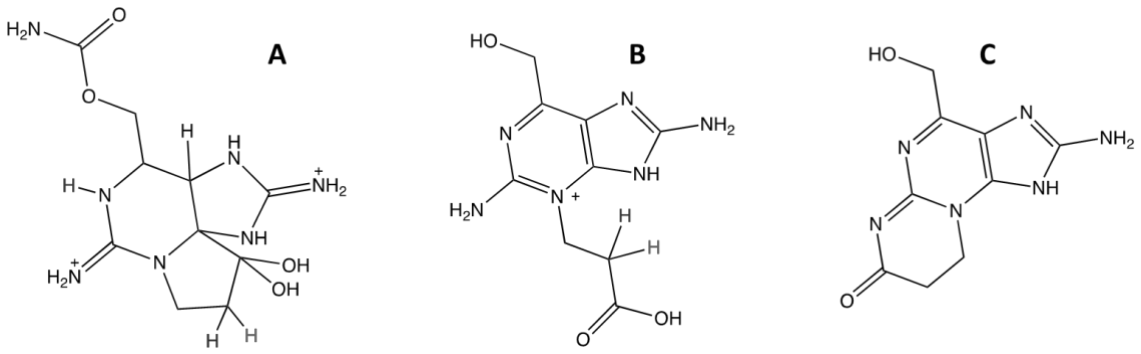

Figure 1.3 Structure **A**, Saxitoxin is reacted with hydrogen peroxide and oxidized to form the fluorescent product, **B**. Isolation of B results in a rearrangement and the non-fluorescent compound **C**.

CHAPTER 2

EMERGING *LYNGBYA WOLLEI* TOXINS: A NEW HIGH RESOLUTION MASS SPECTROMETRY METHOD TO ELUCIDATE A POTENTIAL ENVIRONMENTAL THREAT

2.1 ABSTRACT

Mass spectrometric methods for the quantitative and qualitative analyses of algal biotoxins are often complicated by co-eluting compounds that present analytically as interferences. This issue is particularly critical for organic polyamines, where co-eluting materials can suppress the formation of cations during electrospray ionization. Here we present an extraction procedure designed specifically to overcome matrix-derived ion suppression of algal toxins in samples of *Lyngbya wollei,* a filamentous benthic algae known to produce several saxitoxin analogues. *Lyngbya wollei* samples were collected from a large, persistent harmful algal bloom in Lake Wateree, SC. Six known *Lyngbya wollei*-specific toxins (LWT1-6) were successfully resolved and quantified against saxitoxin using hydrophilic interaction liquid chromatography coupled with triple quadrupole and quadrupole time-of-flight mass spectrometry. The parent ions $[M^{2+} – H^{+}]^{+}$ were observed for LWTs 1-6 and the $[M]^{2+}$ ion was observed for LWT5. High resolution mass spectra and unique fragmentation ions were obtained for LWTs 1-6. The relative retention time vs LWT5 for each toxin was used to validate peak assignment by liquid chromatography. A dilution factor of 50 resulted in a linear calibration of saxitoxin in the algae matrix. Ion suppression was resolved by sample dilution, which led to linear, positive correlations between peak area and mass of the extracted sample ($R^2 > 0.96$). Optimized sample extraction method and instrument parameters are presented.

2.2 INTRODUCTION

Analogues of the neurotoxic alkaloid saxitoxin, also known as paralytic shellfish toxins are members of a class of naturally occurring secondary metabolites produced by

freshwater cyanobacteria and marine dinoflagellates.[1, 2] Saxitoxin is a selective sodium channel blocker that has been documented to be extremely toxic to a wide range of species, including humans.[3-7] To date, there are at least 57 known analogues of saxitoxin[8] with varying levels of toxicity (by mouse bioassay), produced by a variety of genera including *Anabaena* [9-11] *Cylindospermopsis,*[12] *Aphanizomenon,*[13-15] *Planktothrix,*[16] and *Lyngbya.*[17] *Lyngbya wollei* (Farlow ex Gomont) Speziale & Dyck, a filamentous, benthic cyanobacteria, is a source of saxitoxin analogues known as *Lyngbya wollei* toxins (LWTs, Figure B.1).[18-22]

The qualification and quantification of saxitoxin analogues can be challenging. Effect based assays, including the mouse bioassay,[23-25] in-vitro cell viability assays,[26-29] enzyme-linked immune sorbent assay,[30, 31] and receptor binding assay[32-35] can provide qualitative and quantitative toxicity information.[25] However, these techniques report concentrations as summed saxitoxin equivalents and do not report the relative concentrations of different structural analogues. The latter is key for developing a detailed understanding of the relevant toxin biosynthetic pathways and understanding the synergistic toxic effects possible from complex toxin sources like *Lyngbya wollei*.

Mass spectrometric techniques are alternatives that typically have a wider linear dynamic range than most immunoassays and offer a higher level of structural information than effect-based assays.[17, 18, 36-39] However, the use of electrospray ionization mass spectrometry for the identification and quantification of polyamines like the saxitoxin analogues can be complicated by the presence of co-extracted materials that affect ionization efficiency in the source.[17, 18] The most commonly observed effect is

suppression, resulting in non-linear calibration curves for the saxitoxin analogues.[21,40] Here we report the development of a new mass spectrometry method for accurate and precise measurement of *Lyngbya wollei* toxins at ng/L detection limits that overcomes ion suppression.

2.3 MATERIALS AND METHODS

2.3.1 MATERIALS

All chemicals were used as received. All aqueous solutions used 18 MΩ cm^{-1} (Barnstead E-pure) water. All glassware was acid washed in 2 M HCl/0.1 M oxalic acid prior to oxidation in a muffle furnace to ensure it was trace metal and organic free. Acetonitrile (HPLC grade) was obtained from VWR BDH chemicals. Ammonium formate (98+%) was purchased from Alfa Aesar. Formic acid (certified ACS), glacial acetic acid (certified ACS PLUS), and hydrochloric acid (certified ACS Plus) were purchased from Fisher. Saxitoxin dihydrochloride in dilute hydrochloride standard solutions were obtained from NIST and Abraxis Inc.

2.3.2 SAMPLING

Lyngbya wollei grab samples were collected on November 6, 2018 from a surface floating mat on Lake Wateree, SC. Samples were collected in sterile 500-mL collection bottles and stored at 0^{o}C during transport (less than three hours). Samples were processed immediately when received. Samples were rinsed lightly under deionized water to remove entangled detritus, drained of excess water, frozen in liquid nitrogen, and lyophilized. After lyophilization, algae samples were homogenized using a tissue grinder and stored at -20 °C until extraction.

2.3.3 EXTRACTION METHOD

Freeze dried algae samples were returned to room temperature and their masses obtained with an analytical balance. Sample mass varied from 25-300 mg of dry weight algae. All samples were mixed with 10 mL 0.1 M acetic acid, sonicated for 15 minutes and centrifuged for 5 minutes. The resulting supernatant was removed, passed through a 0.45-micron nylon filter and analyzed by liquid chromatography-mass spectrometry. Extractions and subsequent dilutions were repeated using 0.1 M HCl and 0.01 M HCl. The mass to volume ratio was kept constant at 10 mg of dry weight algae for every 1 mL of extraction solvent in the extraction procedure to produce extracts for subsequent sample dilution experiments.

2.3.4 CHROMATOGRAPHY AND MASS SPECTROMETRY

Toxins were analyzed using a Waters (Milford, MA, USA) Acquity ultra performance liquid chromatograph (UPLC) coupled with a Xevo triple quadrupole (TQ) mass spectrometer equipped with an electrospray ionization (ESI) source in positive ion mode. High resolution analyte confirmation was performed on an Agilent (Santa Clara, CA, USA) 1290 Infinity II ultrahigh performance liquid chromatograph (UHPLC) system coupled to an Agilent 6545 quadrupole (Q)-time-of-flight (TOF) tandem mass spectrometer with electrospray ionization (ESI) in positive ion mode. High resolution Q-TOF data was processed using Agilent B.08.00 software. Separations were performed on a BEH Amide (2.1x150 mm) 1.7 µm particle size column (Waters). The mobile phases were aqueous 5.6 mM formate buffered pH 3.5 (A) and 95:5 acetonitrile:water 5.6 mM formate buffer pH 3.5 (B). The gradient LC method used for both instruments (TQ and Q-TOF) was as follows:

80% B held for one minute, ramped to 60% B over the next 3 minutes and held for 2 minutes, at 7 minutes ramped back to the original conditions over one minute (80% B) and held for re-equilibration for 8 minutes (16 minutes total).

Saxitoxin was optimized manually by direct infusion into the source, using an optimized cone voltage of 0.5 kV and cone energy of 80 V. The source temperature was 150 °C. The desolvation temperature, extractor voltage, desolvation gas flow, cone gas flow, and collision gas flow are shown in Table B.1. Due to the lack of commercial standards, optimization of source conditions on the UPLC-TQ mass spectrometer was done by optimizing chromatographic peak areas. A series of source methods was developed varying capillary and cone voltages to determine the optimal ionization parameters for LWT1, 4, 5, and 6 (Figure B.2). A capillary voltage of 0.5 kV was optimal for all LWTs observed, consistent with the voltage for saxitoxin. LWT1 experienced in-source fragmentation at cone potentials significantly above 30 V, therefore this value was maintained at 30 V at the retention time window corresponding to LWT1 elution. The other LWTs did not experience this issue, and a cone energy of 80 V was optimal for LWT4, LWT5, and LWT6.

Instrument parameters previously optimized for identifying small molecules by UHPLC-QTOF were utilized for LWT confirmation.[41] The mass spectrometer was operated at a fragmentation voltage of 110 V, capillary voltage of 4000 V, gas temperature of 300 °C, drying gas flow of 12 L min^{-1}, and nebulizer pressure of 35 psi, with a m/z scan range of 50 to 750. During initial analyte screening, the collision energy was ramped from 0, 20, to 40 eV every scan to obtain both MS and MS/MS spectra for each peak. Once LWTs of

interest were identified in algae extracts, targeted analysis was performed with a collision energy of 30 eV to obtain high resolution MS/MS spectra.

2.4 RESULTS

2.4.1 TOXIN IDENTIFICATION

Previous published studies on the analysis of LWTs were the result of mass spectrometers with unit-mass resolution, along with NMR (nuclear magnetic resonance) spectroscopy.[11, 18, 36, 42] In our study, saxitoxin analogues were initially detected in *Lyngbya wollei* extracts by full scan analysis at unit mass resolution on the UPLC-TQ mass spectrometer (Figure 2.1). LWTs lose a proton during ionization, forming an $[M^{2+} – H^{+}]^{+}$ parent ion, which is consistent with previously published work on doubly charged, low molecular weight poly amines by ESI-MS. [43-45] High resolution analysis by UHPLC-QTOF-MS was utilized for confirmation of the identity of the suspected LWTs (Figure B.3-B.7). High resolution data provided exact masses of precursor and product ions, correlating to a specific molecular formula for each peak, which allowed additional confidence in the chemical structures for these toxins (Table 2).

The structural similarities between the LWTs and saxitoxin means that similar product ion profiles were seen across multiple analytes of interest. For example, fragments with m/z 72.0556 and *m/z* 60.0556, corresponding to elemental formulae of $C_2H_6N_3$ (< 6 ppm mass error) and CH_6N_3 (< 2 ppm mass error), respectively, were observed for all LWTs (Table 2). Fragmentation of LWT1 resulted in ten fragment ions. The sulfur-containing functional group was lost from each fragment ion observed. Thirteen fragment ions were observed for LWT4 (Table 2). Similarly to LWT1, the most abundant fragment was from

loss of the OH functional group, as well loss of nitrogenous fragments (such as CH_5N_3 and CH_4N_3). Six identical product ions were observed between LWT4 and LWT6.

Fragment ions obtained for LWT5 and saxitoxin were nearly identical (Table 2 and Table B.2). Eleven fragment ions were observed for LWT5, of those eleven, eight were identical ions to saxitoxin. The three unique product ions were the result of losses from locations other than the carbamate ester (for saxitoxin) or the acetyl ester (for LWT5). Resulting mass differences in these product ions differed by 1 Da. For example, the loss of water from LWT5 resulted in the product ion *m/z* 281.1357, whereas the loss of water from saxitoxin resulted in *m/z* 282.1309. The agreement between fragments for saxitoxin and LWTs increases the confidence in the LWT identifications. Importantly, this agreement suggests parallels between the ionization chemistry of these two families of analytes, supporting the use of saxitoxin as a quantification standard for the LWTs, in the absence of commercially available standards for these toxins.

LWT2 and LWT3 are structural isomers (hereafter referred to as LWT2/3) with the same molecular weight. They were not detected using the UPLC-TQ mass spectrometer, but at least one isomer was detected with the QTOF mass spectrometer during the high resolution analysis of the algae extract (Figure B.8, Table B.3). LWT2/3 are structural isomers, and likely were not separable with the chromatographic approaches used in this study; thus, it is possible that both isomers were present, but coeluted. Similar to LWT1, LWT2/3 has a sulfur-containing functional group which was lost in four out of the six product ions observed. LWT2/3 were 2 orders of magnitude lower in peak intensity, relative to LWT1, 4, 5, and 6 (which had peak intensities on the order of 10^5) on the QTOF

mass spectrometer, and LWT2/3 were undetectable at these concentrations on the UPLC-TQ mass spectrometer.

2.4.2 MATRIX EFFECTS

The initial extraction procedure used 0.1 M acetic acid, sonication for 15 min, and filtration before analysis by UPLC-MS. However, the method response (peak area) from this extraction procedure showed a non-linear relationship vs the mass of the algae extracted ($R^2 < 0.6838$) for LWT4, 5, and 6. Furthermore, peak area vs mass extracted showed a negative slope for LWT5 (Figure 2.2). This behavior is consistent with the presence of co-extracted materials in the sample acting to suppress the ionization of the LWTs in the mass spectrometer.[40]

A commercially available standard, saxitoxin, was added to the sample as a surrogate LWT to probe for the nature of matrix effects. Saxitoxin calibration curves were prepared from 0.1 M acetic acid and algae extracts for comparative purposes (Figure 2.3). The slope for saxitoxin in acetic acid was 7820 ppb^{-1} with an R^2 of 0.9923, whereas in the algae matrix, the slope was 926 ppb^{-1} saxitoxin with an R^2 of 0.2455. The concentration dependence was determined by diluting saxitoxin-spiked algae extracts in 0.1 M acetic acid (Figure 2.4) over a range of dilution factors (corresponding to a dilution factor of zero to 1000). Comparison of peak areas vs log dilution factor for the LWTs (Figure 2.4) showed a parabolic function for LWT 4, 5, and 6.

Examination of the dilution factor effect revealed that sample dilution of 50 or more reduced the interfering species to a level essentially below “detection” based on their ability to disproportionately affect the standard. The full calibration curve for saxitoxin

was repeated at a dilution factor of 1:50 for extract:acetic acid. The corresponding curve (Figure 2.4 inset) was linear with a slope of 7975 ppb^{-1} and an R^2 of 0.9959. In order to test the linearity of our toxins at a DF of 50, the mass of dry algae was varied over the range of 25 – 300 mg, extracted, and the resulting extracts were diluted by a factor of 50. The peak area vs mass was linear ($R^2 > 0.9522$) for all toxins observed (Figure 2.5).

2.4.3 EXTRACTION IN HYDROCHLORIC ACID

As shown in the literature, the choice of extraction solvent is important and the presence of strong acids of an acid can alter the apparent toxin profile. The effects of varying extracting acids on the magnitude of the suppression were determined. Lyophilized algae were extracted with either 0.01 M HCl or 0.1 M HCl and the extracts were diluted over a dilution factor range of 1 – 1000. The peak area vs. dilution factor function for the LWTs was determined for the differing HCl conditions (Figure B.9). LWT5 and LWT6 were affected strongly by the change in extraction solvent, requiring at least a dilution factor of 10 to ensure dilution of the matrix beyond visible suppression effects. This result points to the importance in testing for suppression when ranking extraction procedures.

2.5 DISCUSSION

The high-resolution fragmentation analysis presented here provides an unprecedented range of fragment ion options that can be used to conclusively indicate the presence and retention time of LWTs 1 through 6 in a sample, even in the absence of commercial standards. These same transitions can be used for MRM-based analyses in quantification. The presence of ion suppression factors can vary within environmental

matrices. Smaller, polar molecules are more susceptible to ion suppression, as well as amine analytes. Biological samples are more likely to contain nonvolatile and less volatile solutes, leading to a change in spray droplet solution properties, which can be a major source of ion suppression when using electrospray. Given that saxitoxin analogues are small, polar molecules, usually extracted from natural samples, matrix effects will most likely be present in any algae extract, therefore, the current results suggest analysis of saxitoxin and its analogues extracted from algae should be subjected to a dilution factor-based assay. A strategy to obtain linear saxitoxin calibration within the algae matrix as well as linear toxin vs. mass correlations is demonstrated. The current work suggests a safe dilution factor of at least 10 for the Lake Wateree based samples, however for our work we chose 50 to ensure adequate dilution of the matrix during lake turnover events.

Accurate risk assessments for *Lyngbya wollei* are extremely difficult due to reference standards for the mixture of toxins produced by this algae being commercially unavailable. Effect-based assays for the analysis of these toxins remain largely non-specific, fail to provide a molecular toxin profile, and often require secondary verification by mass spectrometry. The combination of a lack of standards for quantification and qualification make risk assessment and remediation a gamble each time this species is encountered, as historically the relative concentrations of LWTs are variable and unpredictable. Utilizing a dilution factor-based assay, as presented here, provides selective detection with minimal sampling processing to avoid interferences from ion-suppressing matrix effects.

2.6 REFERENCES

1. Oshima, Y.; Hasegawa, M.; Yasumoto, T.; Hallegraeff, G.; Blackburn, S., Dinoflagellate gymnodinium catenatum as the source of paralytic shellfish toxins in tasmanian shellfish. *Toxicon* **1987,** *25*, (10), 1105-1111.

2. Harada, T.; Oshima, Y.; Yasumoto, T., Studies on paralytic shellfish poisoning in tropical waters .4. Structures of 2 paralytic shellfish toxins, gonyautoxin-v and gonyautoxin-vi isolated from a tropical dinoflagellate, pyrodinium bahamense var compressa. *Agricultural and Biological Chemistry* **1982,** *46*, (7), 1861-1864.

3. Carmichael, W. W., Toxins of cyanobacteria. *Sci.Am.* **1994,** *270*, (1), 78-86.

4. Jochimsen, E. M.; Carmichael, W. W.; An, J. S.; Cardo, D. M.; Cookson, S. T.; Holmes, C. E. M.; Antunes, M. B. D.; de Melo, D. A.; Lyra, T. M.; Barreto, V. S. T.; Azevedo, S.; Jarvis, W. R., Liver failure and death after exposure to microcystins at a hemodialysis center in brazil. *N. Engl. J. Med.* **1998,** *338*, (13), 873-878.

5. Negri, A. P.; Jones, G. J.; Hindmarsh, M., Sheep mortality associated with paralytic shellfish poisons from the cyanobacterium anabaena circinalis. *Toxicon* **1995,** *33*, (10), 1321-1329.

6. Kao, C. Y., Paralytic shellfish poisoning. *Algal toxins in seafood and drinking water.* **1993**, 75-86.

7. Landsberg, J. H., The effects of harmful algal blooms on aquatic organisms. *Reviews in Fisheries Science* **2002,** *10*, (2), 113-390.

8. Wiese, M.; D'Agostino, P. M.; Mihali, T. K.; Moffitt, M. C.; Neilan, B. A., Neurotoxic alkaloids: Saxitoxin and its analogs. *Marine Drugs* **2010,** *8*, (7), 2185-2211.

9. Al-Tebrineh, J.; Mihali, T. K.; Pomati, F.; Neilan, B. A., Detection of saxitoxin-producing cyanobacteria and anabaena circinalis in environmental water blooms by quantitative pcr. *Applied and Environmental Microbiology* **2010,** *76*, (23), 7836-7842.

10. Humpage, A. R.; Rositano, J.; Bretag, A. H.; Brown, R.; Baker, P. D.; Nicholson, B. C.; Steffensen, D. A., Paralytic shellfish poisons from australian cyanobacterial blooms. *Australian Journal of Marine and Freshwater Research* **1994,** *45*, (5), 761-771.

11. Onodera, H.; Oshima, Y.; Watanabe, M. F.; Watanabe, M.; Bolch, C. J.; Blackburn, S.; Yasumoto, T., Screening of paralytic shellfish toxins in freshwater cyanobacteria and chemical confirmation of the toxins in cultured *anabaena circinalis* from australia. In *Harmful and toxic algal blooms*, Yasumoto, T.;Oshima, Y.; Fukuyo, Y., Eds. IOS UNESCO: Paris, 1996; pp 563-566.

12. Lagos, N.; Onodera, H.; Zagatto, P. A.; Andrinolo, D.; Azevedo, S.; Oshima, Y., The first evidence of paralytic shellfish toxins in the freshwater cyanobacterium cylindrospermopsis raciborskii, isolated from brazil. *Toxicon* **1999,** *37*, (10), 1359-1373.

13. Mahmood, N. A.; Carmichael, W. W., Paralytic shellfish poisons produced by the freshwater cyanobacterium aphanizomenon-flos-aquae nh-5. *Toxicon* **1986,** *24*, (2), 175-&.

14. Jackim, E.; Gentile, J., Toxins of a blue green alga - similarity to saxitoxin. *Science* **1968,** *162*, (3856), 915-&.

15. Sawyer, P. J.; Gentile, J. H.; Sasner, J. J., Demonstration of a toxin from aphanizomenon flos aquae (l) ralfs. *Canadian Journal of Microbiology* **1968,** *14*, (11), 1199-&.

16. Pomati, F.; Sacchi, S.; Rosetti, C.; Giovannardi, S.; Onodera, H.; Oshima, Y.; Neilan, B. A., The freshwater cyanobacterium planktothrix sp. Fp1: Molecular identification and detection of paralytic shellfish poisoning toxins. *Journal of Phycology* **2003,** *36*, (3), 553-562.

17. Dell'Aversano, C., Hydrophilic interaction liquid chromatography-mass spectrometry (hilic-ms) of paralytic shellfish poisoning toxins, domoic acid, and assorted cyanobacterial toxins. In *Hydrophilic interaction liquid chromatography*, Wang, P. G.; He, W., Eds. Crc Press-Taylor & Francis Group: Boca Raton, 2011; Vol. 103, pp 105-132.

18. Foss, A. J.; Phlips, E. J.; Yilmaz, M.; Chapman, A., Characterization of paralytic shellfish toxins from lyngbya wollei dominated mats collected from two florida springs. *Harmful Algae* **2012,** *16*, 98-107.

19. Carmichael, W. W.; Evans, W. R.; Yin, Q. Q.; Bell, P.; Moczydlowski, E., Evidence for paralytic shellfish poisons in the freshwater cyanobacterium lyngbya wollei (farlow ex gomont) comb. Nov. *Applied and Environmental Microbiology* **1997,** *63*, (8), 3104-3110.

20. Yin, Q. Q.; Carmichael, W. W.; Evans, W. R., Factors influencing growth and toxin production by cultures of the freshwater cyanobacterium lyngbya wollei farlow ex gomont. *Journal of Applied Phycology* **1997,** *9*, (1), 55-63.

21. Onodera, H.; Satake, M.; Oshima, Y.; Yasumoto, T.; Carmichael, W. W., New saxitoxin analogues from the freshwater filamentous cyanobacterium lyngbya wollei. *Natural Toxins* **1997,** *5*, (4), 146-151.

22. Cowell, B. C.; Botts, P. S., Factors influencing the distribution, abundance and growth of lyngbya wollei in central florida. *Aquatic Botany* **1994,** *49*, (1), 1-17.

23. Schantz, E. J.; McFarren, E. F.; Schafer, M. L.; Lewis, K. H., Purified shellfish poison for bioassay standardization. *Journal of the Association of Official Agricultural Chemists* **1958,** *41*, (1), 160-168.

24. Turner, A. D.; Dhanji-Rapkova, M.; Algoet, M.; Suarez-Isla, B. A.; Cordova, M.; Caceres, C.; Murphy, C. J.; Casey, M.; Lees, D. N., Investigations into matrix components affecting the performance of the official bioassay reference method for quantitation of paralytic shellfish poisoning toxins in oysters. *Toxicon* **2012,** *59*, (2), 215-230.

25. Cusick, K. D.; Sayler, G. S., An overview on the marine neurotoxin, saxitoxin: Genetics, moleuclar targets, methods of detection and ecological functions. *Marine Drugs* **2013,** *11*, 991-1018.

26. Kogure, K.; Tamplin, M. L.; Simidu, U.; Colwell, R. R., A tissue culture assay for tetrodotoxin, saxitoxin and related toxins. *Toxicon* **1988,** *26*, (2), 191-197.

27. Jellett, J. F.; Marks, L. J.; Stewart, J. E.; Dorey, M. L.; Watsonwright, W.; Lawrence, J. F., Paralytic shellfish poison (saxitoxin family) bioassays - automated end-point determination and standardization of the invitro tissue-culture bioassay, and comparison with the standard mouse bioassay. *Toxicon* **1992,** *30*, (10), 1143-1156.

28. Gallacher, S.; Birkbeck, T. H., A tissue culture assay for direct detection of sodium-channel blocking toxins in bacterial culture supernates. *Fems Microbiology Letters* **1992,** *92*, (1), 101-108.

29. Manger, R. L.; Leja, L. S.; Lee, S. Y.; Hungerford, J. M.; Wekell, M. M., Tetrazolium-based cell bioassay for neurotoxins active on voltage sensitive sodium

channels - semiautomated assay for saxitoxins, brevetoxins, and ciguatoxins. *Analytical Biochemistry* **1993,** *214*, (1), 190-194.

30. Chu, F. S.; Huang, X.; Hall, S., Production and characterization of antibodies against neosaxitoxin. *Journal of Aoac International* **1992,** *75*, (2), 341-345.

31. Humpage, A. R.; Magalhaes, V. F.; Froscio, S. M., Comparison of analytical tools and biological assays for detection of paralytic shellfish poisoning toxins. *Analytical and Bioanalytical Chemistry* **2010,** *397*, (5), 1655-1671.

32. Davio, S. R.; Fontelo, P. A., A competitive displacement assay to detect saxitoxin and tetrodotoxin. *Analytical Biochemistry* **1984,** *141*, (1), 199-204.

33. Doucette, G. J.; Logan, M. M.; Ramsdell, J. S.; VanDolah, F. M., Development and preliminary validation of a microtiter plate-based receptor binding assay for paralytic shellfish poisoning toxins. *Toxicon* **1997,** *35*, (5), 625-636.

34. Usup, G.; Leaw, C. P.; Cheah, M. Y.; Ahmad, A.; Ng, B. K., Analysis of paralytic shellfish poisoning toxin congeners by a sodium channel receptor binding assay. *Toxicon* **2004,** *44*, (1), 37-43.

35. Van Dolan, F. M.; Fire, S. E.; Leighfield, T. A.; Mikulski, C. M.; Doucette, G. J., Determination of paralytic shellfish toxins in shellfish by receptor binding assay: Collaborative study. *Journal of Aoac International* **2012,** *95*, (3), 795-812.

36. Dell'Aversano, C.; Hess, P.; Quilliam, M. A., Hydrophilic interaction liquid chromatography-mass spectrometry for the analysis of paralytic shellfish poisoning (psp) toxins. *Journal of Chromatography A* **2005,** *1081*, (2), 190-201.

37. Lajeunesse, A.; Segura, P. A.; Gelinas, M.; Hudon, C.; Thomas, K.; Quilliam, M. A.; Gagnon, C., Detection and confirmation of saxitoxin analogues in freshwater benthic lyngbya wollei algae collected in the st. Lawrence river (canada) by liquid chromatography-tandem mass spectrometry. *Journal of Chromatography A* **2012,** *1219*, 93-103.

38. D'Agostino, P. M.; Boundy, M. J.; Harwood, T. D.; Carmichael, W. W.; Neilan, B. A.; Wood, S. A., Re-evaluation of paralytic shellfish toxin profiles in cyanobacteria using

hydrophilic interaction liquid chromatography-tandem mass spectrometry. *Toxicon* **2019,** *158*, 1-7.

39. Dell'Aversano, C.; Tattaglione, L.; Polito, G.; Dean, K.; Giacobbe, M.; Casabianca, S.; Capellacci, S.; Penna, A.; Turner, A. D., First detection of tetrodotoxin and high levels of paralytic shellfish poisoning toxins in shellfish from sicily (italy) by three different analytical methods. *Chemosphere* **2019,** *215*, 881-892.

40. Annesley, T. M., Ion suppression in mass spectrometry. *Clinical Chemistry* **2003,** *49*, (7), 1041-1044.

41. Huang, Y.; Kong, M.; Westerman, D.; Xu, E. G.; Coffin, S.; Cochran, K. H.; Liu, Y.; Richardson, S. D.; Schlenk, D.; Dionysiou, D. D., Effects of hco3- on degradation of toxic contaminants of emerging concern by uv/no3. *Environmental Science & Technology* **2018,** *52*, (21), 12697-12707.

42. Foss, A. J.; Phlips, E. J.; Aubel, M. T.; Szabo, N. J., Investigation of extraction and analysis techniques for lyngbya wollei derived paralytic shellfish toxins. *Toxicon* **2012,** *60*, (6), 1148-1158.

43. Wang, K. C.; Chen, S. M.; Hsu, J. F.; Cheng, S. G.; Lee, C. K., Simultaneous detection and quantitation of highly water-soluble herbicides in serum using ion-pair liquid chromatography-tandem mass spectrometry. *J. Chromatogr. B* **2008,** *876*, (2), 211-218.

44. Pizzutti, I. R.; Vela, G. M. E.; de Kok, A.; Scholten, J. M.; Dias, J. V.; Cardoso, C. D.; Concenco, G.; Vivian, R., Determination of paraquat and diquat: Lc-ms method optimization and validation. *Food Chemistry* **2016,** *209*, 248-255.

45. Castro, R.; Moyano, E.; Galceran, M. T., Ion-trap versus quadrupole for analysis of quaternary ammonium herbicides by lc-ms. *Chromatographia* **2001,** *53*, (5-6), 273-278.

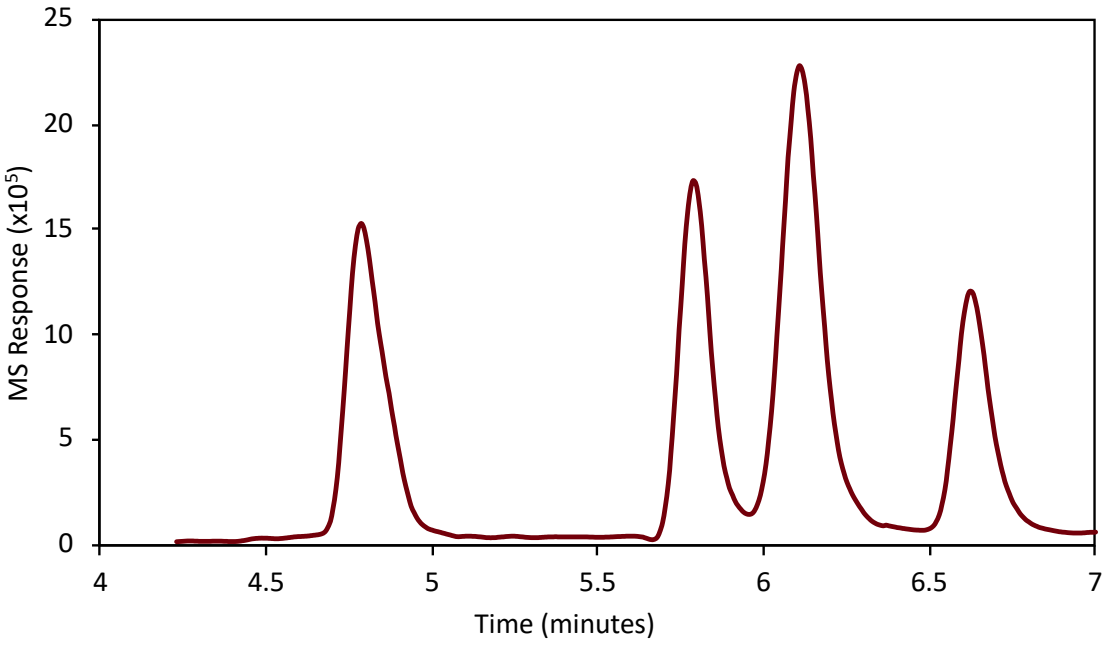

Figure 2.1 LC-MS chromatogram for LWT1 (RT = 4.79 min), LWT4 (RT = 6.64 min), LWT5 (RT = 6.11 min), and LWT6 (RT =5.79 min).

Table 2.1. High resolution fragmentation data for A: LWT1, B:LWT4, C: LWT5, and D: LWT6 (ESI+)

A: LWT1					
m/z	Formula	Mass loss	Formula Loss	Theoretical Mass	ppm Mass Error
379.1040	$C_{11}H_{19}N_6O_7S$			379.1030	2.53
299.1464	$C_{11}H_{19}N_6O_4$	79.958	$-SO_3$	299.1462	0.67
281.1350	$C_{11}H_{17}N_6O_3$	97.969	$-SO_3$, $-H_2O$	281.1351	0.43
221.1145	$C_9H_{13}N_6O$	157.990	$-SO_3$, H_2O, $C_2H_4O_2$	221.1145	0.00
204.0880	$C_9H_{10}N_5O$	175.016	$-SO_3$, $-H_2O$, $-C_2H_4O_2$, $-NH_3$	204.0880	0.20
240.0981	$C_{10}H_{14}N_3O_4$	139.006	$-SO_3$, $-CH_5N_3$	240.0979	0.92
180.0771	$C_8H_{10}N_3O_2$	199.027	$-SO_3$, $-CH_5N_3$, $C_2H_4O_2$	180.0768	1.94
162.0663	$C_8H_8N_3O$	217.038	$-SO_3$, CH_5N_3, $-C_2H_4O_2$, $-H_2O$	162.0662	0.68
102.0661	$C_3H_8N_3O$	277.038	$-C_2H_3O$, $-C_6H_8N_3O_5S$	102.0662	0.88
72.0556	$C_2H_6N_3$	307.048	$-C_9H_{13}N_3O_7S$	72.0556	0.28
60.0557	CH_6N_3	319.048	$-C_{10}H_{13}N_3O_7S$	60.0556	1.33

B: LWT4					
m/z	Formula	Mass loss	Formula Loss	Theoretical Mass	ppm Mass Error
241.1405	$C_9H_{17}N_6O_2$			241.1408	1.04
223.1295	$C_9H_{15}N_6O$	18.011	$-H_2O$	223.1302	3.09
205.1192	$C_9H_{13}N_6$	36.021	$-H_2O$, H_2O	205.1196	2.05
177.0886	$C_7H_9N_6$	64.052	$-H_2O$, H_2O, C_2H_4	177.0883	1.58
164.0821	$C_8H_{10}N_3O$	77.058	$-H_2O$, CH_5N_3	164.0818	1.58
152.0819	$C_7H_{10}N_3O$	89.059	$-CH_4N_3$, $-CH_3O$	152.0818	0.39
136.0867	$C_7H_{10}N_3$	105.054	$-CH_4N_3$, $-H_2O$, $-CH_2O$	136.0869	1.62
122.0711	$C_6H_8N_3$	119.069	$-CH_4N_3$, $-CH_3O$, $-CH_2O$	122.0713	1.39
110.0712	$C_5H_8N_3$	131.069	$-C_4H_8N_3O$, $-OH$	110.0713	0.64
94.0650	C_6H_8N	147.076	$-C_3H_9N_5O_2$	94.0651	1.28
80.0492	C_5H_6N	161.091	$-C_4H_{11}N_5O_2$	80.0495	3.44
72.0556	$C_2H_6N_3$	169.085	$-C_4H_{11}N_5O_2$	72.0556	0.28
69.0447	$C_3H_5N_2$	172.096	$-CH_3O$, $-C_5H_9N_4O$	69.0447	0.29
60.0555	CH_6N_3	181.085	$-C_8H_{11}N_3O_2$	60.0556	2.00

C: LWT5					
m/z	Formula	Mass loss	Formula Loss	Theoretical Mass	ppm Mass Error
299.1460	$C_{11}H_{19}N_6O_4$			299.1462	0.77
281.1353	$C_{11}H_{17}N_6O_3$	18.0107	$-H_2O$	281.1357	1.28
257.1240	$C_{10}H_{17}N_4O_4$	42.0220	$-CH_2N_2$	257.1244	1.67
239.1157	$C_{10}H_{15}N_4O_3$	60.0303	$-H_2O$, $-CH_2N_2$	239.1139	7.65
204.0880	$C_9H_{10}N_5O$	95.0580	$-H_2O$, $-H_2O$, $-NH_2$, -	204.0880	0.05
197.1030	$C_8H_{13}N_4O_2$	102.0430	$-C_2H_4O_2$, $-CH_2N_2$	197.1033	1.52
179.0927	$C_8H_{11}N_4O$	120.0533	$-C_2H_4O_2$, $-CH_2N_2$, $-H_2O$	179.09274	0.22
138.0673	$C_6H_8N_3O$	161.0787	$-C_2H_4O_2$, $-CH_2N_2$, $-H_2O$, -	138.0662	8.04
96.0442	C_5H_6NO	203.1018	$-CH_2N_2$, $-CH_4N_3$, -	96.0444	1.98
83.0604	$C_4H_7N_2$	216.0856	$-C_2H_3O_2$, $-C_5H_9N_4O_2$	83.0604	0.36
72.0552	$C_2H_6N_3$	227.0908	$-C_9H_{13}N_3O_4$	72.0556	5.83
60.0557	CH_6N_3	239.0903	$-C_{10}H_{13}N_3O_4$	60.0556	1.33

D: LWT6					
m/z	Formula	Mass loss	Formula Loss	Theoretical Mass	ppm Mass Error
283.1513	$C_{11}H_{19}N_6O_3$			283.1513	0.04
241.1301	C10H17N4O3	42.0212	$-CH_2N_2$	241.12952	2.41
224.1032	$C_{10}H_{14}N_3O_3$	59.0481	$-CH_5N_3$	224.1030	1.03
205.1194	$C_9H_{13}N_6$	78.0319	$-H_2O$, $-C_2H_4O_2$	205.1196	1.07
190.0958	$C_8H_{10}N_6$	93.0555	$-H_2O$, $-C_2H_4O_2$, $-CH_3$	190.0962	1.84
181.1082	$C_8H_{13}N_4O$	102.0431	$-C_2H_4O_2$, $-CH_2N_2$	181.1084	1.05
177.0883	$C_7H_9N_6$	106.063	-C2H4O2, -H2O, - C2H4	177.0883	0.11
164.0825	$C_8H_{10}N_3O$	119.0688	$-C_2H_4O_2$, $-CH_5N_3$	164.0818	4.02
146.0713	$C_8H_8N_3$	137.08	$-C_2H_4O_2$, $-CH_5N_3$, $-H_2O$	146.0713	0.21
136.08679	$C_7H_{10}N_3$	147.06451	$-C_2H_4O_2$, $-CH_3N_3$, $-CH_2O$	136.0869	0.96
122.0713	$C_6H_8N_3$	161.08	$-C_2H_4O_2$, $-CH_3N_3$, $-C_2H_4O$	122.0713	0.25
110.0713	$C_5H_8N_3$	173.08	$-C_2H_4O_2$, $-C_4H_8N_3O$	110.0713	0.27
72.0554	$C_2H_6N_3$	211.0959	$-C_9H_{13}N_3O_3$	72.0556	3.05
60.0556	CH_6N_3	223.0957	$-C_{10}H_{13}N_3O_3$	60.0556	0.33

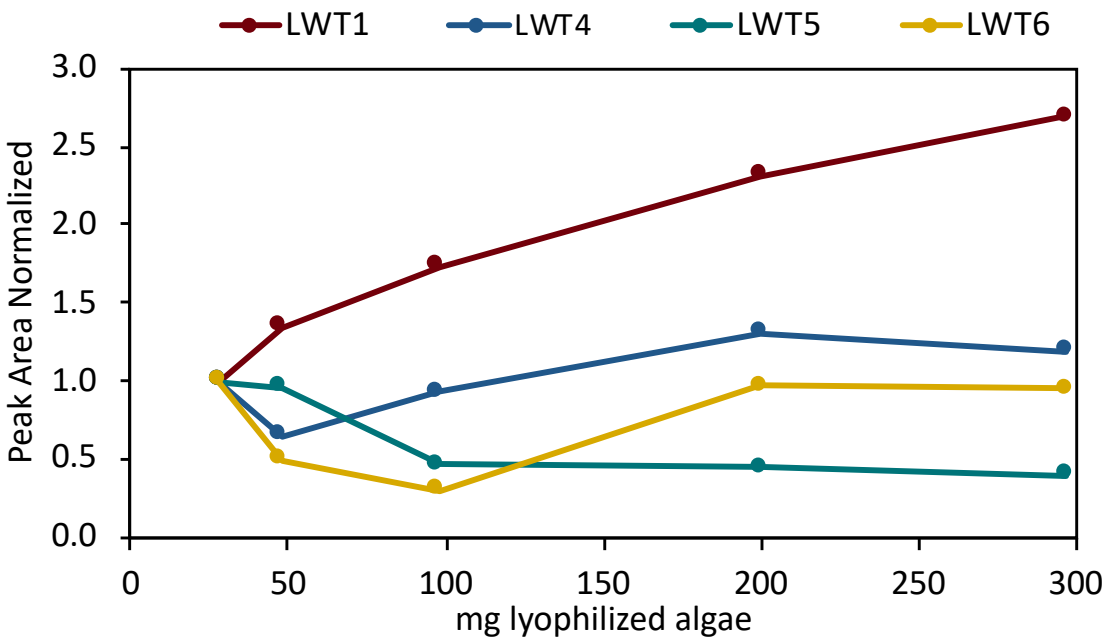

Figure 2.2 Normalized MS peak area vs. mass of lyophilized *L. wollei*. The peak area of each toxin was normalized against the MS response from the lowest mass of algae.

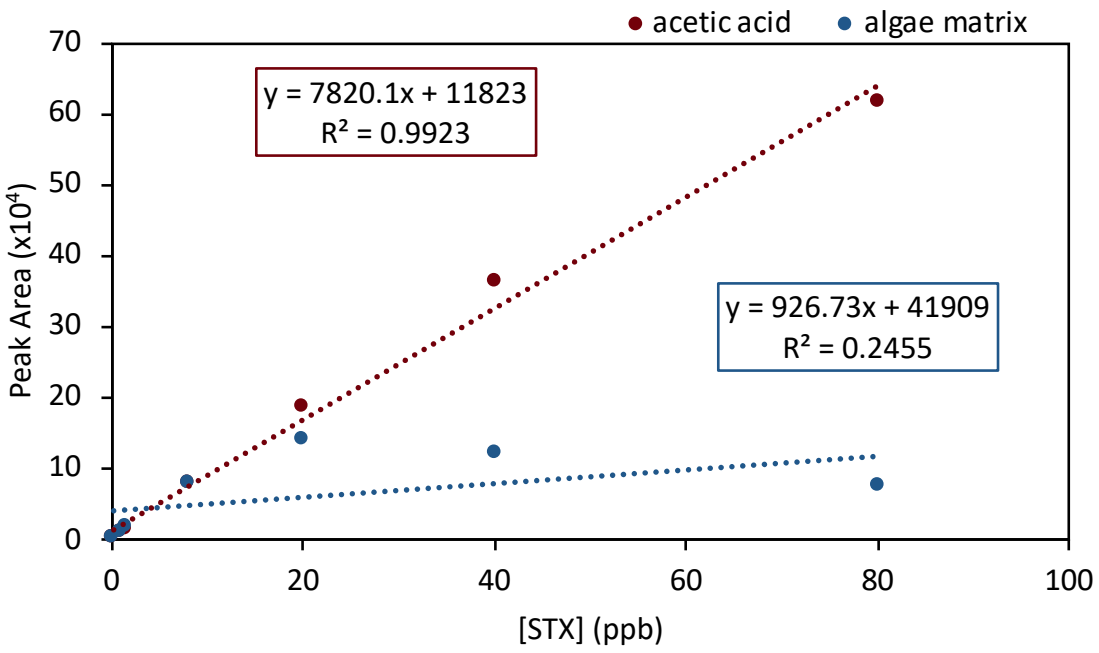

Figure 2.3 Calibration curve for saxitoxin, a model LWT, in 0.1 M acetic acid (red) and in algal extract (blue).

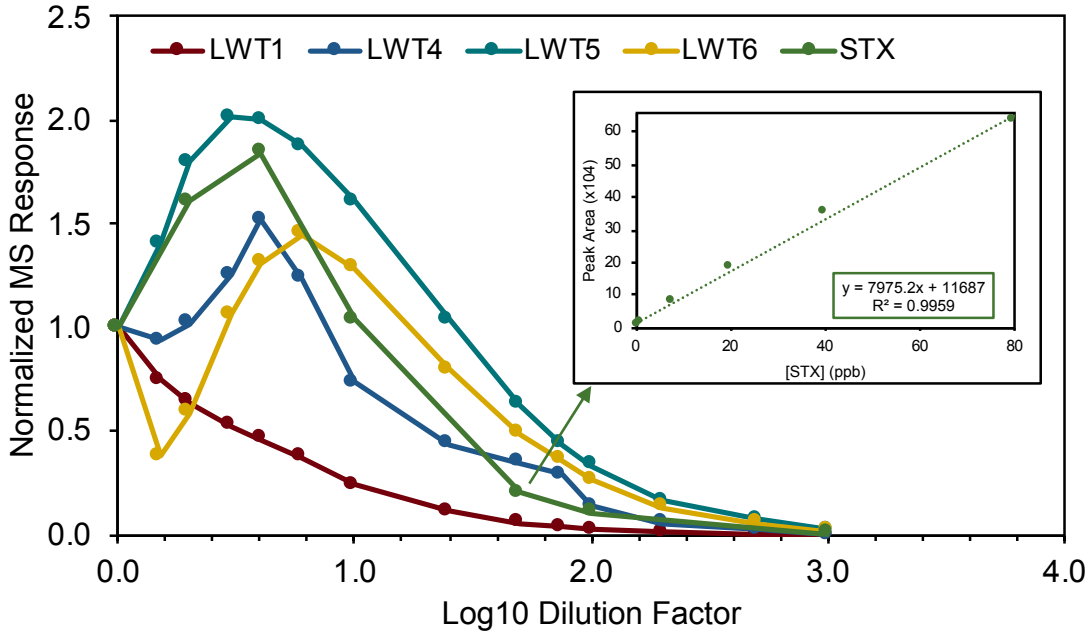

Figure 2.4 Normalized MS peak area of LWTs and saxitoxin in the algal matrix as a function of (log10) dilution factor. Peak area is normalized against the area at a dilution factor of one. Inset: Calibration curve of saxitoxin, a model LWT, in an extract of algae diluted by a factor of 50.

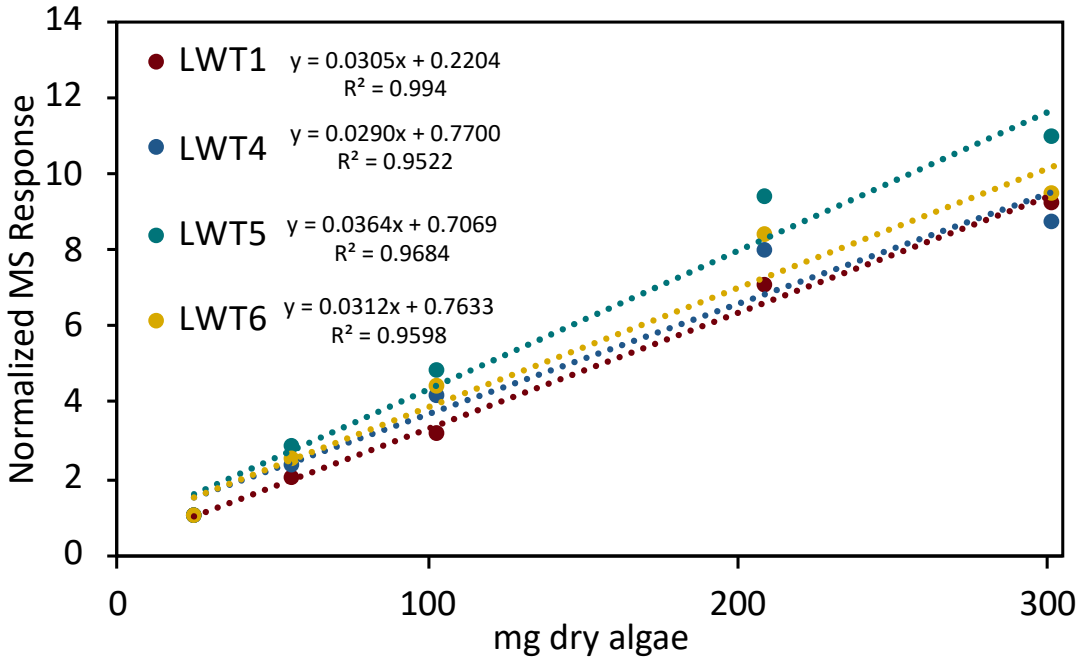

Figure 2.5 Normalized MS peak area vs. mass of lyophilized L. wollei. The peak area of each toxin was normalized against the MS response from the lowest mass of algae (25 mg). Response as a function of dry mass is linear for all 4 toxins (r^2 = 0.952 to 0.994).

CHAPTER 3

INVENTORY OF LYNGBYA WOLLEI TOXINS IN LAKE WATEREE, SOUTH CAROLINA

3.1 ABSTRACT

The occurrence and distribution of the benthic filamentous algae *Lyngbya wollei* was determined for Lake Wateree, SC over the period of July 2018 - February 2019. A 16S rRNA gene sequence was recovered from a sample of collected algae to verify microscopic determination of the presence of *Lyngbya wollei* as the dominant algal species in grab samples from the bloom. Grab samples were routinely collected in Lake Wateree from *Lyngbya wollei* beds over the same time period and evaluated for the presence and concentration of Lyngbya wollei toxins 1-6. Samples were lyophilized, extracted, and extracts were subjected to analysis by liquid chromatography-mass spectrometry (LCMS) for toxin determination. Grab samples presented as fibrous masses and the organic carbon and ash contents were determined for all samples taken. *Lyngbya wollei* toxins 1, 4, 5, and 6 were observed in all locations sampled over the measured time period. Standard reference *Lyngbya wollei* toxins were unavailable; therefore, LWT5 and LWT6 were quantified against their structural analogue saxitoxin and normalized against organic carbon content. The mass of inorganic material trapped in the fibers (~ 35% ash content by dry weight) was recorded. Toxins did not exhibit temporal or location-based trends over the 8-month period ($r^2 < 0.57$). Algal occurrence maps and mean toxin concentrations were used to estimate an approximate total *Lyngbya wollei* toxin inventory for Lake Wateree

3.2 INTRODUCTION

The occurrence of harmful algal blooms (HABs) and associated emergent health risks has increased in recent years with climate change being cited as one of the largest

factors in their growth.[1, 2] HABs develop when aquatic conditions combine to cause the proliferation of algae into the water column due to eutrophication, chemical and biological mechanisms, and anthropogenic activities.[3] The presence of HABs can affect recreational, agricultural, and drinking water resources, leading to a decrease in overall water quality.[4-7] Cyanobacteria are particularly responsive to climate change and their growth rates correlate strongly and positively with higher temperatures, increased stratification, and increased anoxia.[1-3] Cyanobacteria occur naturally in the water column as freely moving and benthic organisms. Benthic cyanobacteria are particularly notable because their communities can support enormous amounts of biomass, exceeding kg wet weight/square meter of sediment surface. Cyanobacteria have a very active secondary metabolism, producing more than 300 bioactive compounds[8-10] some of which are known as cyanotoxins.

The cyanobacterial toxins are a structurally diverse group of secondary metabolites that are produced by a relatively small subset of cyanobacteria.[8, 11, 12] such as *Cylindrospermopsis,*[13-15] *Anabaena,*[16, 17],and *Microcystis.*[18, 19] Several regulatory bodies including the United States Environmental Protection Agency and World Health Organization, have developed drinking water guidelines in recognition of the toxicity of cyanobacterial toxins to human beings.[20-22] Saxitoxins (also known as paralytic shellfish toxins or neurotoxins) are produced from marine genera, such as *Alexandrium*,[23-25] *Gymnodinium,*[26] and *Pyrodinium*,[27, 28] and freshwater species, such as *Anabaena,*[29-31] *Aphanizomenon,*[32-34] *Cylindrospermopsis,*[35] *Planktothrix,*[36] and *Scytonema*.[37, 38] Saxitoxin and its analogues include more than 50 structurally related compounds with varying

toxicity as a function of structure.[39] Although some saxitoxin analogue structures may initially be non-toxic, the structural modifications accompanying their hydrolytic or enzymatic degradation may lead to the formation of structures with toxicity approaching that of saxitoxin. Thus, non-toxin analogues may serve as pro-toxin reservoirs and their presence in the environment cannot be ignored.[40]

Lyngbya wollei is a filamentous benthic cyanobacteria capable of producing biomass in excess of 20 kg/m^2 and has been cited as producing saxitoxin analogues in freshwater and brackish ecosystems.[41-45] More specifically, *Lyngbya wollei* is responsible for the production of several decarbamoyl -saxitoxins and -gonyautoxins, as well as *Lyngbya wollei* toxins 1 thru 6 (LWTs).[40, 45, 46]

An algae bloom of the species *Lyngbya wollei* (Farlow ex Gomont) Speziale & Dyck was identified in Lake Wateree, South Carolina in 2018. Lake Wateree is located in Kershaw, Fairfield, and Lancaster counties in South Carolina. It is a man-made impoundment at the confluence of the Catawba River and Wateree Creek and ultimately joins in with the Santee watershed, draining through the greater Charleston area through the coast. Lake Wateree is a source of water for both recreation and drinking for surrounding communities and encompasses approximately 190 miles of shoreline. The presence of algae within the lake was mapped several times throughout the summer months and nutrient data was collected throughout the lake on separate trips.

Algae samples were collected to survey the biomass and to monitor its spread and potential toxin accumulation (Figure 3.1). Three locations (Coves 1, 2, and 3) were monitored biweekly from June 2018 through February 2019. The presence of LWT1,

LWT4, LWT5, and LWT6 was observed in all algal samples collected and their accumulation in three locations was analyzed. The purpose of this study was to monitor the presence of algae and estimate a total toxin inventory within the lake.

3.3 MATERIALS AND METHODS

3.3.1 MATERIALS

All chemicals were used as received. All aqueous solutions used 18 MΩ cm^{-1} (Barnstead E-pure) water. All glassware was acid washed in 2M HCl/0.1 M oxalic acid prior to oxidation in a muffle furnace. Acetonitrile (LCMS grade) was obtained from VWR BDH chemicals. Ammonium formate (98+%) was purchased from Alfa Aesar. Formic acid (certified ACS), glacial acetic acid (certified ACS Plus), and hydrochloric acid (certified ACS Plus) were purchased from Fisher. Saxitoxin dihydrochloride in dilute hydrochloride standard solutions were obtained from NIST and Abraxis Inc.

3.3.2 SAMPLING

Five sampling trips were taken to map the presence of algae along the shoreline of Lake Wateree during 2018 (Figure 3.1). Samples were collected from the surface of floating mats into 50-mL sterile centrifuge vials. Three locations readily accessible from land were chosen to monitor the presence of algae routinely throughout the year: Cove 1 (Deer Run Cove [34.416054, -80.863473]), Cove 2 (Buck Hill Landing [34.334926, -80.708297]), and Cove 3 ([34.364058, -80.699524]). Collected samples were stored on ice for transport.

3.3.3 EXTRACTION METHOD

Samples stored on ice were further frozen using liquid nitrogen and then lyophilized using a Labconco FreeZone 6 lyophilizer immediately upon arrival to the laboratory. Lyophilized samples were stored at -20°C until extraction. Approximately 100 mg of dry weight algae was extracted with 10 mL of 0.1 M acetic acid. Samples were shaken, sonicated for 15 minutes, and centrifuged for 5 minutes. An aliquot was removed, filtered through a 0.45-micron nylon filter, diluted by a factor of 50 in 0.1 M acetic acid, and analyzed by liquid chromatography mass spectrometry.

3.3.4 UPLC-MS/MS

Algae samples were analyzed by a Waters (Milford, MA, USA) Acquity ultra performance liquid chromatography (UPLC) coupled with a Xevo triple quadrupole mass spectrometer (MS/MS) equipped with an electrospray ionization source (ESI). Separations were performed on a BEH Amide (2.1x150 mm) 1.7 µm particle size column (Waters). The mobile phases were aqueous 5.6 mM formate buffered at pH 3.5 (A) and 95/5, acetonitrile/water 5.6mM formate buffer at pH 3.5 (B) The chromatographic method began initially with 80% B held for one minute, ramped to 60% B over the next 3 minutes and held for 2 minutes, at 7 minutes ramped back to the original conditions over one minute (80% B) and held for re-equilibration for 8 minutes (16 minutes total).

Saxitoxin (*m/z* = 300) was used as a model calibration standard for LWT5 since no commercial standard is available. All saxitoxin calibrations solutions were made up in 3 mM HCl and source conditions were optimized manually. All algae samples collected were analyzed by UPLC-MS/MS in the positive ion mode. Analytes of interest were optimized

manually through chromatography from solutions of extracted algae. Selected ion monitoring (SIM) was used for analysis of LWT1 (*m/z* = 379), LWT4 (*m/z* = 241), LWT5 (*m/z* = 299) and LWT6 (*m/z* = 283).

3.3.5 ORGANIC CARBON AND ASH ANALYSIS

Carbon was analyzed from lyophilized algae samples using a solid sample total organic carbon analyzer (Shimadzu Inc., Columbia, MD). Approximately 40 mg dry weight of algae was placed into a tared ceramic boat, which was then combusted in a 900° C furnace with excess ultra-high purity oxygen (Airgas Inc.). Glucose was used as the calibration standard. Post-combustion weight was recorded to determine inorganic (non-combustible) content.

3.3.6 16S RRNA ANALYSIS

Amplification and sequencing of the 16S rRNA was performed at MR DNA (www.mrdnalab.com, Shallowater, TX). BLASTn was used to taxonomically classify the final operational taxonomical units using databases derived from RDPII and NCBI.

3.4 RESULTS

3.4.1 CARBON AND INORGANIC CONTENT

Total carbon and inorganic material were measured for each algae sample obtained. Samples showed a broad range of carbon and inorganic content between samples collected at the same time and location as well as throughout the sampling period. Average percent carbon ranged from 21% to 40%, while average percent inorganic material ranged from 14% to 49% (Figure S1). Variation shows a random distribution with

no clear trend, indicating the inorganic content is unique to each sample and cannot be examined as a bulk average property.

3.4.2 TOXIN INVENTORY

Algae samples were collected from Coves 1, 2, and 3 regularly between June 2018 and May 2019. LWT1, 4, 5, and 6 were qualified in every sample taken at every location over the sampling period. Reference standards for the LWTs are not commercially available, therefore LWT5 and LWT6 were quantified against saxitoxin, a close structural analogue. Qualitative differences in the fragmentation behavior of LWT1 and LWT4 compare to saxitoxin made the direct quantification of the former by the same technique inadvisable. The raw peak areas of LWT1 and LWT4 combined comprised 6% or less of the total toxin method response and were considered trace components of the system. Trends in the LWTs over time were investigated by determining the slope of $LWTX/LWTX_{min}$ vs sampling date over the 8 month sampling periods for each location, where LWTX refers to the given *Lyngbya wollei* toxin and $LWTX_{min}$ refers to the lowest method response obtained from the same toxin over the sampling period. The normalized LWTX response, normalized on a per g carbon basis showed essentially a flat relationship vs time (Figure 3.2, Cove 1 for LWT1, 4, 5, and 6 is presented for illustrative purposes in text and the same data for Coves 2 and 3 in Figure C.2 and C.3). The hypothesis of seasonal and conditional variation affecting the concentration of the LWTs has been proposed previously [45, 47] however no statistically significant variation was observed in this work (Table 3.1, $r^2 < 0.57$ for all toxin measured vs time). Sample to sample variation of less than a factor of five indicated unusually tight agreement between grab samples from a

harmful algal bloom. An average toxin amount from each location demonstrates the variation between location and location composition (Figure 3.3). The lake wide average total toxin loading (micrograms of LWT5 and LWT6 summed/g carbon) for the algae samples collected from Cove 1, 2, and 3 over the sampling season were 276 μg/g carbon, 466 μg/g carbon, and 450 μg/g carbon respectively.

3.5 DISCUSSION

The toxin amount of LWT1, LWT4, LWT5, and LWT6 over time presented here provides unprecedented time resolution for these four toxin's presence in *Lyngbya wollei*. Total carbon in *Lyngbya wollei* is presented as a normalization technique to decrease noise from inorganic material inherent to the sampling technique. Variation in inorganic content in samples is large; therefore, inorganic content must be measured in each individual sample as an important quality control step to ensure the sample is properly corrected. Toxin amounts were monitored in Lake Wateree over a growing and dormant season (June thru February), however no spatial or temporal trends were observed. Without commercially available standards, saxitoxin was used as a surrogate calibration standard to generate LWT concentrations in saxitoxin equivalents within *Lyngbya wollei* cells. Normalized against g carbon, high μg saxitoxin equivalents were observed in three locations in Lake Wateree (276 μg/g carbon, 466 μg/g carbon, and 450 μg/g carbon). On average, Lyngbya wollei is 32% carbon (±7%) and loses approximately 82% of its weight during freeze drying. *Lyngbya wollei* is a high biomass producing benthic algae, with biomass estimates in the literature that range from 20-30 kg/m^2 fresh weight.

Concentrations of LWTs in Lake Wateree could range from 477 mg/m^2 to 805 mg/m^2 of saxitoxin equivalent toxin concentration.

3.6 REFERENCES

1. Paerl, H. W.; Huisman, J., Climate change: A catalyst for global expansion of harmful cyanobacterial blooms. *Environmental Microbiology Reports* **2009,** *1*, (1), 27-37.

2. Paerl, H. W.; Huisman, J., Climate - blooms like it hot. *Science* **2008,** *320*, (5872), 57-58.

3. O'Neil, J. M.; Davis, T. W.; Burford, M. A.; Gobler, C. J., The rise of harmful cyanobacteria blooms: The potential roles of eutrophication and climate change. *Harmful Algae* **2012,** *14*, 313-334.

4. Jancula, D.; Marsalek, B., Critical review of actually available chemical compounds for prevention and management of cyanobacterial blooms. *Chemosphere* **2011,** *85*, (9), 1415-1422.

5. Ho, J. C.; Michalak, A. M., Challenges in tracking harmful algal blooms: A synthesis of evidence from lake erie. *Journal of Great Lakes Research* **2015,** *41*, (2), 317-325.

6. Westrick, J. A.; Szlag, D. C.; Southwell, B. J.; Sinclair, J., A review of cyanobacteria and cyanotoxins removal/inactivation in drinking water treatment. *Analytical and Bioanalytical Chemistry* **2010,** *397*, (5), 1705-1714.

7. Diaz, J. M.; Plummer, S., Production of extracellular reactive oxygen species by phytoplankton: Past and future directions. *Journal of Plankton Research* **2018,** *40*, (6), 655-666.

8. Carmichael, W. W., Cyanobacteria secondary metabolites - the cyanotoxins. *Journal of Applied Bacteriology* **1992,** *72*, (6), 445-459.

9. Pearson, L. A.; Dittmann, E.; Mazmouz, R.; Ongley, S. E.; D'Agostino, P. M.; Neilan, B. A., The genetics, biosynthesis and regulation of toxic specialized metabolites of cyanobacteria. *Harmful Algae* **2016,** *54*, 98-111.

10. Chapter 38 - phycotoxins. **2013**, 1155 - 1186.

11. Carmichael, W. W., Toxins of cyanobacteria. *Sci.Am.* **1994,** *270*, (1), 78-86.

12. Codd, G. A.; Morrison, L. F.; Metcalf, J. S., Cyanobacterial toxins: Risk management for health protection. *Toxicology and Applied Pharmacology* **2005,** *203*, (3), 264-272.

13. Ohtani, I.; Moore, R. E.; Runnegar, M. T. C., Cylindrospermopsin - a potent hepatotoxin from the blue green alga cylindrospermopsis raciborskii. *Journal of the American Chemical Society* **1992,** *114*, (20), 7941-7942.

14. Cheng, X.; Shi, H.; Adams, C. D.; Timmons, T.; Ma, Y., Effects of oxidative and physical treatments on inactivation of cylindrospermopsis raciborskii and removal of cylindrospermopsin. *Water Science and Technology* **2009,** *60*, (3), 689-697.

15. Soto-Liebe, K.; Murillo, A. A.; Krock, B.; Stucken, K.; Fuentes-Valdes, J. J.; Trefault, N.; Cembella, A.; Vasquez, M., Reassessment of the toxin profile of cylindrospermopsis raciborskii t3 and function of putative sulfotransferases in synthesis of sulfated and sulfonated psp toxins. *Toxicon* **2010,** *56*, (8), 1350-1361.

16. Monegue, R. L.; Philips, E. J., The effect of cyanophages on the growth and survival of lyngbya-wollei, anabaena-flos-aquae, and anabaena-circinalis. *Journal of Aquatic Plant Management* **1991,** *29*, 88-93.

17. Allen, M. B.; Arnon, D. I., Studies on nitrogen-fixing blue-green algae .1. Growth and nitrogen fixation by anabaena-cylindrica lemm. *Plant Physiology* **1955,** *30*, (4), 366-372.

18. Orr, P. T.; Jones, G. J.; Douglas, G. B., Response of cultured microcystis aeruginosa from the swan river, australia, to elevated salt concentration and consequences for bloom and toxin management in estuaries. *Marine and Freshwater Research* **2004,** *55*, (3), 277-283.

19. Qian, H. F.; Hu, B. L.; Yu, S. Q.; Pan, X. J.; Wu, T.; Fu, Z. W., The effects of hydrogen peroxide on the circadian rhythms of microcystis aeruginosa. *Plos One* **2012,** *7*, (3).

20. Merel, S.; Walker, D.; Chicana, R.; Snyder, S.; Baures, E.; Thomas, O., State of knowledge and concerns on cyanobacterial blooms and cyanotoxins. *Environment International* **2013,** *59*, 303-327.

21. Weirich, C. A.; Miller, T. R., Freshwater harmful algal blooms: Toxins and children's health. *Current Problems in Pediatric and Adolescent Health Care* **2014,** *44*, (1), 2-24.

22. Dunlap, C. R.; sklenar, K. S.; Blake, L. J., A costly endeavor: Addressing algae problems in a water supply. *Journal of American Water works Association* **2015,** *107*, (5), 102-102.

23. Anderson, D. M.; Kulis, D. M.; Sullivan, J. J.; Hall, S.; Lee, C., Dynamics and physiology of saxitoxin production by the dinoflagellates alexandrium spp. *Marine Biology* **1990,** *104*, (3), 511-524.

24. Chang, F. H.; Anderson, D. M.; Kulis, D. M.; Till, D. G., Toxin production of alexandrium minutum (dinophyceae) from the bay of plenty, new zealand. *Toxicon* **1997,** *35*, (3), 393-409.

25. Cho, Y.; Tsuchiya, S.; Yoshioka, R.; Omura, T.; Konoki, K.; Oshima, Y.; Yotsu-Yamashita, M., The presence of 12 beta-deoxydecarbamoylsaxitoxin in the japanese toxic dinoflagellate alexandrium determined by simultaneous analysis for paralytic shellfish toxins using hilic-lc-ms/ms. *Harmful Algae* **2015,** *49*, 58-67.

26. Oshima, Y.; Hasegawa, M.; Yasumoto, T.; Hallegraeff, G.; Blackburn, S., Dinoflagellate gymnodinium catenatum as the source of paralytic shellfish toxins in tasmanian shellfish. *Toxicon* **1987,** *25*, (10), 1105-1111.

27. Usup, G.; Kulis, D. M.; Anderson, D. M., Growth and toxin production of the toxic dinoflagellate pyrodinium bahamense var. Compressum in laboratory cultures. *Natural Toxins* **1994,** *2*, (5), 254-262.

28. Harada, T.; Oshima, Y.; Yasumoto, T., Studies on paralytic shellfish poisoning in tropical waters .4. Structures of 2 paralytic shellfish toxins, gonyautoxin-v and gonyautoxin-vi isolated from a tropical dinoflagellate, pyrodinium bahamense var compressa. *Agricultural and Biological Chemistry* **1982,** *46*, (7), 1861-1864.

29. Humpage, A. R.; Rositano, J.; Bretag, A. H.; Brown, R.; Baker, P. D.; Nicholson, B. C.; Steffensen, D. A., Paralytic shellfish poisons from australian cyanobacterial blooms. *Australian Journal of Marine and Freshwater Research* **1994,** *45*, (5), 761-771.

30. Onodera, H.; Oshima, Y.; Watanabe, M. F.; Watanabe, M.; Bolch, C. J.; Blackburn, S.; Yasumoto, T., Screening of paralytic shellfish toxins in freshwater cyanobacteria and chemical confirmation of the toxins in cultured *anabaena circinalis* from australia. In *Harmful and toxic algal blooms*, Yasumoto, T.;Oshima, Y.; Fukuyo, Y., Eds. IOS UNESCO: Paris, 1996; pp 563-566.

31. Al-Tebrineh, J.; Mihali, T. K.; Pomati, F.; Neilan, B. A., Detection of saxitoxin-producing cyanobacteria and anabaena circinalis in environmental water blooms by quantitative pcr. *Applied and Environmental Microbiology* **2010,** *76*, (23), 7836-7842.

32. Sawyer, P. J.; Gentile, J. H.; Sasner, J. J., Demonstration of a toxin from aphanizomenon flos aquae (l) ralfs. *Canadian Journal of Microbiology* **1968,** *14*, (11), 1199-&.

33. Jackim, E.; Gentile, J., Toxins of a blue green alga - similarity to saxitoxin. *Science* **1968,** *162*, (3856), 915-&.

34. Mahmood, N. A.; Carmichael, W. W., Paralytic shellfish poisons produced by the freshwater cyanobacterium aphanizomenon-flos-aquae nh-5. *Toxicon* **1986,** *24*, (2), 175-&.

35. Lagos, N.; Onodera, H.; Zagatto, P. A.; Andrinolo, D.; Azevedo, S.; Oshima, Y., The first evidence of paralytic shellfish toxins in the freshwater cyanobacterium cylindrospermopsis raciborskii, isolated from brazil. *Toxicon* **1999,** *37*, (10), 1359-1373.

36. Pomati, F.; Sacchi, S.; Rosetti, C.; Giovannardi, S.; Onodera, H.; Oshima, Y.; Neilan, B. A., The freshwater cyanobacterium planktothrix sp. Fp1: Molecular identification and detection of paralytic shellfish poisoning toxins. *Journal of Phycology* **2003,** *36*, (3), 553-562.

37. Smith, F. M. J.; Wood, S. A.; Wilks, T.; Kelly, D.; Broady, P. A.; Williamson, W.; Gaw, S., Survey of scytonema (cyanobacteria) and associated saxitoxins in the littoral zone of recreational lakes in canterbury, new zealand. *Phycologia* **2012,** *51*, (5), 542-551.

38. Smith, F. M. J.; Wood, S. A.; van Ginkel, R.; Broady, P. A.; Gaw, S., First report of saxitoxin production by a species of the freshwater benthic cyanobacterium, scytonema agardh. *Toxicon* **2011,** *57*, (4), 566-573.

39. Wiese, M.; D'Agostino, P. M.; Mihali, T. K.; Moffitt, M. C.; Neilan, B. A., Neurotoxic alkaloids: Saxitoxin and its analogs. *Marine Drugs* **2010,** *8*, (7), 2185-2211.

40. Foss, A. J.; Phlips, E. J.; Aubel, M. T.; Szabo, N. J., Investigation of extraction and analysis techniques for lyngbya wollei derived paralytic shellfish toxins. *Toxicon* **2012,** *60*, (6), 1148-1158.

41. Onodera, H.; Satake, M.; Oshima, Y.; Yasumoto, T.; Carmichael, W. W., New saxitoxin analogues from the freshwater filamentous cyanobacterium lyngbya wollei. *Natural Toxins* **1997,** *5*, (4), 146-151.

42. Cowell, B. C.; Botts, P. S., Factors influencing the distribution, abundance and growth of lyngbya wollei in central florida. *Aquatic Botany* **1994,** *49*, (1), 1-17.

43. Yin, Q. Q.; Carmichael, W. W.; Evans, W. R., Factors influencing growth and toxin production by cultures of the freshwater cyanobacterium lyngbya wollei farlow ex gomont. *Journal of Applied Phycology* **1997,** *9*, (1), 55-63.

44. Carmichael, W. W.; Evans, W. R.; Yin, Q. Q.; Bell, P.; Moczydlowski, E., Evidence for paralytic shellfish poisons in the freshwater cyanobacterium lyngbya wollei (farlow ex gomont) comb. Nov. *Applied and Environmental Microbiology* **1997,** *63*, (8), 3104-3110.

45. Foss, A. J.; Phlips, E. J.; Yilmaz, M.; Chapman, A., Characterization of paralytic shellfish toxins from lyngbya wollei dominated mats collected from two florida springs. *Harmful Algae* **2012,** *16*, 98-107.

46. Mihali, T. K.; Carmichael, W. W.; Neilan, B. A., A putative gene cluster from a lyngbya wollei bloom that encodes paralytic shellfish toxin biosynthesis. *Plos One* **2011,** *6*, (2).

47. Hudon, C.; Gagnon, P.; Larabie, S. P.; Gagnon, C.; Lajeunesse, A.; Lachapelle, M.; Quilliam, M. A., Spatial and temporal variations of a saxitoxin analogue (lwtx-1) in

lyngbya wollei (cyanobacteria) mats in the st. Lawrence river (quebec, canada). *Harmful Algae* **2016,** *57*, 69-77.

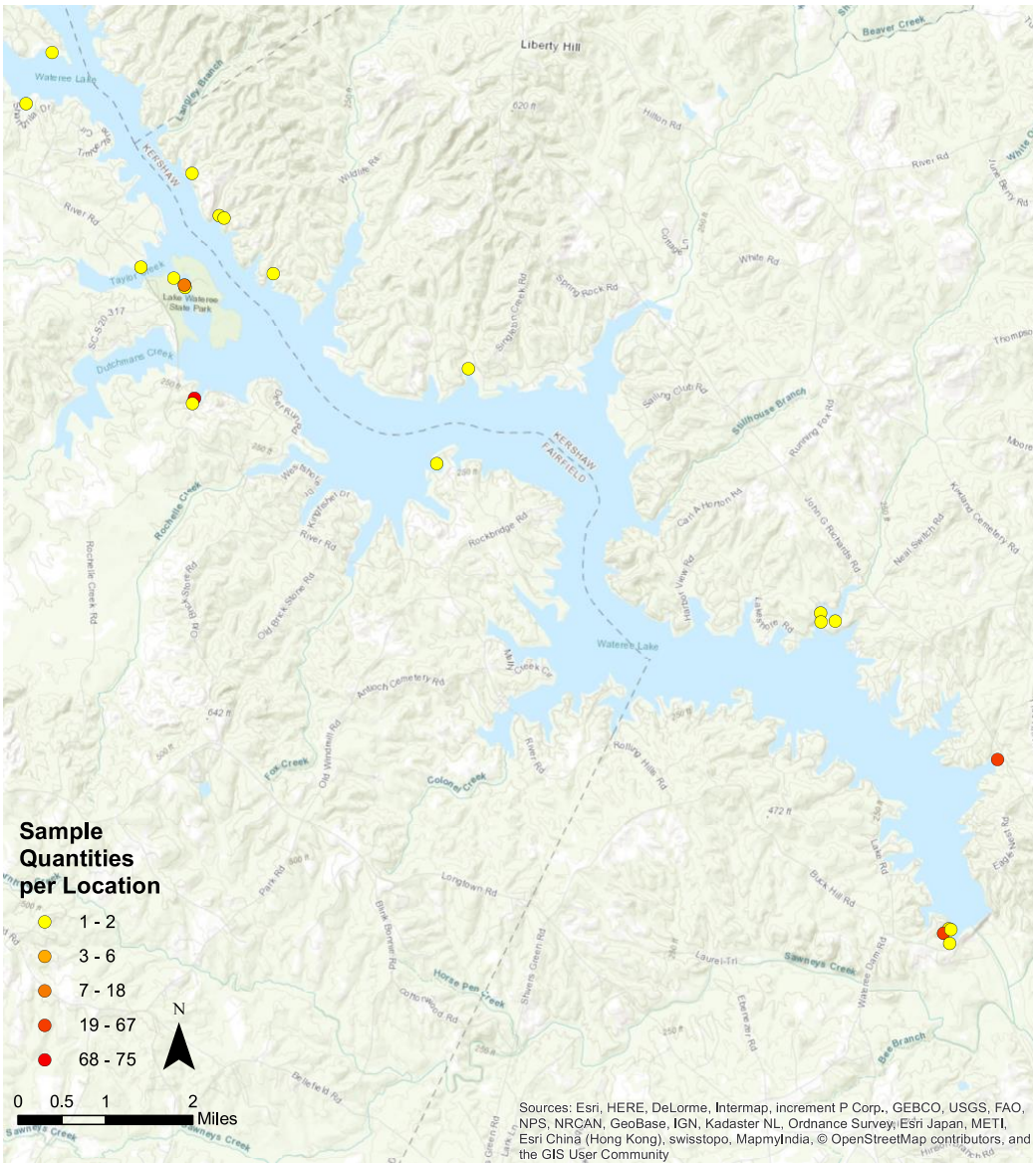

Figure 3.1. Map of Lake Wateree, recorded occurrence of *Lyngbya wollei,* and quantity of samples per each location.

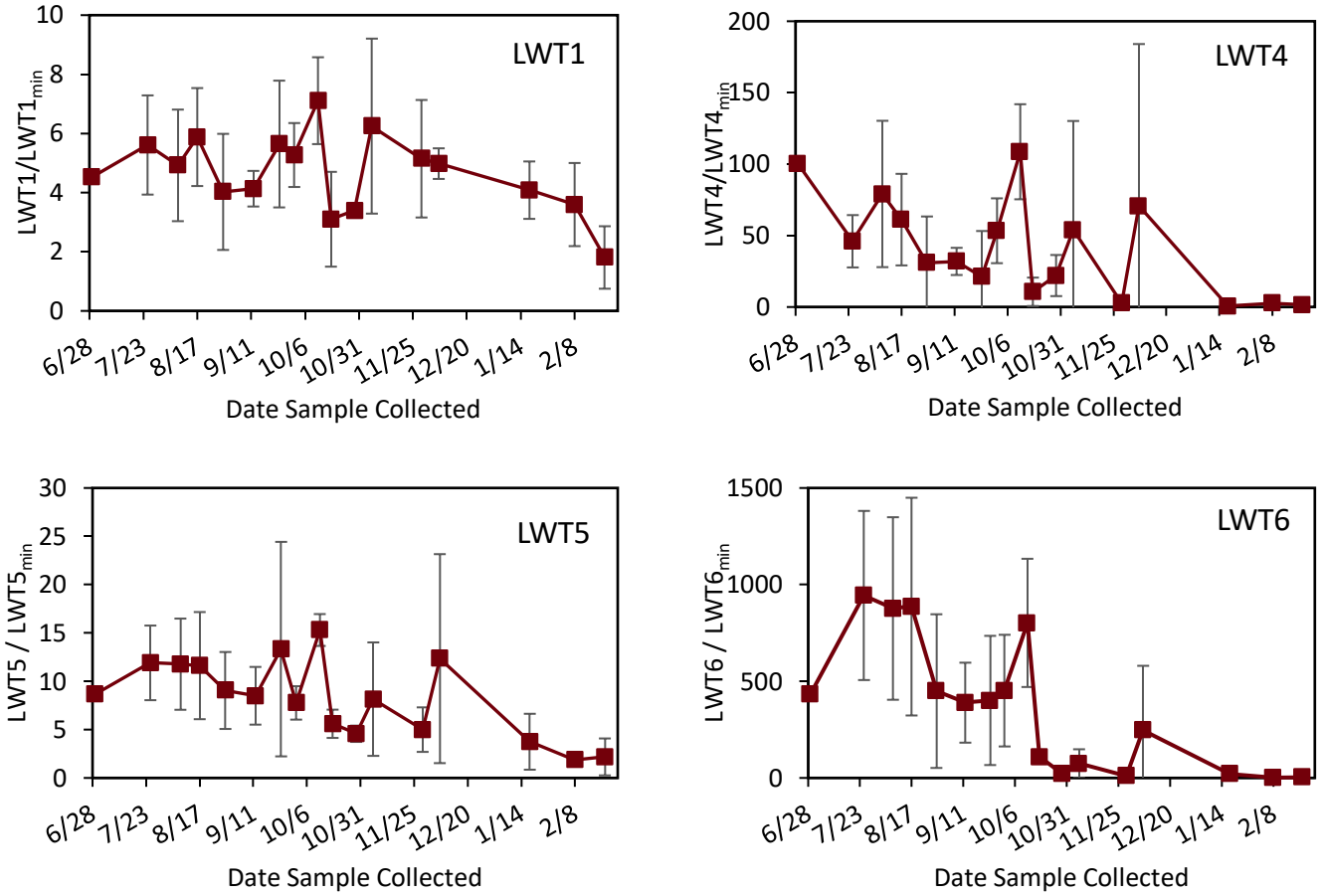

Figure 3.2. LWTX/LWTX$_{min}$ for LWT1, LWT4, LWT5, and LWT6 for Cove 1 from June 2018 to February 2019.

Table 3.1. Slope and R^2 from best fit line of each toxin's peak area vs. date from Cove 1, Cove 2, and Cove 3.

Toxin	Cove 1		Cove 2		Cove 3	
	Slope	R^2	Slope	R^2	Slope	R^2
LWT1	-0.311	0.2021	NA	NA	-0.5657	0.0771
LWT4	-0.900	0.3800	0.2344	0.0195	-0.2638	0.0014
LWT5	-12.15	0.4308	-8.523	0.0320	-4.846	0.0234
LWT6	-24.60	0.5736	-14.185	0.4179	-29.737	0.5247

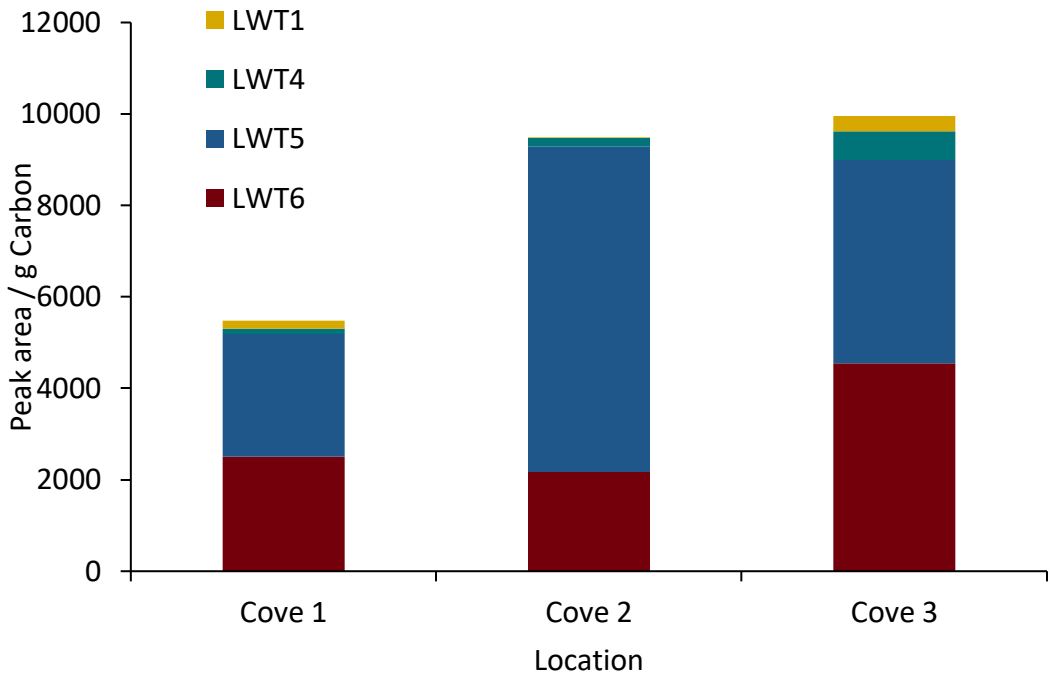

Figure 3.3. Total average LWT amount for Cove 1, Cove 2, and Cove 3.

CHAPTER 4

AUTOXIDATION PROVOKES SYNERGISTIC REACTIVE OXYGEN SPECIES FORMATION IN NATURAL WATER

4.1 ABSTRACT

Reactive oxygen species (ROS) including hydrogen peroxide and superoxide have been measured in many natural waters but their provenance is poorly understood. Here we show the importance of the autoxidation to the rate and yield of hydrogen peroxide formation in several different natural waters in the absence of photons, using the autoxidation of gallic acid as a source of ROS. Baseline hydrogen peroxide generation from the autoxidation of GA was established over the pH range 5-9 and compared to that observed after the addition of GA to a series of natural waters (filtered and unfiltered). The direct oxidation of GA by dioxygen initiated the process but the bulk of the oxidation was through a free radical chain reaction that relied on superoxide as the primary carrier (indicated by the effects of added superoxide dismutase). In unfiltered natural waters the rate of GA oxidation increased by a factor of 5-10 relative to laboratory water, depending on the water source. The addition of a metal chelating agent reduced this rate to the same as laboratory water, indicating metals were important catalysts for this process. An experimental rate constant for superoxide and NOM was determined (2.18 ppm DOC^{-1} hr^{-1}). Results indicated that up to approximately 90% of hydrogen peroxide in natural waters may be tied to the autoxidation of natural organic matter.

4.2 INTRODUCTION

The autoxidation of organic carbon by dioxygen is thermodynamically favorable but spin forbidden, and so is kinetically limited under conditions common to surface waters.[1] However, a few naturally occurring organic molecules, including some of the

hydrolysis products of lignin, are known to react directly with dioxygen to produce reactive oxygen species (ROS). ROS are the partial reduction products of dioxygen and include several species whose reactions with organic carbon are kinetically facile, particularly superoxide, hydrogen peroxide, and hydroxyl radical (presented in aggregate because the concentrations of the three ROS are proportionate with each other through Fenton-type reactions, although their instantaneous concentrations are typically quite different).[2] ROS are widespread in natural waters, but typically only present at micromolar or lower concentrations, a consequence of their high bimolecular rate constants for reactions with natural organic carbon.[3]

Sources of ROS in surface waters include a manifold of photochemical and other processes (Figure 4.1). The photolysis of aqueous nitrate leads to the formation of oxide radical (pKa = 11.5),[4] which protonates at pH values commonly found in surface waters to yield the hydroxyl radical.[5, 6] The photolysis of Fe(III)-ligand (L) complexes can directly lead to hydroxyl radical formation when L = H_2O or HO^- with concurrent production of Fe(II). However, dissolved Fe(III) is more likely to be associated with an organic ligand, leading to oxidation of the ligand and production of ferrous species that in turn can be oxidized by atmospheric oxygen to yield ferric iron and superoxide (pKa 4.8).[3, 7, 8] The photoexcitation of dissolved organic matter leads to the apparent formation of several ROS, including superoxide, hydrogen peroxide, singlet oxygen, and hydroxyl radical.[9, 10] Outside the photic zone, ROS production appears to be dominated by the redox chemistry of Fe(II). Underwater groundwater discharge and tidal water movement releases Fe(II) species from sedimentary porewaters to oxygen-containing regions in the water column,

resulting in the production of superoxide and hydrogen peroxide as it oxidizes.[11-13] Catalytic versions of this system exist where reduced natural organic matter (NOM) or hydrogen sulfide drive the reduction of resultant Fe(III) species back to Fe(II).[13-15] Reactive oxygen species are also associated with surface and groundwaters in both marine and freshwater environments, as in microbial production of superoxide.[3, 16-19]

The reactions illustrated in Figure 4.1 are **primary** sources (i.e. radicals derived from non-radical species during initiation) of ROS and the provenance of ROS is usually ascribed to them. However, another possible source of ROS in surface waters are the **secondary** reactions associated with the decay of peroxyl radicals (i.e. radicals derived from radicals during chain propagation, particularly related to autoxidation).[20-24] The reactions of hydroxyl radical and superoxide with organic carbon are known to lead to the production of carbon centered radicals.[25] Carbon centered radicals may react with themselves through dimerization, fragmentation, or dismutation, but they also react (generally) with dioxygen with very high bimolecular rate constants that typically approach diffusion controlled. This coupling reaction leads to the formation of peroxyl radicals.[26] Peroxyl radicals experience a manifold of decay pathways including several that result in the release of additional superoxide or hydrogen peroxide.[27] The latter ROS enable the oxidation of additional organic matter, with the net radical chain process described as autoxidation.[20, 25, 28-31]

Autoxidative processes have been shown to be important for the redox cycling of naturally occurring and anthropogenic metals, as well as several classes of organic materials, particularly quinones and halogenated molecules.[29, 32-39] The autoxidation of

phenolic acids in the presence of redox-active transition metals is thermodynamically capable of supporting the incidental co-oxidation of several pesticides, including carbaryl, atrazine, and 2,4,5-T (although the kinetics of this are dependent on solution conditions).[40] The oxidation of phenolics by hydroxyl radical leads to the formation of significant amounts of hydrogen peroxide in solution.[41, 42] This is not limited to aromatic structures; the oxidation of aliphatic acids has also been shown to lead to hydrogen peroxide formation under conditions ranging from laboratory grade water to cloud water.[43] Here we report the potential of NOM, derived from several different natural waters, to develop ROS through autoxidation in the absence of added photons, transition metals, or peroxides. This was accomplished by the addition of a radical initiator; gallic acid (GA), with its autoxidation serving as the initiator for the superoxide driven production of ROS from NOM.[44, 45]

The autoxidation of GA in laboratory and natural waters was characterized with respect to its ability to influence the rate of ROS production and consume GA at pH 5-10, representative of most surface waters.[46] This process was systematically repeated in surface waters collected from several locations in the Saluda and Santee watersheds in South Carolina, including the Congaree River, a secondary stream (Cedar Creek), a stagnant slough (Old Bates River), and a lake (Lake Marion). Natural waters were characterized for pH, dissolved organic carbon, and a suite of transition metals (Tables 1 and C.2). In all cases the addition of GA to these waters resulted in dramatic increases in the rate of ROS formation relative to that observed in solutions of GA or NOM alone.

Hydrogen peroxide production was also dependent on dissolved transition metals, although the relationship was not rectilinear (*vide infra*).

4.3 MATERIALS AND METHODS

4.3.1 MATERIALS

Gallic acid (98+%, 3,4,5-trihydroxybenzoic acid) and diethylenetriaminepenta-acetic acid (98+%, DTPA) were purchased from Alfa Aesar. Sodium bicarbonate, acetonitrile (HPLC Grade), and hydrochloric acid were obtained from BDH. Horseradish peroxidase (HRP) was obtained from Sigma-Aldrich and 10-acetyl-3,7-dihydroxy-phenoxazine (Amplex Red, 97%) was purchased from American Advanced Scientific. Both were stored in a desiccator at -5°C. Dibasic sodium phosphate (certified ACS) and formic acid (certified ACS) was purchased from Fisher. All chemicals were used as received. Laboratory water was deionized to a resistivity of 18 MΩ cm^{-1} (Barnstead E-pure) and ozonated for at least 5 hours to remove all organic material. Aqueous solutions were made up in this water; residual ozone had been purged by N_2. All glassware was acid washed in 2 M HCl/0.1 M oxalic acid prior to oxidation in a muffle furnace.

4.3.2 PROCEDURE

All experiments were performed in triplicate and results averaged. The resulting standard deviations are presented in figures as error bars. All experiments were conducted under dim red light. GA stock solutions were made fresh daily in 0.1 M sodium bicarbonate, with pH pre-adjusted to the desired condition. Experiments were initiated by the addition of GA stock solutions to air saturated solutions (10-fold molar excess of

oxygen relative to GA, [O_2] = 250 μM) made from either ASTM grade water or natural waters buffered with 0.1M sodium bicarbonate at the desired pH condition. Experiments took place in 20 mL vials open to the atmosphere with continuous stirring. Aliquots of the resulting mixture were removed periodically and quenched by acidification. Samples were immediately measured for hydrogen peroxide and GA (below).

4.3.3 HYDROGEN PEROXIDE BY FLUORESCENCE

Hydrogen peroxide was measured indirectly by the Amplex Red™ technique,[47-49] which is based on conversion of the Amplex Red™ reagent to resorufin by HRP. Amplex Red™ indicator solution (ARI), 100 mM, was made fresh in 50 mM sodium phosphate buffer (pH = 7.5) before each use. Hydrogen peroxide samples were transferred into pre-charged vials containing 0.01 M DTPA in 50 mM phosphate buffer adjusted to a pH of 7.5. 200 μL of the resulting solution was mixed with 100 μL of ARI solution in a 96-well plate. After a 30-minute incubation period fluorescence was measured with a SpectraMax M5 microplate reader (Molecular Devices Corporation). Stock solutions of hydrogen peroxide were standardized by direct absorbance of H_2O_2 at 254 nm and calibration curves generated daily. The concentration of Amplex Red™ was at least 10 times higher than GA during analysis in the 96-well plate to minimize the possibility of artifacts from competitive GA oxidation. Net oxidation of GA at the conditions required for the Amplex Red™ technique could have contributed a maximum of 5% positive systematic error to the maximum measured hydrogen peroxide concentration under the given pH condition (Figure D.4).

4.3.4 GALLIC ACID BY UPLC-ESI-MS/MS

The concentration of GA was monitored with a Waters (Milford, MA, USA) Acquity ultra performance liquid chromatography (UPLC) coupled with a Xevo triple quadrupole mass spectrometer (MS/MS) equipped with an electrospray ionization source (ESI). Separations were performed on a BEH C18 (2.1x50 mm) 1.7 µm particle size column (Waters). The mobile phase was initially 95%/5% aqueous (A)/acetonitrile (B), with both phases made up to 0.1% formic acid (v/v) with the following gradient program: at 0.8 mins, 80% A, at 1 min 10% for 0.05 mins, 1.5 mins back to 95% A. GA eluted at 0.49 min at a flow rate of 0.6 mL/min (Figure D.1). Full scan spectra of standard solutions were acquired for qualification of GA (Figure D.2). Multiple reaction monitoring (MRM) was used to quantify GA using the transition of m/z = 169 to m/z = 125, corresponding to the loss of the carboxylic acid group in the negative ionization mode. Source parameters for this transition were optimized manually (Table D.1). Data was processed using MassLynx software (V.4.1). A calibration curve was done with GA standard solutions made up in aqueous mobile phase to prevent oxidation artifacts.

4.3.5 NATURAL WATER SAMPLES

Water samples were obtained from four locations within South Carolina (Figure D.3). Sample locations included a lake site; (Site 1, Low Falls Landing in Lake Marion, 33.632256, -80.543134), a forested slough on the Congaree River (Site 2, Old Bates River, 33.785559, -80.635637), a forested secondary creek exiting the Congaree National Park (Site 3, Cedar Creek, 33.818651, -80.787909), and an urban boat landing on the Congaree River (Site 4, Rosewood Landing, 33.964918, -81.036215). Filtered samples were passed

through a 0.45-micron filter and buffered to pH 8.3 in 0.1M sodium bicarbonate. Buffered natural water blank experiments had no observable hydrogen peroxide formation (Figure D.4).

The total dissolved organic carbon (DOC) content in each sample was determined using a TOC-L Total Organic Carbon Analyzer (Shimadzu Corporation, Table 4.1). Samples were filtered using a 0.2-micron pore size filter and acidified with HCl. Potassium hydrogen phthalate was used for calibration standards.

4.3.6 METAL ANALYSIS

Inductively coupled plasma mass spectrometry (ICP-MS) was used to analyze metals in the natural water samples using a modified EPA method 200.8. Each natural water was also filtered and analyzed to resolve between total and dissolved metal sources. Particulate metals were determined by subtracting dissolved from total. Non-redox active and trace metals and elements are reported in Table C.2. Redox active metals (iron, copper, manganese, and nickel; dissolved and particulate) are shown in Table 4.1.

4.4 RESULTS AND DISCUSSION

4.4.1 GALLIC ACID AS AN ROS SOURCE

This work was based on the application of GA autoxidation as a consistent source of superoxide in the absence of applied photons or transition metals. GA is tetraprotic with two pKas in the environmentally relevant range (in bold): **4.8, 8.8**, 11.0, and 13.0. Its oxidation was initiated by the direct reaction of the GA dianion with dioxygen to yield superoxide and a suite of unstable GA-derived radical intermediates.[50] GA oxidation,

defined as the net oxidation of GA and its kinetically unstable products, was spontaneous in air saturated solutions under all conditions tested (Figure 4.2). The kinetics of GA oxidation were complex and often displayed an induction period, consistent with autoxidation (Figure D.4).[51] The induction period was defined in this work as the period post-GA addition corresponding to an experimentally observed loss rate statistically indistinguishable from zero. All experimental rates of GA oxidation were obtained after the induction period. GA oxidation was zero order in GA under all conditions. Rates were pH sensitive (Figure 4.2) consistent with the proposed initiation step in which dioxygen has been proposed to react directly with the dianion (Figure 4.3, Equation 4.1). [50]

A series of reactions was proposed consistent with the observed results (Figure 4.3), based on the observation that superoxide was the chain carrier. The reactions presented in Figure 4.3 are simplified proposed steps for possible reactions. Superoxide was also proposed as the primary source of hydrogen peroxide, either through its direct reduction by an organic substrate or through dismutation. Superoxide was generated by the direct one electron reduction of oxygen by GA (Equation 4.1) and the reaction of GA oxidation products (GA_{ox}) with oxygen (Equation 4.4). Superoxide acted as the chain carrier by reacting with either GA, GA derived oxidation products, or with itself (Equations 4.3, 4.5, and 4.11, respectively). Hydrogen peroxide generated in the system can also react with either GA or GA derived oxidation products (Equations 4.6 and 4.7). The involvement of superoxide and its conjugate acid, the hydroperoxyl radical as chain carriers and sources of hydrogen peroxide was the chief justification for the use of this system as a probe for the ability of NOM to produce ROS during autoxidation. We

proposed that NOM can react with either GA, superoxide, or hydrogen peroxide, to be oxidized and produce ROS, such as hydrogen peroxide and hydroxyl radical (Equations 4.8, 4.9, and 4.10).

Hydrogen peroxide was generated during GA oxidation at all pHs tested (pH 5-10), as indicated by the Amplex Red method (Figure D.5). Hydrogen peroxide formation was constant after an initiation period (Figure 4.4). The post-induction experimental rate varied with pH in a manner consistent with the rate of GA oxidation (Figure 4.4). The mean ratio of the rates of GA oxidation over hydrogen peroxide formation was constant over the studied pH range, with a value of 1.51 and an RSD of 15.5% (Figure D.6). This ratio indicated a constancy in mechanism for the rate determining step of the process. The induction period between GA loss and hydrogen peroxide formation was consistent with an extensive autoxidation mechanism that involved the extraction of multiple reductive equivalents per mole of GA (Figure D.7). The constancy of hydrogen peroxide produced per mole of GA in the system was probed by monitoring the ratio of the instantaneous concentration of hydrogen peroxide relative to the initial concentration of GA for a range of GA concentrations (Figure 4.5). The development of hydrogen peroxide over time varied linearly with the amount of GA in the sample under all conditions tested, consistent with the hypothesis that hydrogen peroxide formation was independent of the initial concentration of GA.

The source of hydrogen peroxide was tested by the addition of superoxide dismutase (SOD) to the system (Figure 4.6). SOD addition at t=0 caused the net rate of GA oxidation to fall by a factor of 12**,** from 17.2 ($\pm$ 5.5) μM/hr to 1.4 ($\pm$ 0.7) μM/hr, indicating

that GA oxidation was dominated by the chain reaction with superoxide as the chief carrier. The possible reaction of GA with hydrogen peroxide (Equation 4.6, Figure 4.3) was shown to be insignificant on the timescale of the experiment (Figure D.8), therefore oxidation of GA can be achieved by either the reaction of GA with dioxygen (Equation 4.1, Figure 4.3) or by superoxide (Equation 4.3, Figure 4.3). SOD was added to resolve between these two routes, by removing superoxide and converting it to hydrogen peroxide and oxygen. Accordingly, in the presence of SOD, GA oxidation was due solely to the relatively slow initiation reaction of GA oxidation by dioxygen (Equation 4.1, Figure 4.3). Since the rate of GA oxidation decreased in the presence of SOD, it was assumed that the chief chain propagation step for the oxidation of GA was oxidation by superoxide, Equation 4.3. Although SOD added dissolved oxygen back to the system, and oxygen was an important initiator, the amount added was trivial relative to dissolved oxygen present from constant aeration (approximately 250 μM). The ratio of these rates indicated only 8% of the hydrogen peroxide produced was a consequence of dismutation, where 92% of the production was a result of the chain reaction; i.e. chain propagation was approximately 12 repeat reactions. In the absence of added photons and transition metals, GA was able to produce ROS, thus acting as a source of superoxide and hydrogen peroxide.

4.4.2 GA OXIDATION IN NATURAL WATERS

Natural water samples, collected from four different sites in South Carolina (vide supra), contained 7.31-13.06 ppm NOM (as DOC). Total Fe in the natural waters ranged from 0.12-5.51 ppm). Hydrogen peroxide, spiked into unfiltered and filter-sterilized

natural waters as a control (buffered to pH 8.3), decreased with less than 10% decay rate over 240 min in all samples (Figure D.9).

The role of photochemically derived sources of ROS in surface waters has been previously explored.[3-10] Work presented here focused on characterizing the interaction of natural waters with ROS from non-photochemical sources, particularly those derived from the autoxidation of phenols. The experimental approach was based on incorporating the constituents of natural waters as factors in the GA autoxidation process, rather than apply GA as a selective and innocent probe for ROS.[52, 53] This procedure provided insight on the capability of natural waters to support autoxidation, similar to previous work exploring the process by which ozone-initiated autoxidation of NOM affected its molecular weight.[54, 55] GA oxidation was carried out in unfiltered natural water samples, buffered to pH 8.3 and the rate of GA autoxidation was observed along with concurrent hydrogen peroxide formation (Figure 4.7). GA oxidation was also carried out in filtered natural water samples (Figure D.10), under the same conditions. No significant difference was observed between the filtered and unfiltered samples under the tested conditions. In these conditions, GA oxidation was rapid relative to laboratory water experiments with an approximate increase in the rate of oxidation by a factor of 4 averaged for all natural waters relative to laboratory water and was essentially complete within 30 minutes of initiation. The rate of hydrogen peroxide production also increased by an approximate factor of 11 in natural waters relative to laboratory water experiments. Neither the experimental rate of GA oxidation, rate of hydrogen peroxide formation, or maximum

hydrogen peroxide level linearly correlated to the NOM or to particulate or dissolved metals (all $r2 \leq 0.65$).

The experiments were repeated, under the same pH conditions, in the presence of 2 mM DTPA to remove transition metals as a factor (Figure 4.8). In the absence of transition metals, the rate of GA oxidation and subsequent ROS formation were within the 95% CI to those seen in laboratory water, indicating that transition metals were clearly essential for achieving the maximum rate of ROS formation. GA was also oxidized, and hydrogen peroxide was measured in the absence of added NOM but in the presence of Fe(III) at concentrations that approximated the highest iron loadings (Figure D.11). Added Fe(III) suppressed the formation of hydrogen peroxide essentially to the zero, presumably by acting as a hydrogen peroxide scavenger. In natural waters, GA oxidation conditions that generated ROS at the highest rate contained transition metals and NOM; this indicated synergism between NOM and transition metals (Figure 4.8) during hydrogen peroxide production from GA oxidation (i.e. both were required to obtain the highest possible extent and rate of oxidation). Direct GA oxidation by dioxygen was minimal relative to the oxidation of NOM and GA by superoxide (Figure 4.6). The added Fe(III) experiment was unfortunately not exclusive, particularly if the rate of reaction of Fe(III) with superoxide ($k = 1.5x108\ M^{-1}\ s^{-1}$) was conditionally competitive with the rate of Fe(III) sequestration (implying precipitation) by phosphate. In addition, neither DTPA nor phosphate were kinetically selective for Fe(III) alone, and other redox active transition metals such as Cu could have played an important role in the outcome. Indeed, the failure

of NOM and Fe(III) to perfectly model the natural water suggested the system must be more complex.

4.4.3 HYDROGEN PEROXIDE PRODUCTION RATES

A goal of the work presented here was the development of a bimolecular rate constant for the reaction of superoxide with NOM, analogous to the procedures applied for the reaction of NOM with HO.[56, 57] The role of superoxide as an essential chain carrier in this system imposed limitations on which strategy to use to solve for this rate constant. Free radical oxidations in environmental systems are often modeled as a series of summed first order processes; however, *all* superoxide-dependent reactions are barred from this by the constant role of superoxide disproportionation as a kinetically significant sink for superoxide and source for hydrogen peroxide (i.e. the analytically required inclusion of a parallel second order process). Given that these two species were the essential chain carrier for the measured reaction and measured product it would have been inappropriate to make the first order simplification in this case. The calculation for the bimolecular rate constant for the reaction of superoxide with NOM follows.

The rate of hydrogen peroxide generation during GA oxidation in 18 MΩ water was developed as a comparative index for measuring the ROS contribution from the autoxidation of GA in the presence of NOM, and NOM's potential to act as a source of ROS under these conditions.

In laboratory water, the rate of hydrogen peroxide production $\left(\frac{d\mathrm{H_2O_2}}{d\mathrm{t}}_{LW}\right)$ was expressed (based on reactions in Figure 4.3) as:

$$[4.12] \qquad \frac{d\mathrm{H_2O_2}}{d\mathrm{t}}_{LW} = \mathrm{k_3[GA][O_2^{-\cdot}]} + \mathrm{k_5[GA_{ox}][O_2^{-\cdot}]} - \mathrm{k_6[GA][H_2O_2]} - \mathrm{k_7[GA_{ox}][H_2O_2]} + \mathrm{k_{11}[O_2^{-\cdot}]^2}$$

The consumption of hydrogen peroxide by GA and its oxidation species (Equations 6 and 7) was not significantly affected by exogenous hydrogen peroxide spiked into the reaction at relevant concentrations (Figure D.8). Addition of 5 μM hydrogen peroxide did not significantly change the slope of hydrogen peroxide production over the timescale of the experiment. This suggests hydrogen peroxide is formed as a stable or metastable termination step, therefore the contribution from Equations 4.6 and 4.7 were minimal under the given conditions. The equation then simplified to:

$$[4.13] \qquad \frac{d\mathrm{H_2O_2}}{d\mathrm{t}}_{LW} = \mathrm{k_3[O_2^{-\cdot}][GA]} + \mathrm{k_5[O_2^{-\cdot}][GA_{ox}]} + \mathrm{k_{11}[O_2^{-\cdot}]^2}$$

The rate of hydrogen peroxide production during the GA autoxidation carried out in natural water $\left(\frac{d\mathrm{H_2O_2}}{d\mathrm{t}}_{NW}\right)$ experiments included a summative term "NOM" to describe the effects of NOM (unfiltered), so was expressed as:

$$[4.14] \qquad \frac{d\mathrm{H_2O_2}}{d\mathrm{t}}_{NW} = \mathrm{k_3[GA][O_2^{-\cdot}]} + \mathrm{k_5[GA_{ox}][O_2^{-\cdot}]} + \mathrm{k_{11}[O_2^{-\cdot}]^2} + \mathrm{k_9[O_2^{-\cdot}][NOM]} - \mathrm{k_{10}}[H_2O_2][\mathrm{NOM}]$$

The reaction between hydrogen peroxide and NOM was interrogated by spiking in hydrogen peroxide into the natural waters in the absence of GA. Hydrogen peroxide in the resulting solution was stable for the measured period (6 hours) in unfiltered and filtered waters (Figure D.9). Therefore, the contribution from Equation 4.10 was minimal under our conditions allowing 4.14 to be simplified to:

$$\left(\frac{d\mathrm{H_2O_2}}{d\mathrm{t}}\right)_{NW} = \mathrm{k_3[GA][O_2^{-\cdot}]} + \mathrm{k_5[GA_{ox}][O_2^{-\cdot}]} + \mathrm{k_{11}[O_2^{-\cdot}]^2} + \mathrm{k_9[O_2^{-\cdot}][NOM]} \quad [4.15]$$

The hydrogen peroxide production from GA oxidation was either expressed as Equation 4.13 (in laboratory water) or Equation 4.15 (in natural water) and they differ by the summative "NOM" term. Under both conditions the initiation of these reactions is controlled by the addition of GA into the reaction, Equations 4.13 and 4.15 were combined and rearranged to solve for the value of k_9, an experimentally derived bimolecular rate constant for the reaction between superoxide and NOM (expressing NOM as ppm C):

$$\mathrm{k_9} = \frac{\left(\left(\frac{d\mathrm{H_2O_2}}{d\mathrm{t}}\right)_{NW} - \left(\frac{d\mathrm{H_2O_2}}{d\mathrm{t}}\right)_{LW}\right)}{\mathrm{[O_2^{-\cdot}][NOM]}} \quad [4.16]$$

The rate of hydrogen peroxide production in laboratory experiments was 11.1 $\pm$ 3.6 μM/hr (n=7) and the average rate of hydrogen peroxide production in the four natural water experiments was 55.1 $\pm$ 9.4 μM/hr (n=4). The concentration of superoxide (2.11 μM) was estimated experimentally from the rate of hydrogen peroxide formation in the presence of SOD, with the assumption that dismutation only accounted for a fraction of the fate of superoxide (Scheme D.1).[58] A second order mass dependent rate constant (Equation 4.16) for the reaction of superoxide with NOM was determined from the steady state concentration of superoxide and the experimental rates of hydrogen peroxide production for laboratory and natural water experiments using the averaged NOM concentration in the natural water experiments as 9.53 $\pm$ 2.5 ppm.

$$[4.17] \qquad k_9 = \frac{(55.1\ \mu M/hr - 11.1\ \mu M/hr)}{[2.11\ \mu M][9.53\ ppm]} = 2.18\ ppm^{-1}\ hr^{-1}$$

The numerator in Equation 4.17 was positive under all conditions studied, an indication of the positive contribution of NOM to formation of superoxide in the system. Although superoxide has been shown to be an effective nucleophile in aprotic solvents[59] in aqueous solution its probable reactivity with NOM is expected to be dominated by one-electron oxidation or direct addition, with both leading to the formation of organoperoxides. Two possible termination steps that both produce hydrogen peroxide are dismutation of superoxide or peroxidation of NOM by superoxide. Under conditions when peroxidation 1 of NOM dominated the fate of superoxide, hydrogen peroxide continued to evolve at a rate that was approximately a factor of 11 times faster than predicted based on dismutation alone. Therefore, the experimental rate constant for hydrogen peroxide formation from NOM was used to solve for conditions where superoxide was more likely to terminate with the stoichiometric production of hydrogen peroxide than by dismutation or progress through peroxidation to generate hydrogen peroxide at higher than predicted rates. Based on the measured rate constant, peroxidation dominated as the source of hydrogen peroxide at all conditions where the fractional fate of superoxide was equal or greater to 50%, as in:

$$[4.18] \qquad \text{Fraction of } O_2^{-\cdot} \text{ reacting with NOM} = \frac{k_9[O_2^{-\cdot}][NOM]}{k_9[O_2^{-\cdot}][NOM] + k_{11}[O_2^{-\cdot}]^2}$$

The dismutation of superoxide was pH dependent with the net rate of dismutation increasing from basic pH to a maximum at 4.8. The rate constant developed in Equation 4.17 was used to estimate the fraction of superoxide reacting with NOM over the NOM

concentration range of 0 – 15 ppm at pHs of 6.2, 7.2, 8.2. (Figure 4.9). The model suggested that at basic pHs autoxidation of NOM was a significant if not dominant source for total hydrogen peroxide in natural waters, barring enzymatic loss of superoxide.

4.5 CONCLUSIONS

ROS are critically important abiotic links connecting reduced carbon and carbon dioxide in the carbon cycle. They are significant because they directly mineralize recalcitrant carbon and can structurally modify organic carbon to make it more bioavailable. The autoxidation of organic carbon is an intrinsically bimolecular process[60-63] that is often used to describe the chemistry of aqueous organoperoxyl radicals. Therefore, autoxidation can be expected to be a particularly significant source of ROS in waters with high concentrations of DOC; including runoff from melting permafrost,[14, 15, 64, 65] pore waters in episodically inundated soils,[11-13] hydrothermal vent plumes,[66-69] etc. The results discussed illustrate the need to examine ROS in natural waters in the context of initiation, propagation, and termination. Currently the bulk of studies that discuss the phenomena in the context of initiation, either photochemical or geochemical, and the role of the nature of NOM with respect to sources or molecular structure and its ability to affect autoxidative ROS yields is unknown. The possible effects on biota in surface waters are difficult to assess in a well-mixed water column, like in the sample sites at this study. It is also appropriate to point out a possible marine analogy, where several investigators have recently documented a deep water (depth > 1 km) superoxide maxima associated with microbial superoxide sources.[3, 16, 17, 19] Indirect effects on biota can also be seen in work examining the natural distribution of antioxidant enzymes in the water

column. This work showed that metals were essential participants in this process but under the natural water conditions interrogated the native abundance of total metals saturated the system. This indicated a critical reaction between redox metals, organic oxidation intermediates, and superoxide, with metals far more in excess than the latter two in the studied system. These results imply that in environments with relatively low concentrations of dissolved metals like the Southern Ocean autoxidation of NOM may not be as significant a source of ROS as could be expected in fresh waters.

4.6 REFERENCES

1. Luther, G. W., The role of one- and two-electron transfer reactions in forming thermodynamically unstable intermediates as barriers in multi-electron redox reactions. *Aquat. Geochem.* **2010,** *16*, (3), 395-420.

2. Bertini, I.; Gray, H. B.; Lippard, S. J.; Valentine, J. S., Bioinorganic chemistry. In *Bioinorganic chemistry*, University Science Books: Mill Valley, CA, 1994; pp 253-313.

3. Rose, A. L.; Godrant, A.; Furnas, M.; Waite, T. D., Dynamics of nonphotochemical superoxide production and decay in the great barrier reef lagoon. *Limnol. Oceanogr.* **2010,** *55*, (4), 1521-1536.

4. Poskrebyshev, G. A.; Neta, P.; Huie, R. E., Temperature dependence of the acid dissociation constant of the hydroxyl radical. *Journal of Physical Chemistry A* **2002,** *106*, (47), 11488-11491.

5. Goldstein, S.; Rabani, J., Mechanism of nitrite formation by nitrate photolysis in aqueous solutions: The role of peroxynitrite, nitrogen dioxide, and hydroxyl radical. *Journal of the American Chemical Society* **2007,** *129*, (34), 10597-10601.

6. Buxton, G. V.; Greenstock, C. L.; Helman, W. P.; Ross, A. B., Critical-review of rate constants for reactions of hydrated electrons, hydrogen-atoms and hydroxyl radicals (.Oh/.O-) in aqueous-solution. *Journal of Physical and Chemical Reference Data* **1988,** *17*, (2), 513-886.

7. Rose, A. L., The influence of reactive oxygen species on local redox conditions in oxygenated natural waters. *Front. Earth Sci.* **2016,** *4*, 11.

8. Fujii, M.; Rose, A. L.; Waite, T. D.; Omura, T., Oxygen and superoxide-mediated redox kinetics of iron complexed by humic substances in coastal seawater. *Environ. Sci. Technol.* **2010,** *44*, (24), 9337-9342.

9. Garg, S.; Rose, A. L.; Waite, T. D., Photochemical production of superoxide and hydrogen peroxide from natural organic matter. *Geochim. Cosmochim. Acta* **2011,** *75*, (15), 4310-4320.

10. Cooper, W. J.; Zika, R. G.; Petasne, R. G.; Plane, J. M. C., Photochemical formation of h2o2 in natural-waters exposed to sunlight. *Environ. Sci. Technol.* **1988,** *22*, (10), 1156-1160.

11. Dias, D. M. C.; Copeland, J. M.; Milliken, C. L.; Shi, X. M.; Ferry, J. L.; Shaw, T. J., Production of reactive oxygen species in the rhizosphere of a spartina-dominated salt marsh systems. *Aquat. Geochem.* **2016,** *22*, (5-6), 573-591.

12. Murphy, S. A.; Meng, S.; Solomon, B. M.; Dias, D. M. C.; Shaw, T. J.; Ferry, J. L., Hydrous ferric oxides in sediment catalyze formation of reactive oxygen species during sulfide oxidation. *Frontiers in Marine Science* **2016,** *3*, (227).

13. Murphy, S. A.; Solomon, B. M.; Meng, S. N.; Copeland, J. M.; Shaw, T. J.; Ferry, J. L., Geochemical production of reactive oxygen species from biogeochemically reduced fe. *Environ. Sci. Technol.* **2014,** *48*, (7), 3815-3821.

14. Page, S. E.; Kling, G. W.; Sander, M.; Harrold, K. H.; Logan, J. R.; McNeill, K.; Cory, R. M., Dark formation of hydroxyl radical in arctic soil and surface waters. *Environ. Sci. Technol.* **2013,** *47*, (22), 12860-12867.

15. Trusiak, A.; Treibergs, L. A.; Kling, G. W.; Cory, R. M., The role of iron and reactive oxygen species in the production of co_2 in arctic soil waters. *Geochim. Cosmochim. Acta* **2018,** *224*, 80-95.

16. Zhang, T.; Hansel, C. M.; Voelker, B. M.; Lamborg, C. H., Extensive dark biological production of reactive oxygen species in brackish and freshwater ponds. *Environ. Sci. Technol.* **2016,** *50*, (6), 2983-2993.

17. Marsico, R. M.; Schneider, R. J.; Voelker, B. M.; Zhang, T.; Diaz, J. M.; Hansel, C. M.; Ushijima, S., Spatial and temporal variability of widespread dark production and decay of hydrogen peroxide in freshwater. *Aquat. Sci.* **2015,** *77*, (4), 523-533.

18. Dixon, T. C.; Vermilyea, A. W.; Scott, D. T.; Voelker, B. M., Hydrogen peroxide dynamics in an agricultural headwater stream: Evidence for significant nonphotochemical production. *Limnol. Oceanogr.* **2013,** *58*, (6), 2133-2144.

19. Vermilyea, A. W.; Hansard, S. P.; Voelker, B. M., Dark production of hydrogen peroxide in the gulf of alaska. *Limnol. Oceanogr.* **2010,** *55*, (2), 580-588.

20. von Sonntag, C.; Schuchmann, H. P., The elucidation of peroxyl radical reactions in aqueous-solution with the help of radiation-chemical methods. *Angew. Chem.-Int. Edit. Engl.* **1991,** *30*, (10), 1229-1253.

21. Tamba, M.; Torreggiani, A.; Tubertini, O., Thiyl-radicals and thiyl-peroxyl radicals produced from the irradiation of antioxidant thiol compounds. *Radiation Physics and Chemistry* **1995,** *46*, (4-6), 569-574.

22. Khaikin, G. I.; Alfassi, Z. B.; Huie, R. E.; Neta, P., Oxidation of ferrous and ferrocyanide ions by peroxyl radicals. *Journal of Physical Chemistry* **1996,** *100*, (17), 7072-7077.

23. Goldstein, S.; Lind, J.; Merenyi, G., Reaction of organic peroxyl radicals with (no2)-n-center dot and (no)-n-center dot in aqueous solution: Intermediacy of organic peroxynitrate and peroxynitrite species. *Journal of Physical Chemistry A* **2004,** *108*, (10), 1719-1725.

24. Flyunt, R.; Makogon, O.; Naumov, S.; Schoneich, C.; Asmus, K. D., Reactions of halogenated hydroperoxides and peroxyl and alkoxyl radicals from isoflurane in aqueous solution. *Journal of Physical Chemistry A* **2007,** *111*, (45), 11618-11625.

25. von Sonntag, C.; Schuchmann, H.-P., Peroxyl radicals in aqueous solution. In *Peroxyl radicals*, Alfassi, Z. B., Ed. J. Wiley & Sons Ltd: New York, 1997.

26. Pratt, D. A.; Tallman, K. A.; Porter, N. A., Free radical oxidation of polyunsaturated lipids: New mechanistic insights and the development of peroxyl radical clocks. *Accounts Chem. Res.* **2011,** *44*, (6), 458-467.

27. von Sonntag, C.; Dowideit, P.; Fang, X. W.; Mertens, R.; Pan, X. M.; Schuchmann, M. N.; Schuchmann, H. P., The fate of peroxyl radicals in aqueous solution. *Water Science and Technology* **1997,** *35*, (4), 9-15.

28. Bi, R.; Lu, Q.; Yu, W. M.; Yuan, Y.; Zhou, S. G., Electron transfer capacity of soil dissolved organic matter and its potential impact on soil respiration. *J. Soils Sediments* **2013,** *13*, (9), 1553-1560.

29. Qin, W. X.; Wang, Y. J.; Fang, G. D.; Wu, T. L.; Liu, C.; Zhou, D. M., Evidence for the generation of reactive oxygen species from hydroquinone and benzoquinone: Roles in arsenite oxidation. *Chemosphere* **2016,** *150*, 71-78.

30. Yuan, X.; Davis, J. A.; Nico, P. S., Iron-mediated oxidation of methoxyhydroquinone under dark conditions: Kinetic and mechanistic insights. *Environ. Sci. Technol.* **2016,** *50*, (4), 1731-1740.

31. Vonsonntag, C.; Schuchmann, H. P., The elucidation of peroxyl radical reactions in aqueous-solution with the help of radiation-chemical methods. *Angewandte Chemie-International Edition in English* **1991,** *30*, (10), 1229-1253.

32. Gulkowska, A.; Krauss, M.; Rentsch, D.; Hollender, J., Reactions of a sulfonamide antimicrobial with model humic constituents: Assessing pathways and stability of covalent bonding. *Environ. Sci. Technol.* **2012,** *46*, (4), 2102-2111.

33. Tan, L.; Liang, B.; Fang, Z. Q.; Xie, Y. Y.; Tsang, E. P., Effect of humic acid and transition metal ions on the debromination of decabromodiphenyl by nano zero-valent iron: Kinetics and mechanisms. *J. Nanopart. Res.* **2014,** *16*, (12), 13.

34. Tobiszewski, M.; Namiesnik, J., Abiotic degradation of chlorinated ethanes and ethenes in water. *Environ. Sci. Pollut. Res.* **2012,** *19*, (6), 1994-2006.

35. Yu, Z. G.; Peiffer, S.; Gottlicher, J.; Knorr, K. H., Electron transfer budgets and kinetics of abiotic oxidation and incorporation of aqueous sulfide by dissolved organic matter. *Environ. Sci. Technol.* **2015,** *49*, (9), 5441-5449.

36. Zheng, W.; Liang, L. Y.; Gu, B. H., Mercury reduction and oxidation by reduced natural organic matter in anoxic environments. *Environ. Sci. Technol.* **2012,** *46*, (1), 292-299.

37. Krumina, L.; Lyngsie, G.; Tunlid, A.; Persson, P., Oxidation of a dimethoxyhydroquinone by ferrihydrite and goethite nanoparticles: Iron reduction versus surface catalysis. *Environ. Sci. Technol.* **2017,** *51*, (16), 9053-9061.

38. Scharko, N. K.; Martin, E. T.; Losovyj, Y.; Peters, D. G.; Raff, J. D., Evidence for quinone redox chemistry mediating daytime and nighttime no_2^- to-hono conversion on soil surfaces. *Environ. Sci. Technol.* **2017,** *51*, (17), 9633-9643.

39. Taran, O., Electron transfer between electrically conductive minerals and quinones. *Front. Chem.* **2017,** *5*, 13.

40. Sun, Y. F.; Pignatello, J. J., Activation of hydrogen-peroxide by iron(iii) chelates for abiotic degradation of herbicides and insecticides in water. *Journal of Agricultural and Food Chemistry* **1993,** *41*, (2), 308-312.

41. Danilewicz, J. C.; Wallbridge, P. J., Further studies on the mechanism of interaction of polyphenols, oxygen, and sulfite in wine. *Am. J. Enol. Vitic.* **2010,** *61*, (2), 166-175.

42. Kozmer, Z.; Arany, E.; Alapi, T.; Rozsa, G.; Hernadi, K.; Dombi, A., New insights regarding the impact of radical transfer and scavenger materials on the (oh)-o-center dot-initiated phototransformation of phenol. *J. Photochem. Photobiol. A-Chem.* **2016,** *314*, 125-132.

43. Leitner, N. K. V.; Dore, M., Hydroxyl radical induced decomposition of aliphatic acids in oxygenated and deoxygenated aqueous solutions. *J. Photochem. Photobiol. A-Chem.* **1996,** *99*, (2-3), 137-143.

44. Danilewicz, J. C., Mechanism of autoxidation of polyphenols and participation of sulfite in wine: Key role of iron. *Am. J. Enol. Vitic.* **2011,** *62*, (3), 319-328.

45. Lebeuf, R.; Zhu, Y.; Nardello-Rataj, V.; Lallier, J. P.; Aubry, J. M., Natural polyphenols as safe alternatives to hydroquinone for the organocatalyzed reduction of dioxygen dissolved in water by diethylhydroxylamine (deha). *Green Chem.* **2012,** *14*, (3), 825-831.

46. USGS, Usgs national water quality assessment data warehouse. In 2007.

47. Zhao, B. Z.; Summers, F. A.; Mason, R. P., Photooxidation of amplex red to resorufin: Implications of exposing the amplex red assay to light. *Free Radical Biology and Medicine* **2012,** *53*, (5), 1080-1087.

48. Zhou, M. J.; Diwu, Z. J.; PanchukVoloshina, N.; Haugland, R. P., A stable nonfluorescent derivative of resorufin for the fluorometric determination of trace hydrogen peroxide: Applications in detecting the activity of phagocyte nadph oxidase and other oxidases. *Analytical Biochemistry* **1997,** *253*, (2), 162-168.

49. Burns, J. M.; Cooper, W. J.; Ferry, J. L.; King, D. W.; DiMento, B. P.; McNeill, K.; Miller, C. J.; Miller, W. L.; Peake, B. M.; Rusak, S. A.; Rose, A. L.; Waite, T. D., Methods for reactive oxygen species (ros) detection in aqueous environments. *Aquat. Sci.* **2012,** *74*, (4), 683-734.

50. Milenkovic, D.; Dorovic, J.; Petrovic, V.; Avdovic, E.; Markovic, Z., Hydrogen atom transfer versus proton coupled electron transfer mechanism of gallic acid with different peroxy radicals. *Reaction Kinetics Mechanisms and Catalysis* **2018,** *123*, (1), 215-230.

51. Misra, H. P., Generation of superoxide free radical during the autoxidation of thiols *The Journal of Biological Chemistry* **1973,** *249*, (7), 2151-2155.

52. Lindsey, M. E.; Tarr, M. A., Quantitation of hydroxyl radical during fenton oxidation following a single addition of iron and peroxide. *Chemosphere* **2000,** *41*, (3), 409-417.

53. Yang, M.; Jonsson, M., Evaluation of the o2 and ph effects on probes for surface bound hydroxyl radicals. *Journal of Physical chemistry C* **2014,** *118*, (15), 7971-7979.

54. Yu, W.; Zhang, D.; Graham, N. J. D., Membrane fouling by extracellular polymeric substances after ozone pre-treatment: Variation of nano-particles size. *Water Research* **2017,** *120*, 146-155.

55. Jekel, M., Flocculation effects of ozone. *Ozone Science and Engineering* **1994,** *16*, (1), 55-66.

56. Brezonik, P. L.; Fulkerson-Brekken, J., Nitrate-induced photolysis in natural waters: Controls on concentrations of hydroxyl radical photo-intermediates by natural scavenging agents. *Environ. Sci. Technol.* **1998,** *32*, (19), 3004-3010.

57. Vaughan, P. P.; Blough, N. V., Photochemical formation of hydroxyl radical by constituents of natural waters. *Environ. Sci. Technol.* **1998,** *32*, (19), 2947-2953.

58. Rush, J. D.; Bielski, B. H. J., Pulse radiolytic studies of the reactions of ho_2/o_2^- with fe(ii)/fe(iii) ions - the reactivity of ho_2/o_2^- with ferric ions and its implication on the occurrence of the haber-weiss reaction. *Journal of Physical Chemistry* **1985,** *89*, (23), 5062-5066.

59. Hojo, M.; Sawyer, D. T., Oxygenation by superoxide ion of halogenofluorocarbons (freons and haloforms) in aprotic-solvents. *Chemical Research in Toxicology* **1989,** *2*, (3), 193-196.

60. Russell, G. A., The autoxidation of 2-nitropropane in basic solution. *Journal of the American Chemical Society* **1954,** *76*, (6), 1595-1600.

61. Russell, G. A., Fundamental processes of autoxidation. *Journal of Chemical Education* **1959,** *36*, (3), 111.

62. Russell, G. A., Deuterium-isotope effects in the autoxidation of aralkyl hydrocarbons - mechanism of the interaction of peroxy radicals. *Journal of the American Chemical Society* **1957,** *79*, (14), 3871-3877.

63. Russell, G. A., Mechanism of the termination step in autoxidation reactions. *Chemistry & Industry* **1956**, (49), 1483-1483.

64. Fimmen, R. L.; Cory, R. M.; Chin, Y. P.; Trouts, T. D.; McKnight, D. M., Probing the oxidation-reduction properties of terrestrially and microbially derived dissolved organic matter. *Geochim. Cosmochim. Acta* **2007,** *71*, (12), 3003-3015.

65. Belicka, L. L.; Harvey, H. R., The sequestration of terrestrial organic carbon in arctic ocean sediments: A comparison of methods and implications for regional carbon budgets. *Geochim. Cosmochim. Acta* **2009,** *73*, (20), 6231-6248.

66. Hoer, D. R.; Gibson, P. J.; Tommerdahl, J. P.; Lindquist, N. L.; Martens, C. S., Consumption of dissolved organic carbon by caribbean reef sponges. *Limnol. Oceanogr.* **2018,** *63*, (1), 337-351.

67. Ingram, W. C.; Meyers, S. R.; Martens, C. S., Chemostratigraphy of deep-sea quaternary sediments along the northern gulf of mexico slope: Quantifying the source and burial of sediments and organic carbon at mississippi canyon 118. *Mar. Pet. Geol.* **2013,** *46*, 190-200.

68. Johnston, S. G.; Keene, A. F.; Bush, R. T.; Burton, E. D.; Sullivan, L. A.; Smith, D.; McElnea, A. E.; Martens, M. A.; Wilbraharn, S., Contemporary pedogenesis of severely degraded tropical acid sulfate soils after introduction of regular tidal inundation. *Geoderma* **2009,** *149*, (3-4), 335-346.

69. Lapham, L. L.; Chanton, J. P.; Martens, C. S.; Higley, P. D.; Jannasch, H. W.; Woolsey, J. R., Measuring temporal variability in pore-fluid chemistry to assess gas hydrate stability: Development of a continuous pore-fluid array. *Environ. Sci. Technol.* **2008,** *42*, (19), 7368-7373.

Table 4.1 Redox active metal and dissolved organic carbon content in the water at the four sites.

Location		Redox active metal concentration (ppb)*				DOC (ppm) (standard deviation)
		^{55}Fe	^{59}Ni	^{63}Cu	^{55}Mn	
Low Falls Landing	Total	393	2.53	3.2	42	9.34 (0.16)
	Dissolved	221	1.39	0.97	1.3	
	Particulate	172	1.14	2.23	41	
Oxbow Lake	Total	5507	24	2.18	906	13.06 (0.05)
	Dissolved	2294	9.78	3.07	492	
	Particulate	3213	14.22	ND	414	
Cedar Creek	Total	1609	6.96	0.8	27	8.42 (0.03)
	Dissolved	748	3.55	1.33	14	
	Particulate	861	3.41	ND	13	
Rosewood Landing	Total	118	1.26	2.06	46	7.31 (0.08)
	Dissolved	60	1.46	1.6	22	
	Particulate	58	ND	0.46	24	

* Total and dissolved concentrations of the metals are represented by analysis of the unfiltered and filtered water samples, respectively, particulate concentrations were found by subtracting the dissolved from the total. ND means non-detect.

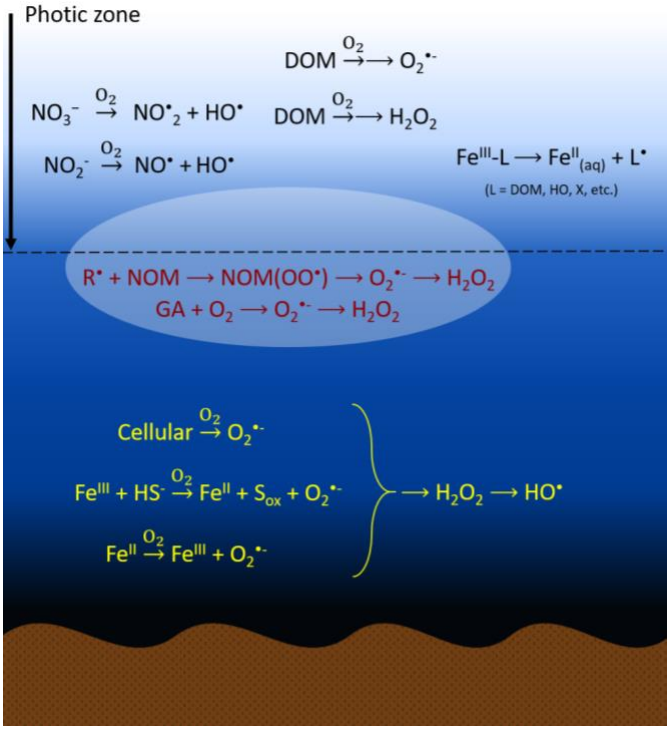

Figure 4.1 Sources of reactive oxygen species in the water column. Reactions below the dashed line represent reactions that are not restricted to the photic zone.

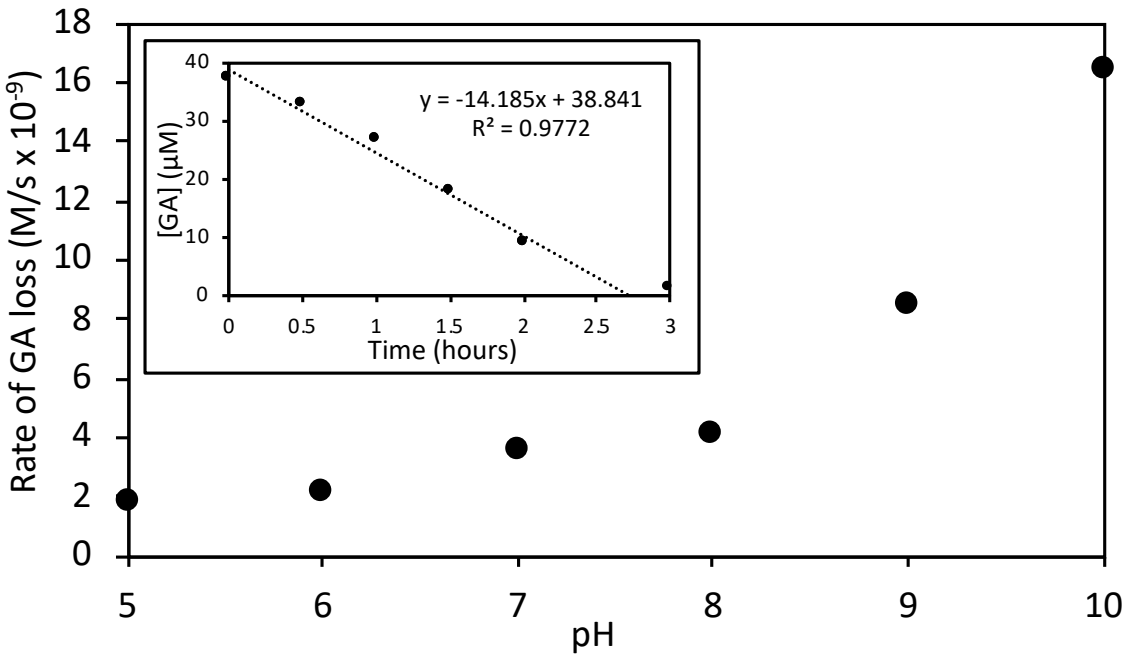

Figure 4.2 Rate of gallic acid loss over the pH range 5 – 10, Insert: gallic acid concentration over time at pH 7. The oxidation of gallic acid was zero order in GA in pH 7 buffered air-saturated solution (insert). The observed slopes varied with pH (5-10 shown), corresponding with oxidation of the GA^{2-} anion as the initiating step. All reactions took place in air-saturated 0.1 M sodium bicarbonate buffered solutions adjusted to the appropriate pH.

Initiation

[4.1] $\mathrm{GA} + \mathrm{O_2} \rightarrow \mathrm{GA_{ox}} + \mathrm{HO_2^{\cdot}}$ k_1

[4.2] $\mathrm{HO_2^{\cdot}} \rightleftharpoons \mathrm{H^+} + \mathrm{O_2^{-\cdot}}$ $pKa = 4.8$

Propagation

[4.3] $\mathrm{GA} + \mathrm{O_2^{-\cdot}} \rightarrow \mathrm{GA_{ox}} + \mathrm{H_2O_2}$ k_3

[4.4] $\mathrm{GA_{ox}} + \mathrm{O_2} \rightarrow \mathrm{GA_{ox}} + \mathrm{O_2^{-\cdot}}$ k_4

[4.5] $\mathrm{GA_{ox}} + \mathrm{O_2^{-\cdot}} \rightarrow \mathrm{GA_{ox}} + \mathrm{H_2O_2}$ k_5

[4.6] $\mathrm{GA} + \mathrm{H_2O_2} \rightarrow \mathrm{GA_{ox}} + \mathrm{ROS}$ k_6

[4.7] $\mathrm{GA_{ox}} + \mathrm{H_2O_2} \rightarrow \mathrm{GA_{ox}} + \mathrm{ROS}$ k_7

[4.8] $\mathrm{GA} + \mathrm{NOM} \rightarrow \mathrm{GA_{ox}} + \mathrm{NOM_{red}}$ k_8

[4.9] $\mathrm{O_2^{-\cdot}} + \mathrm{NOM} \rightarrow \mathrm{H_2O_2} + \mathrm{NOM_{ox}}$ k_9

[4.10] $\mathrm{H_2O_2} + \mathrm{NOM} \rightarrow \mathrm{NOM_{ox}} + \mathrm{ROS}$ k_{10}

Termination

[4.11] $\mathrm{O_2^{-\cdot}} + \mathrm{HO_2^{\cdot}} \rightarrow \mathrm{H_2O_2} + \mathrm{O_2}$ k_{11}

Figure 4.3 Proposed set of equations in the free radical chain reaction initiated by the direct oxidation of gallic acid by dioxygen. GAox refers to all gallic acid oxidation products in the generic sense. Here, superoxide acts as the chain carrier continuing the chain propagation generating more ROS and oxidized versions of gallic acid. Added NOM acts a propagation step for the reaction series and a termination step for superoxide. The chain is terminated upon dismutation of superoxide to produce hydrogen peroxide. The reactions provided are simplified proposed steps that include generalized reactants and products.

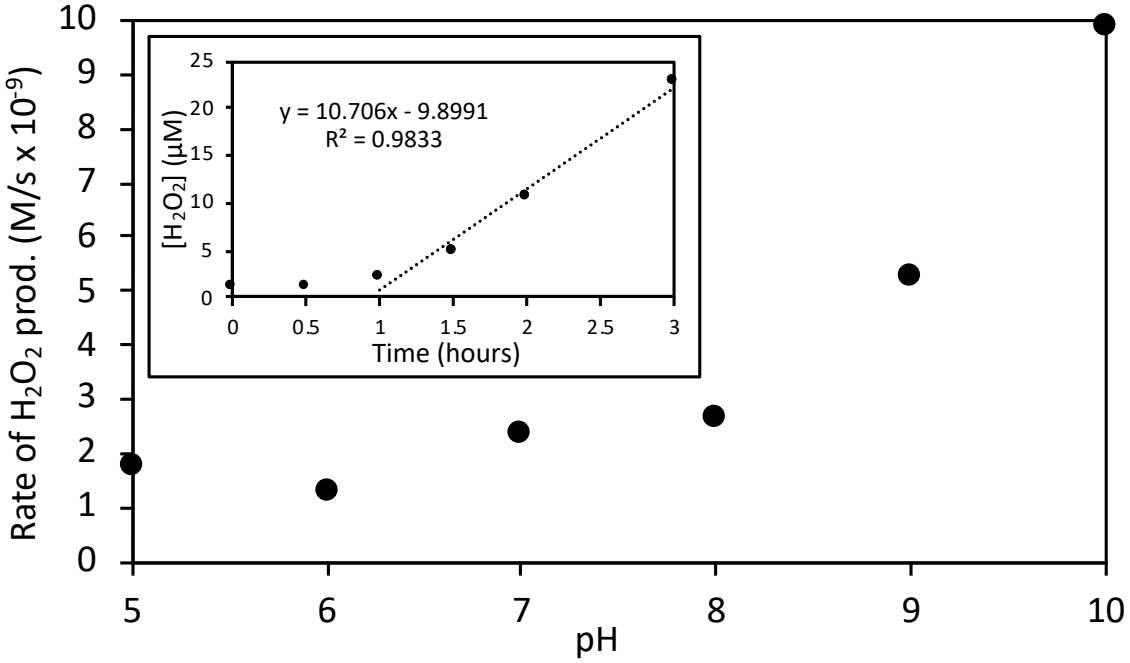

Figure 4.4 Rate of hydrogen peroxide production over the pH of range 5 – 10, insert: hydrogen peroxide concentration over time at pH 7. The production of hydrogen peroxide was zero order in hydrogen peroxide over the pH range (5-10). The rates of hydrogen peroxide production were calculated after the induction period at pH 7(insert). The increase in the slopes with increasing pH was consistent with the hypothesis that the mechanism to produce hydrogen peroxide was constant across the measured conditions. All reactions took place in air-saturated 0.1M sodium bicarbonate buffered solutions adjusted to the appropriate pH.

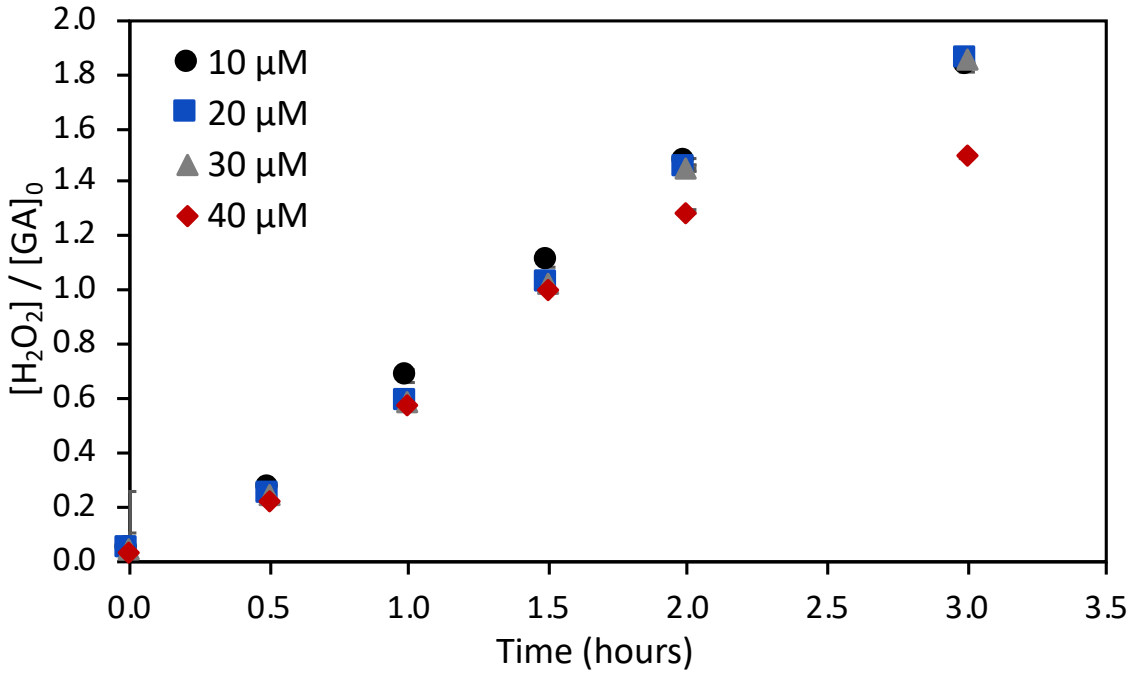

Figure 4.5 Ratio of the concentration of hydrogen peroxide to nominal gallic acid concentration over time. The concentration of hydrogen peroxide per GA nominal concentration was constant over various initial GA concentrations. This constancy indicates that the oxidation of GA and production of hydrogen peroxide was independent of GA nominal. All solutions were buffered to pH 8.3 in 0.1M sodium bicarbonate, GA aliquots were spiked in from a freshly prepared stock solution.

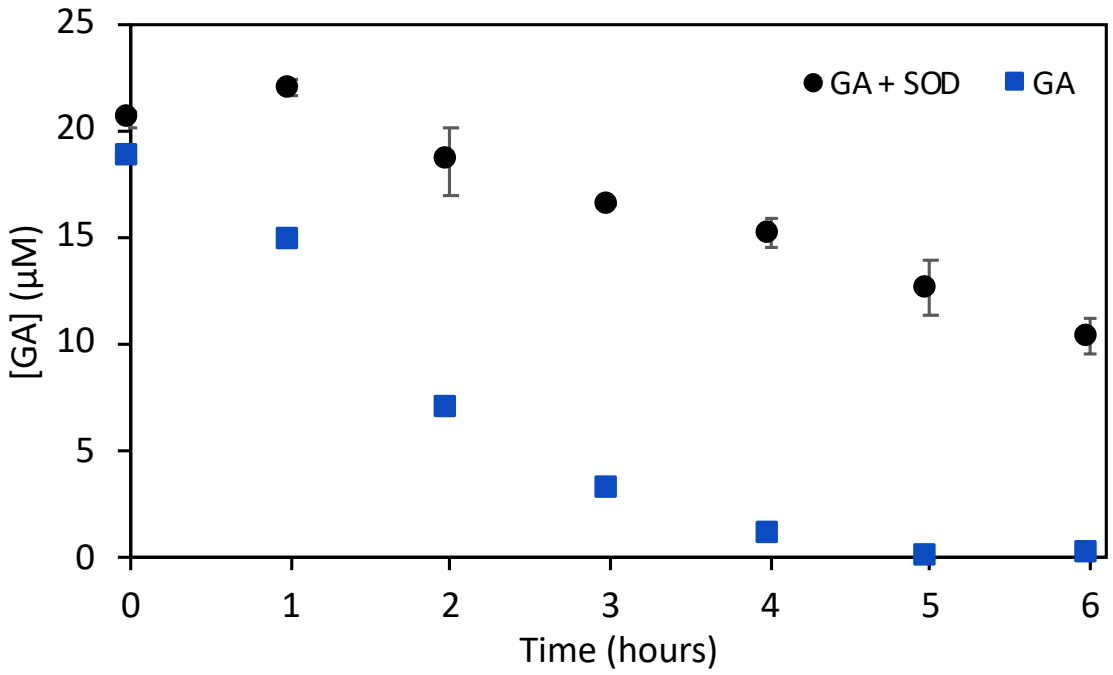

Figure 4.6 Gallic acid concentration loss over time in the presence and absence of superoxide dismutase (SOD). SOD preserved GA in solution and decreased the rate of hydrogen peroxide production (not shown). SOD effectively scavenged superoxide and GA oxidation was solely due to the presence of oxygen. The decreased rate showed that superoxide was the chain carrier for GA oxidation in aqueous solutions. All solutions were buffered with 0.1 M sodium bicarbonate to a pH of 8.3, nominal starting concentration of GA was 20µM.

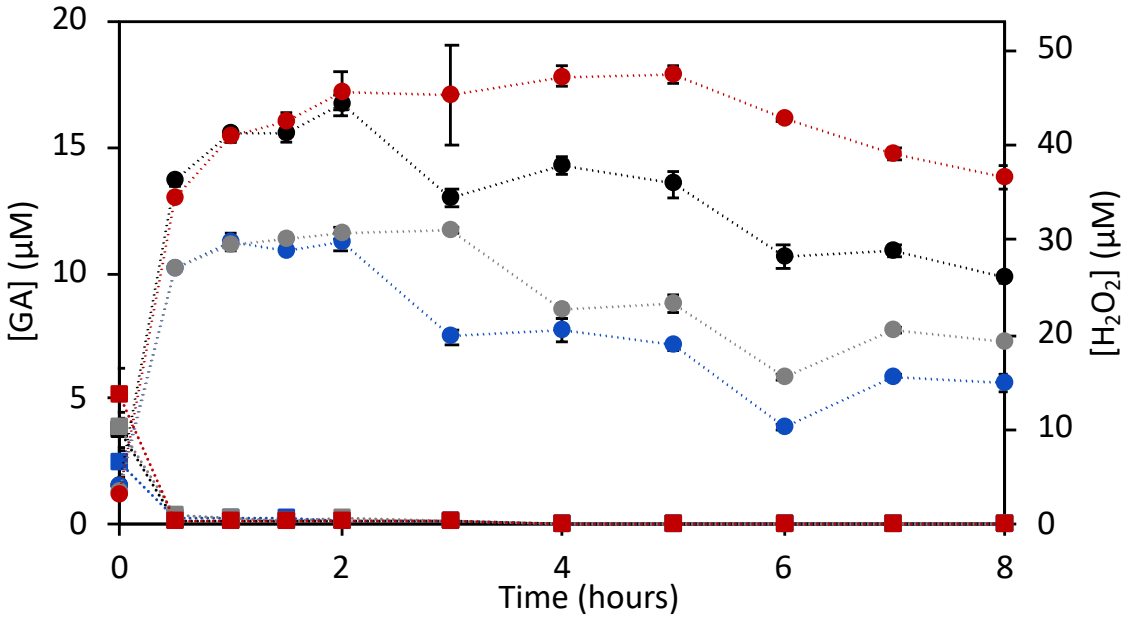

Figure 4.7 Concentration of GA (squares) and hydrogen peroxide (circles) over time in natural water. All samples were buffered to pH 8.3 in sodium bicarbonate, collected from around South Carolina. Site 1: black, Site 2: blue, Site 3: grey, Site 4: red. Nominal starting concentration of GA was 20 µM, but oxidation was rapid and T0 represented 75% of nominal already oxidized. Production of peroxide reached maxima after 1 hour. Error bars represent standard deviation from n=3 replicates.

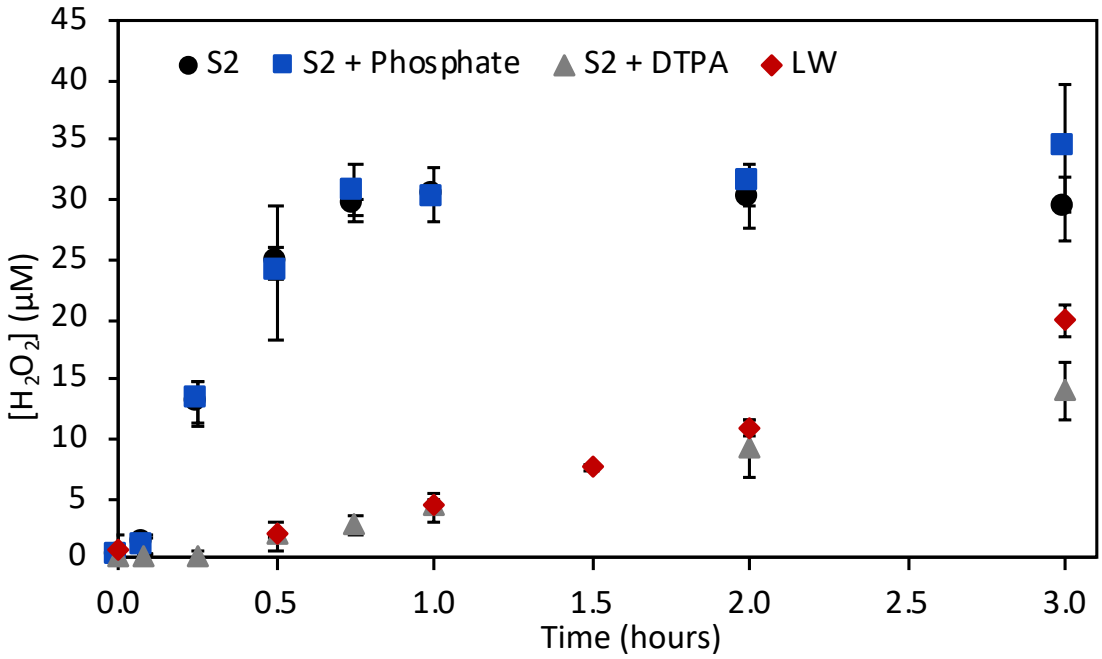

Figure 4.8 Production of hydrogen peroxide from Site 2, Old Bates River, during GA oxidation. The concentration of added phosphate was at 1 mM, added DTPA was 0.2 mM, nominal starting concentration of GA was 20 µM, and pH was 8.3, buffered with 0.1M sodium bicarbonate. Addition of the DTPA to complex native transition metals decreased the rate of production to that of laboratory water (LW).

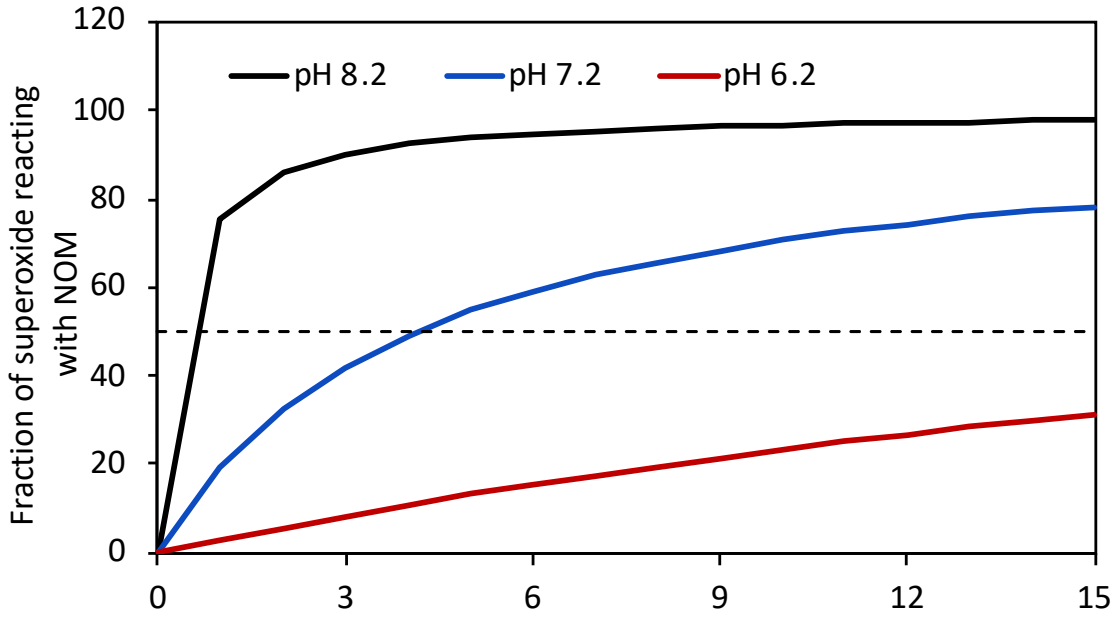

Figure 4.9 Fraction of superoxide reacting with NOM at three pHs. This was modeled from Equation 18 and since superoxide dismutase is pH dependent, this model was carried out over three pHs: 6.2, 7.2, and 8.2. The dashed line represents the transition from the fate of superoxide; below 50% the fate of superoxide is through dismutation and above 50%, peroxidation of NOM.

APPENDIX A

CHAPTER 1 SUPPLEMENTAL MATERIAL

Table A.1 Literature results from June 30, 2019. Search terms were "genera" followed by "ROS" in Web of Science.

Genera	Hydrogen Peroxide	Hydroxyl Radical	Ozone
Anabaena	143	13	72
Aphanizomenon flos-aquae	6	2	3
Cylindrospermopsis	5	2	5
Lyngbya	17	5	13
Microcystis	169	50	101
Nodularia	1	0	5
Nostoc	64	13	61
Oscillatoria	25	3	19
Phormidium	16	4	10
Planktothrix	16	2	5
Pseudanabaena	6	0	3
Raphidiopsis	4	0	0
Synechococcus	128	6	30
Trichodesmium	5	1	5

Table A.2. Literature results from June 30, 2019. Search terms were "toxin" followed by "ROS" in Web of Science.

Toxin	Hydrogen Peroxide	Hydroxyl radical	Ozone
Anatoxin-a	21	8	19
BMAA	0	0	0
Cylindrospermopsin	26	26	14
Microcystin	186	123	85
Nodularin	5	3	4
Saxitoxin (Paralytic shellfish toxins)	24 (27)	3 (0)	6 (11)

APPENDIX B

CHAPTER 2 SUPPLEMENTAL MATERIAL

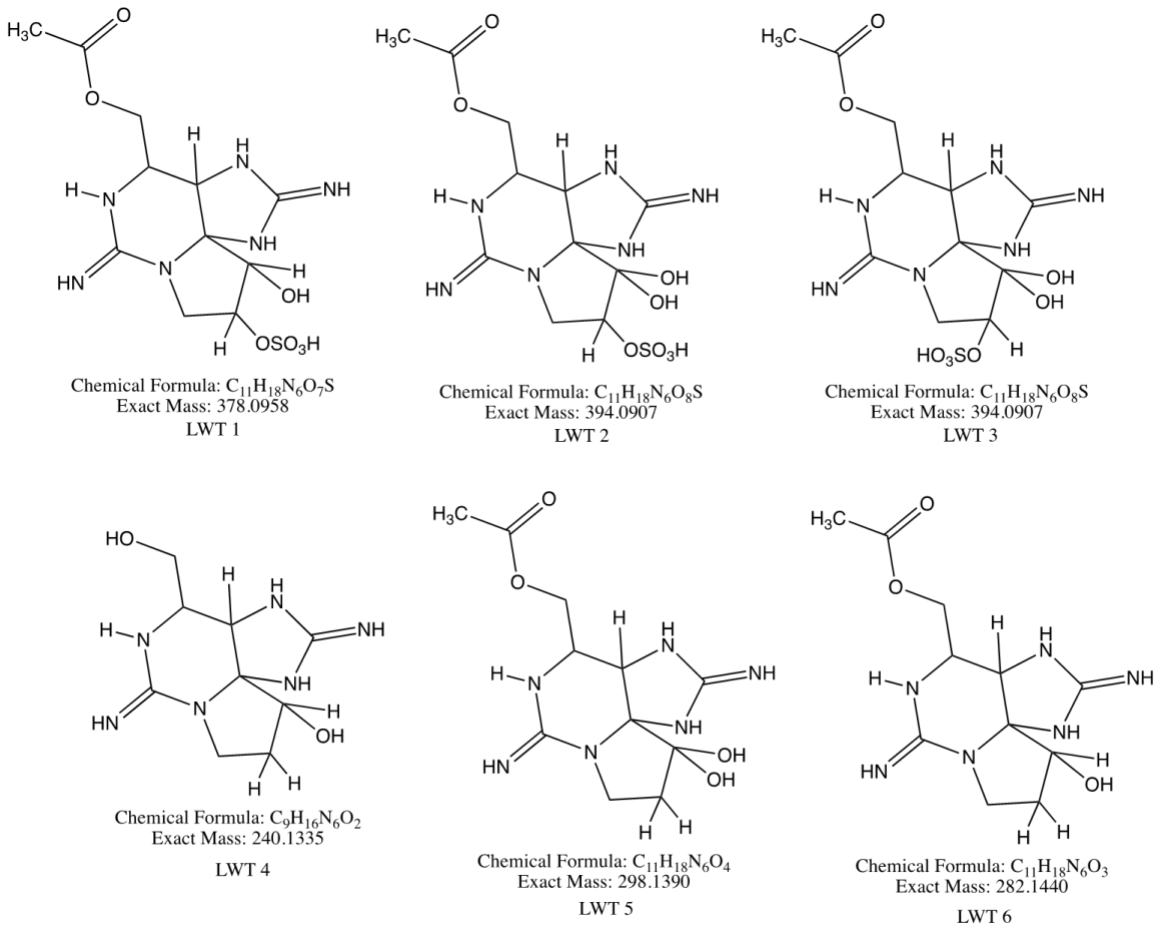

Figure B.1 Molecular structures of the *Lyngbya wollei* toxins (LWTs) 1-6 (free base).

Table B.1 LC-TQ source parameters for detection of LWTs. All parameters were optimized manually using MassLynx (V.4.1) using saxitoxin as a model LWT and kept constant.

Polarity	ES+
Extractor (V)	3
Source Temperature (°C)	150
Desolvation Temperature (°C)	400
Cone Gas Flow (L/Hr)	25
Desolvation Gas Flow (L/Hr)	600
Collision Gas Flow (mL/Min)	0.15

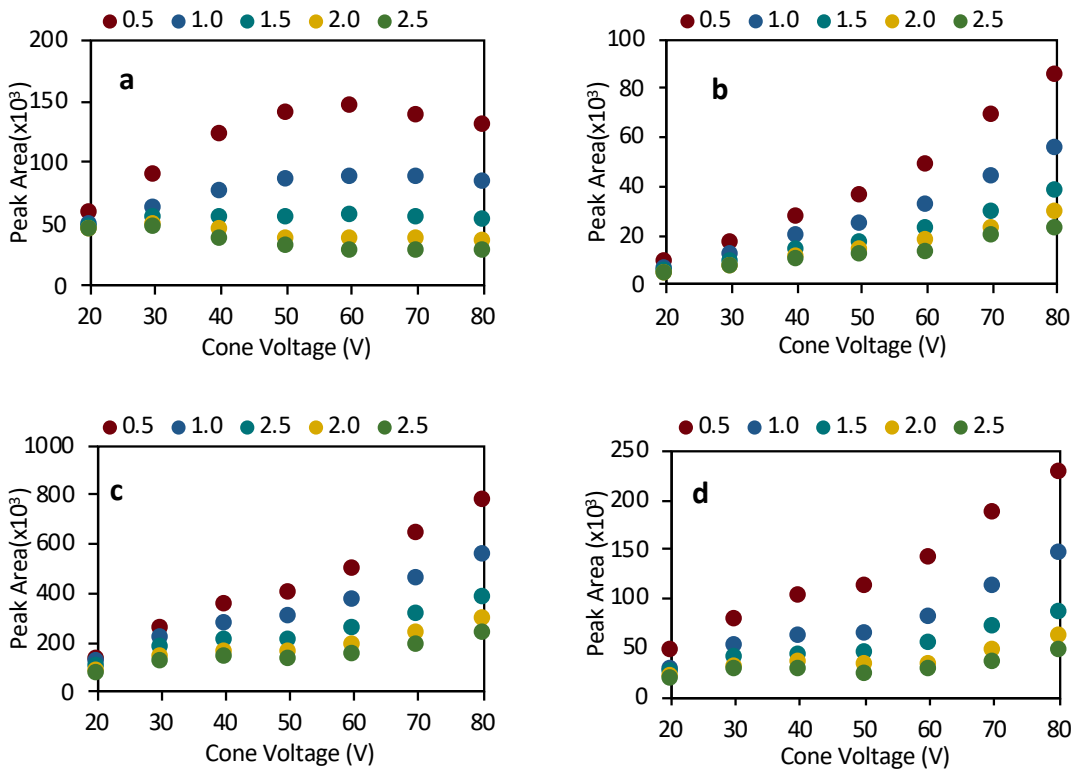

Figure B.2 Peak area vs. cone voltage for LWT1 (a), LWT4 (b), LWT5 (c), and LWT6 (d). Each cone voltage series was done at a capillary voltage ranging from 0.5 kV - 2.5 kV. A capillary voltage of 0.5 kV was chosen for all LWTs, consistent with the optimal capillary voltage for saxitoxin, the model LWT.

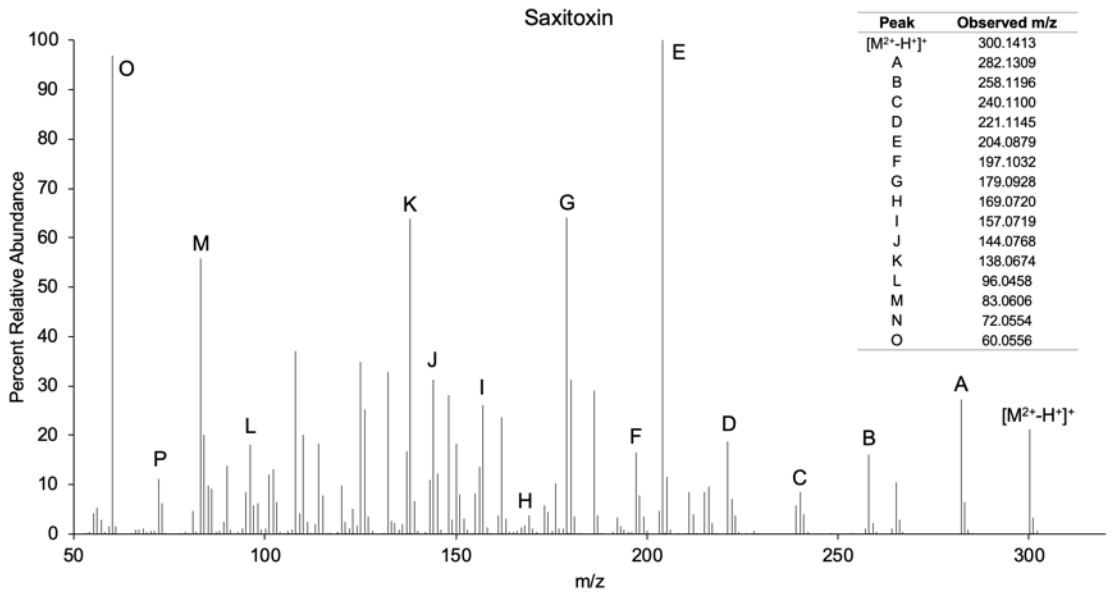

Figure B.3 High resolution spectra obtained from the UHPLC-QTOF for Saxitoxin at 6.38 mins.

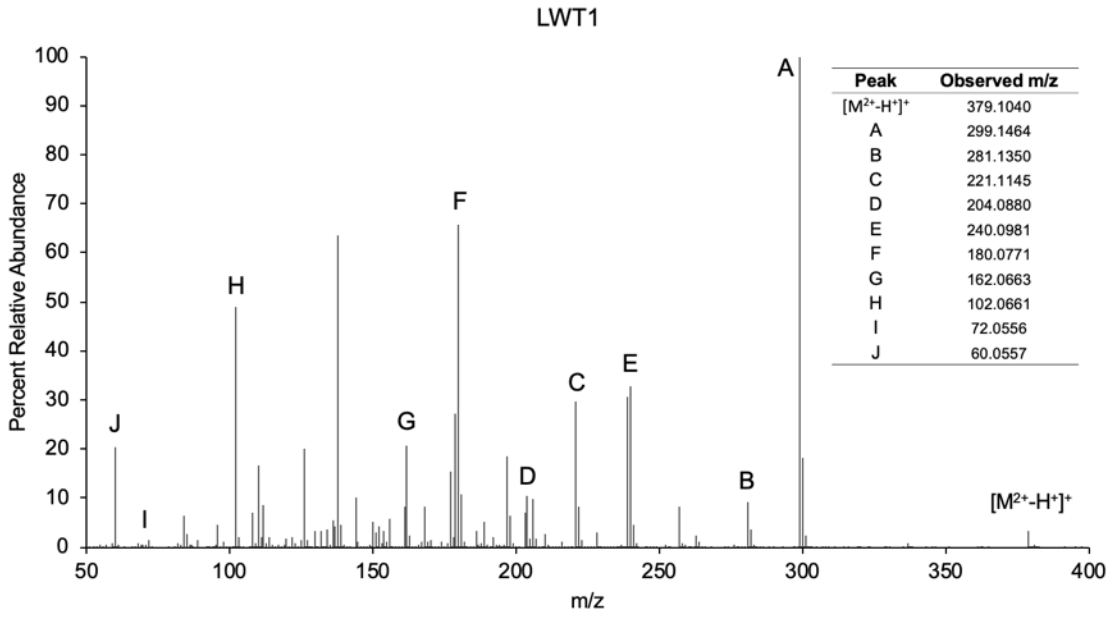

Figure B.4 High resolution spectra obtained from the UHPLC-QTOF for LWT1 at 3.87 mins.

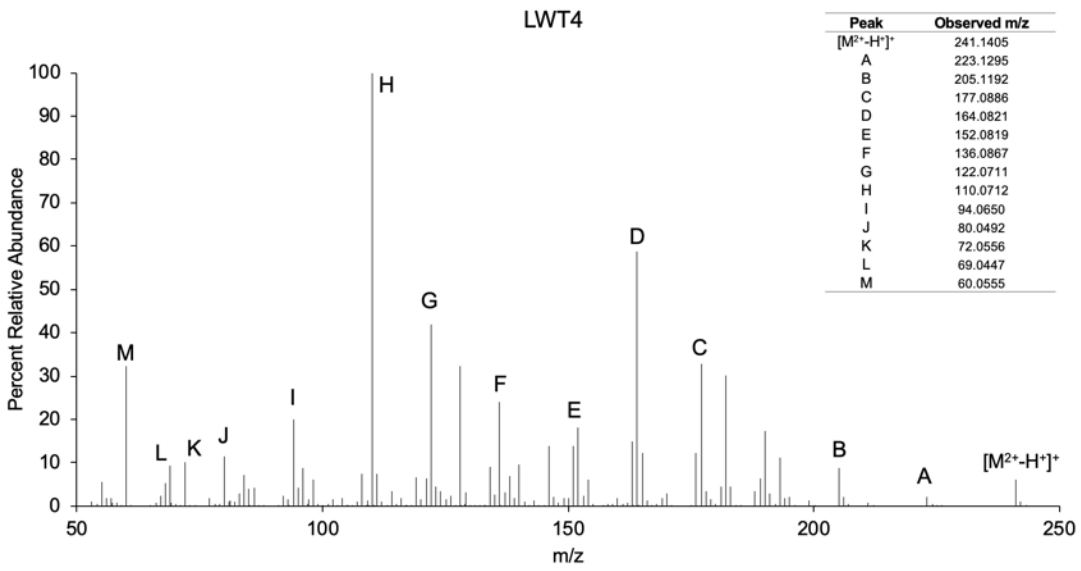

Figure B.5 High resolution spectra obtained from the UHPLC-QTOF for LWT4 at 6.13 mins.

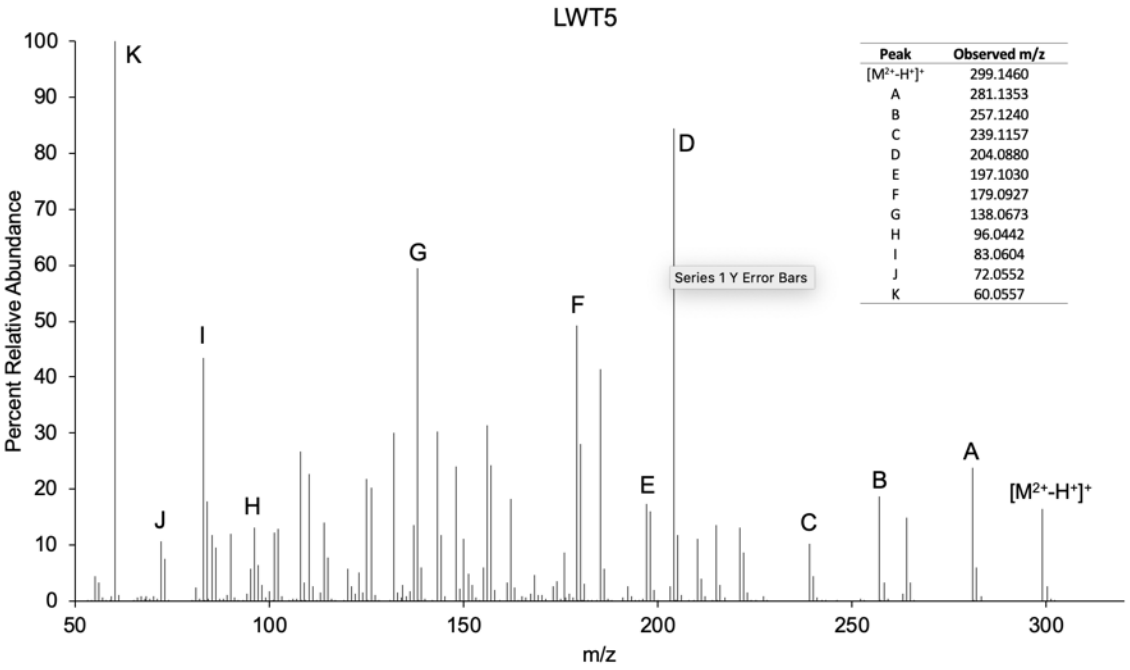

Peak	Observed m/z
$[M^{2+}-H^{+}]^{+}$	299.1460
A	281.1353
B	257.1240
C	239.1157
D	204.0880
E	197.1030
F	179.0927
G	138.0673
H	96.0442
I	83.0604
J	72.0552
K	60.0557

Figure B.6 High resolution spectra obtained from the UHPLC-QTOF for LWT5 at 5.84 mins.

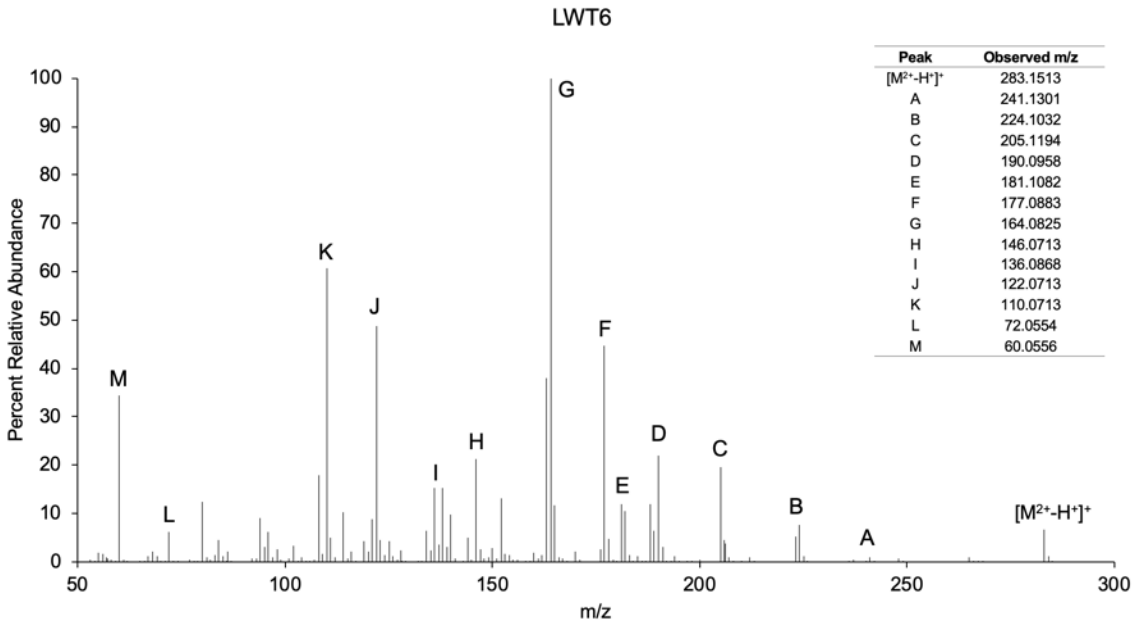

Figure B.7 High resolution spectra obtained from the UHPLC-QTOF for LWT6 at 4.96 mins.

Table B.2 Fragmentation ions, losses, and ppm mass error for STX on the UHPLC-QTOF

Saxitoxin					
Observed m/z	Formula	Mass loss	Loss	Theoretical m/z	ppm mass diff
300.1413	$C_{10}H_{18}N_7O_4$			300.14148	0.600
282.1309	$C_{10}H_{16}N_7O_3$	18.0104	$-H_2O$	282.13091	0.035
258.1196	$C_9H_{16}N_5O_4$	42.0217	$-CH_2N_2$	258.11968	0.310
240.1100	$C_9H_{14}N_5O_3$	60.0313	$-CH_2N_2$, $-H_2O$	240.10912	3.665
221.1145	$C_9H_{13}N_6O$	79.0268	$-CH_3NO$, $-H_2O$	221.11454	0.181
204.0879	$C_9H_{10}N_5O$	96.0534	$-CH_2NO$, $-NH_2$, $-H_2O$, $-H_2O$	204.08799	0.441
197.1032	$C_8H_{13}N_4O_2$	103.0381	$-CH_3NO_2$, $-CH_2N_2$	197.10330	0.507
179.0928	$C_8H_{11}N_4O$	121.0485	$-CH_3NO_2$, $-CH_2N_2$, $-H_2O$	179.09274	0.335
169.072	$C_6H_9N_4O_2$	131.0693	$-CH_3N_3$, $-C_3H_6O_2$	169.072	0.000
157.0719	$C_5H_9N_4O_2$	143.0694	$-C_5H_9N_3O_2$	157.0720	0.637
144.0768	$C_5H_{10}N_3O_2$	156.0645	$-C_5H_8N_4O_2$	144.07675	0.347
138.0674	$C_6H_8N_3O$	162.0739	$-H_2O$, $-CH_2N_2$, $-C_3H_6N_2O_2$	138.06619	8.764
96.0458	C_5H_6NO	204.0955	$-CH_2NO$, $-CH_2N_2$, $-CH_4N_3$, $-C_2H_4O_2$	96.04439	14.681
83.0606	$C_4H_7N_2$	217.0807	$-CH_2NO_2$, $-C_5H_9N_4O_2$	83.06037	2.769
72.0554	$C_2H_6N_3$	228.0859	$-C_8H_{12}N_4O_4$	72.05562	3.053
60.0556	CH_6N_3	240.0857	$-C_9H_{12}N_4O_4$	60.05562	0.333

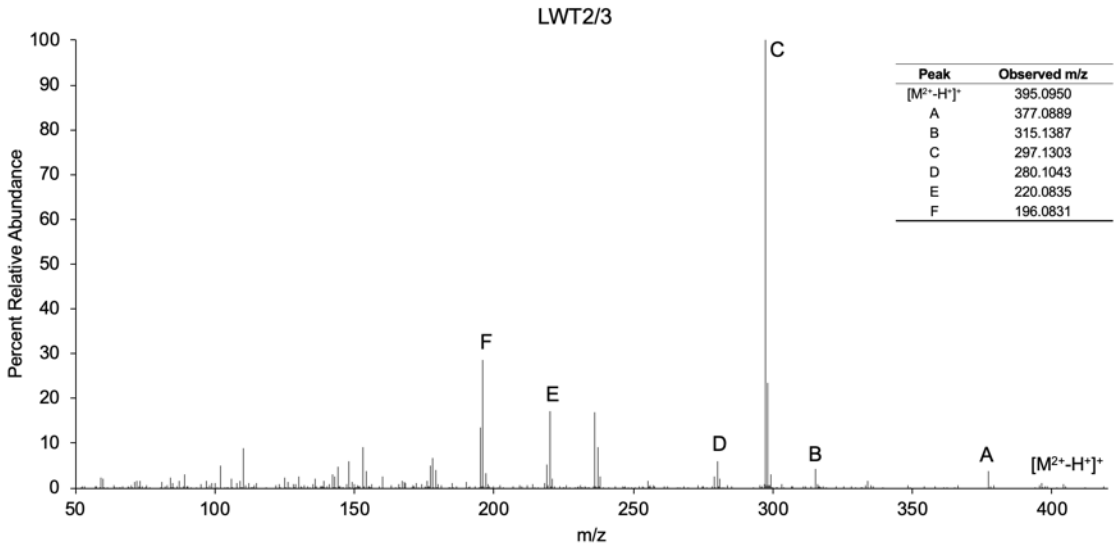

Figure B.8 High resolution spectra obtained from the UHPLC-QTOF for LWT2/3 at 3.94 mins.

Table B.3 Fragmentation ions, losses, and ppm mass error for LWT2/3 on the UHPLC-QTOF

LWT2/3					
Observed m/z	Formula	Mass loss	Loss	Theoretical m/z	ppm mass diff
395.095	$C_{11}H_{19}N_6O_8S$			395.09796	7.492
377.0889	$C_{11}H_{17}N_6O_7S$	18.0061	$-H_2O$	377.08739	4.004
315.1387	$C_{11}H_{19}N_6O_5$	79.9563	$-SO_3$	315.14114	7.743
297.1303	$C_{11}H_{17}N_6O_4$	97.9647	$-SO_3$, $-H_2O$	297.13058	0.942
280.1043	$C_{11}H_{14}N_5O_4$	114.9907	$-SO_3$, $-H_2O$, $-NH_3$	280.10403	0.964
220.0835	$C_9H_{10}N_5O_2$	175.0115	$-SO_3$, $-H_2O$, $-C_2H_4O_2$, $-NH_3$	220.08345	0.227
196.0831	$C_7H_{10}N_5O_2$	199.0119	$-C_4H_7NO_2$, $-H_2O$	196.0829	1.020

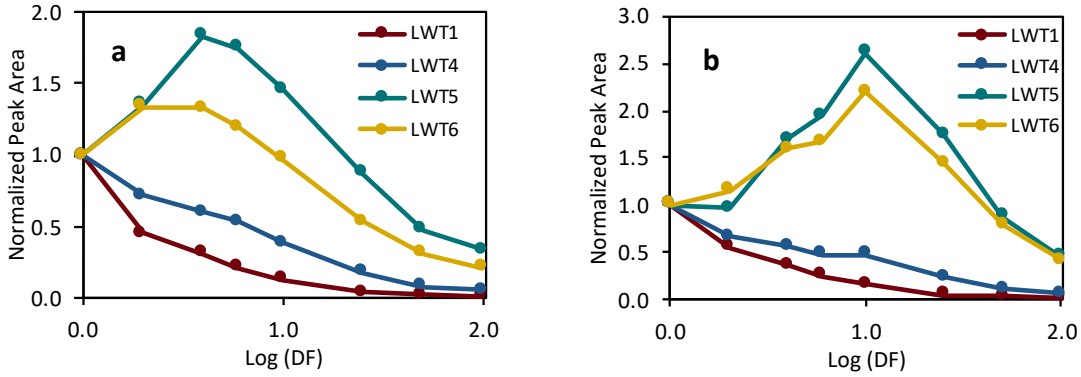

Figure B.9 Normalized MS peak area of LWTs as a function of log10(dilution factor) in different extraction solvents. Approx. 100 mg of dry algae was extracted with 100 mM HCl (a), or 10 mM HCl (b). This acid extract was then diluted by a factor of up to 100 in its original extraction solvent. Peak area is normalized against the area at a dilution factor of one.

APPENDIX C

CHAPTER 3 SUPPLEMENTAL MATERIAL

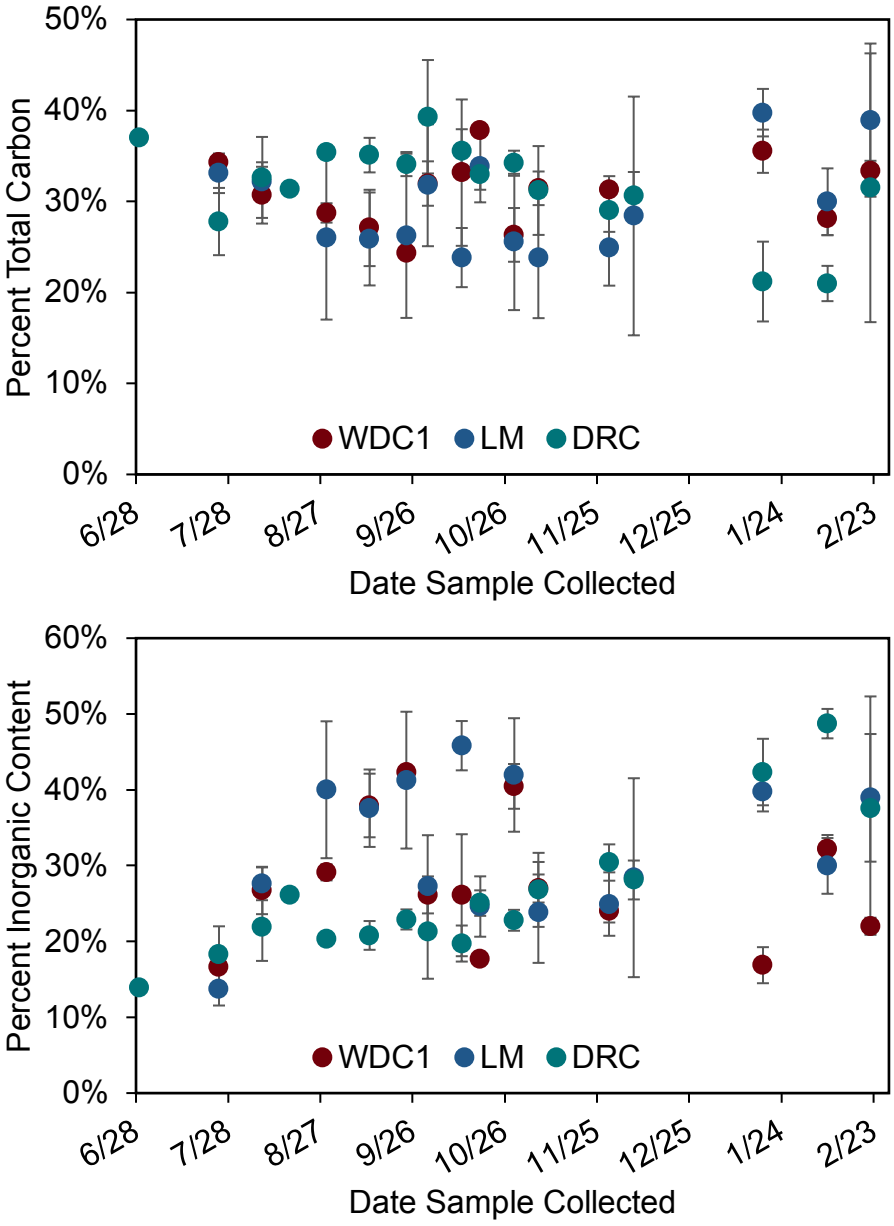

Figure C.1. Percent total carbon (top) and percent inorganic content (bottom) for Cove 1, Cove 2, and Cove 3 over the sampled time season. Average and standard deviation are presented as the average from three grab samples obtained on one day.

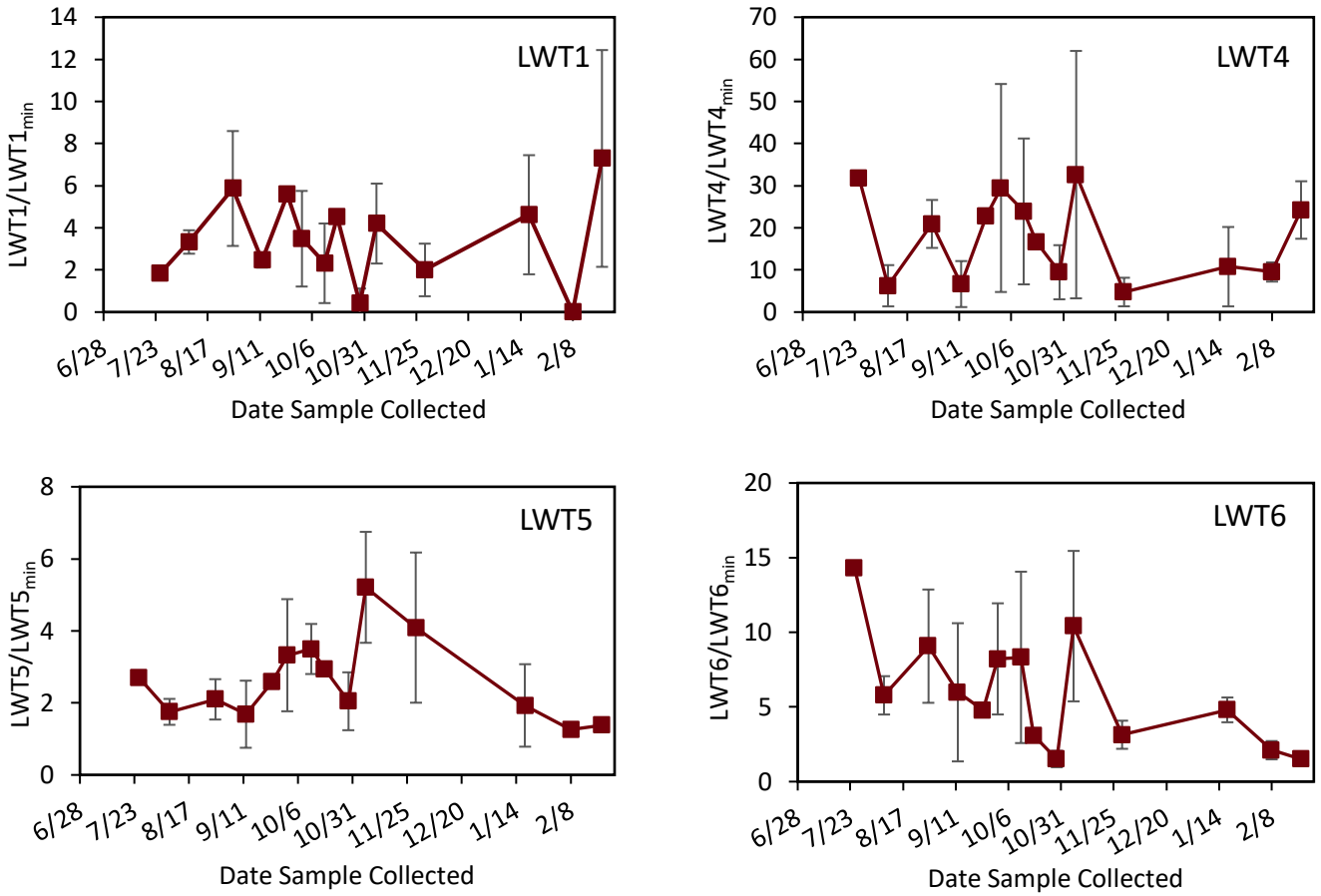

Figure C.2. LWTX/LWTX$_{min}$ for LWT1, LWT4, LWT5, and LWT6 for Cove 2 from June 2018 to February 2019.

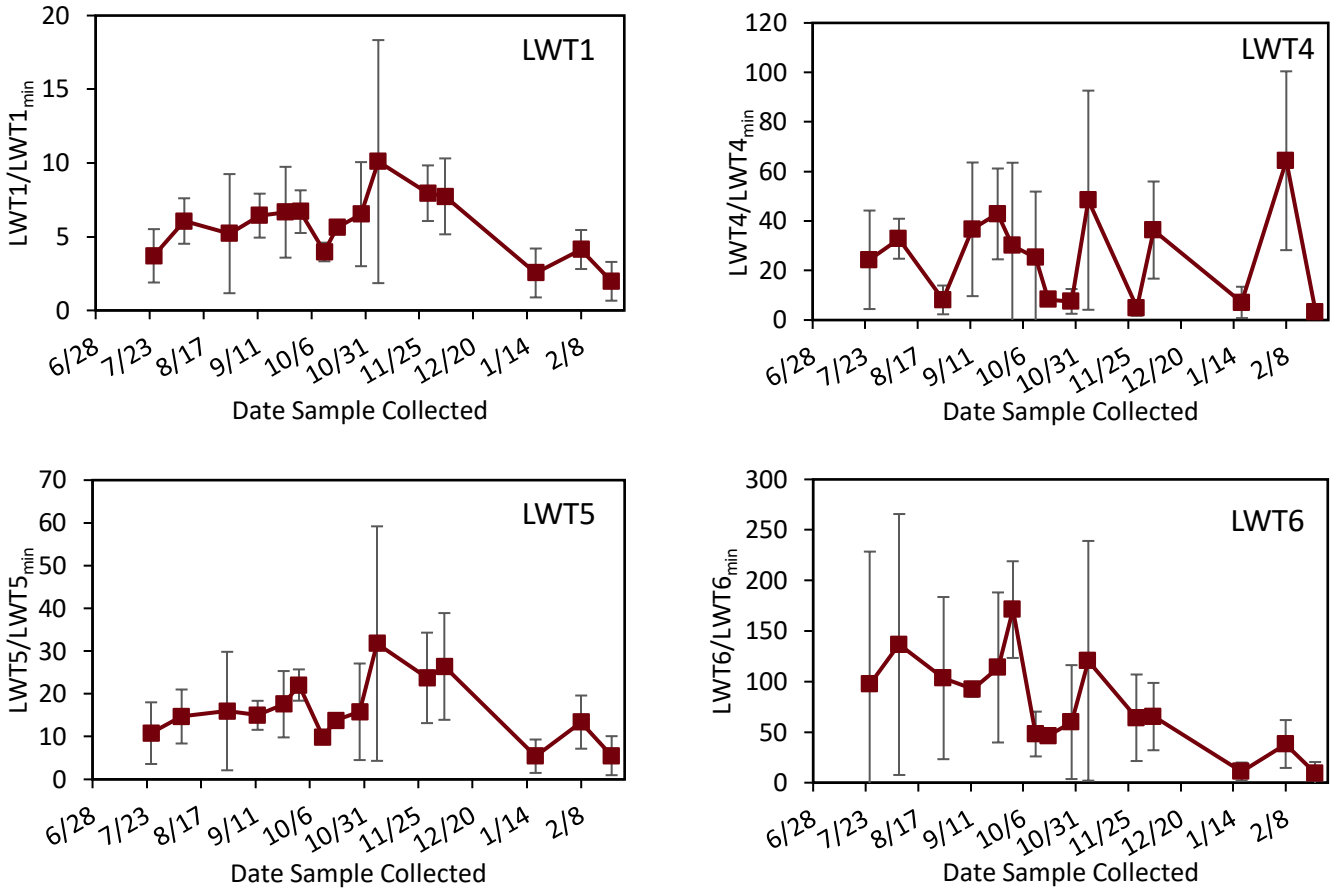

Figure C.3. LWTX/LWTX$_{min}$ for LWT1, LWT4, LWT5, and LWT6 for Cove 3 from June 2018 to February 2019

APPENDIX D

CHAPTER 4 SUPPLEMENTAL MATERIAL

Table D.1 UPLC-MS source parameters for gallic acid detection. Cone and collision voltages for the MRM transition of gallic acid (*m/z*=169 to *m/z*=125) were determined from Intellistart software. All other parameters optimized manually using MassLynx (V.4.1)

Polarity	ES-
Capillary (V)	2000
Cone (V)	28
Extractor (V)	3
Source Temperature (°C)	150
Desolvation Temperature (°C)	600
Cone Gas Flow (L/Hr)	0
Desolvation Gas Flow (L/Hr)	1000
Collision Gas Flow (mL/Min)	0.15

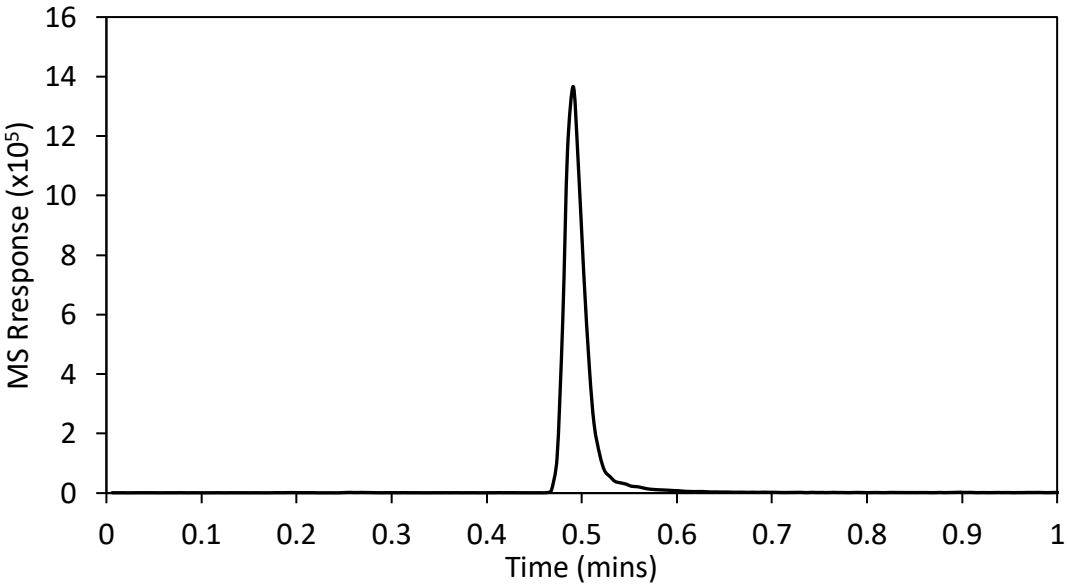

Figure D.1 MRM chromatogram for gallic acid which eluted at 0.49 mins during the gradient flow. Response correlates to the mass transition from *m/*z = 169 to *m/z* = 125.

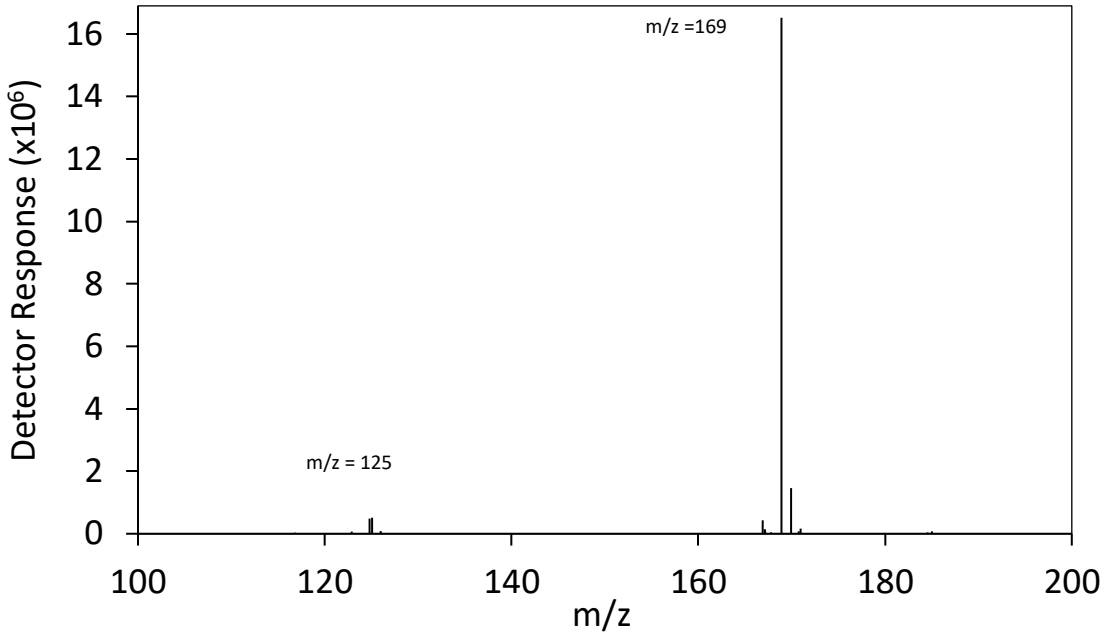

Figure D.2 Full MS spectra of GA, eluted at 0.49 mins under the instrument conditions. The m/z of 169 represents the molecular ion of GA ($[M-H]^-$), and *m/z* of 125 as the main fragment of GA ($[M-H-CO_2]^-$)

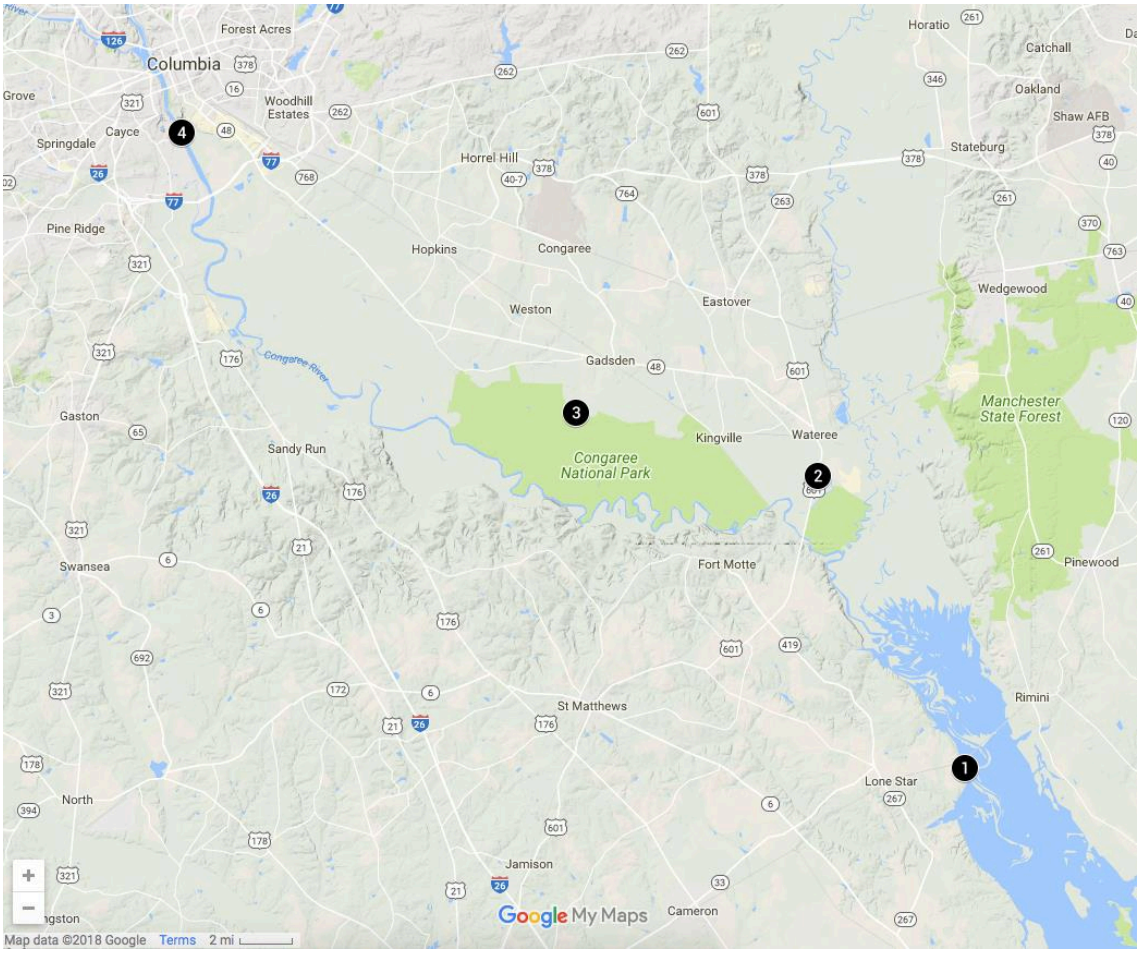

Figure D.3 The locations of the four sampling locations in South Carolina: Low Falls Landing in Lake Marion (Site 1, 33.632256, -80.543134), Old Bates River (Site 2, 33.785559, -80.635637), Cedar Creek in the Congaree National Park (Site3, 33.818651, -80.787909), and Rosewood Landing in the Congaree River (Site 4, 33.964918, -81.036215).

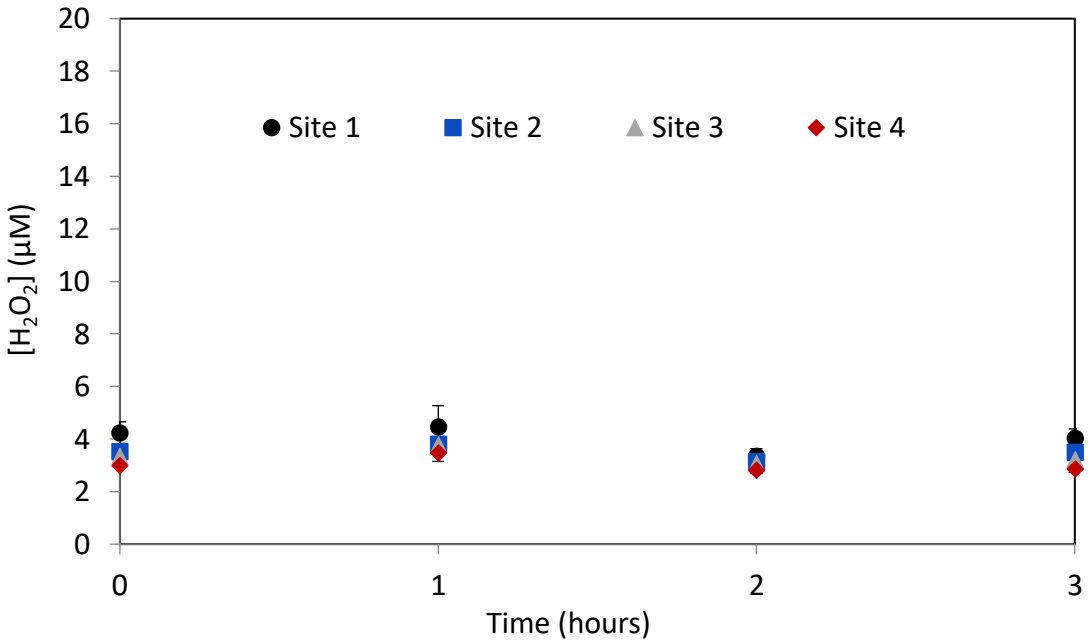

Figure D.4 Background hydrogen peroxide over three hours in the four locations where water was collected.

Table D.2 ICP-MS results of raw and filtered river waters from the four natural water samples collected.

Location (unfiltered/ filtered)	Metal ion detected									
	^{7}Li	^{9}Be	^{11}B	^{23}Na	^{24}Mg	^{27}Al	^{39}K	^{44}Ca	^{51}V	^{52}Cr
Low Falls Landing	2.58	0.02	48	9179	2813	28	3538	649	1.00	0.17
	2.82	0.01	47	8824	2777	1.73	3516	605	0.67	0.08
Old Bates River	1.77	0.06	25	6359	2861	3.07	4905	795	1.77	0.48
	0.82	0.03	19	4799	2021	13	3346	443	0.72	0.28
Cedar Creek	0.71	0.03	9.3	2703	637	9.42	814	117	0.76	0.25
	0.41	0.03	9.3	2890	612	7.06	934	121	0.40	0.18
Rosewood Landing	2.73	0.01	29	5587	1961	18	2784	472	0.87	0.10
	2.82	0.00	29	5904	1950	0.64	2779	465	0.76	0.13

Location (unfiltered/ filtered)	^{59}Co	^{64}Zn	^{75}As	^{88}Sr	^{98}Mo	^{107}Ag	^{111}Cd	^{121}Sb	^{138}Ba	^{205}Ti
Low Falls Landing	0.08	21.0	0.47	49	1.53	0.09	0.00	0.22	21	0.01
	0.01	1.93	0.43	49	1.21	0.00	0.00	0.38	20	0.00
Old Bates River	1.20	32.0	1.21	65	0.31	0.00	0.02	0.06	82	0.02
	0.45	2.05	0.58	46	0.16	0.00	0.00	0.08	46	0.00
Cedar Creek	0.97	5.15	0.53	10	0.12	0.00	0.00	0.02	17	0.00
	0.04	14.0	0.39	9.5	0.06	0.00	0.02	0.02	16	0.00
Rosewood Landing	0.11	3.02	0.44	40	2.15	0.03	0.00	0.29	10	0.00
	0.04	9.82	0.39	39	2.68	58.09	0.03	0.32	9.80	0.00

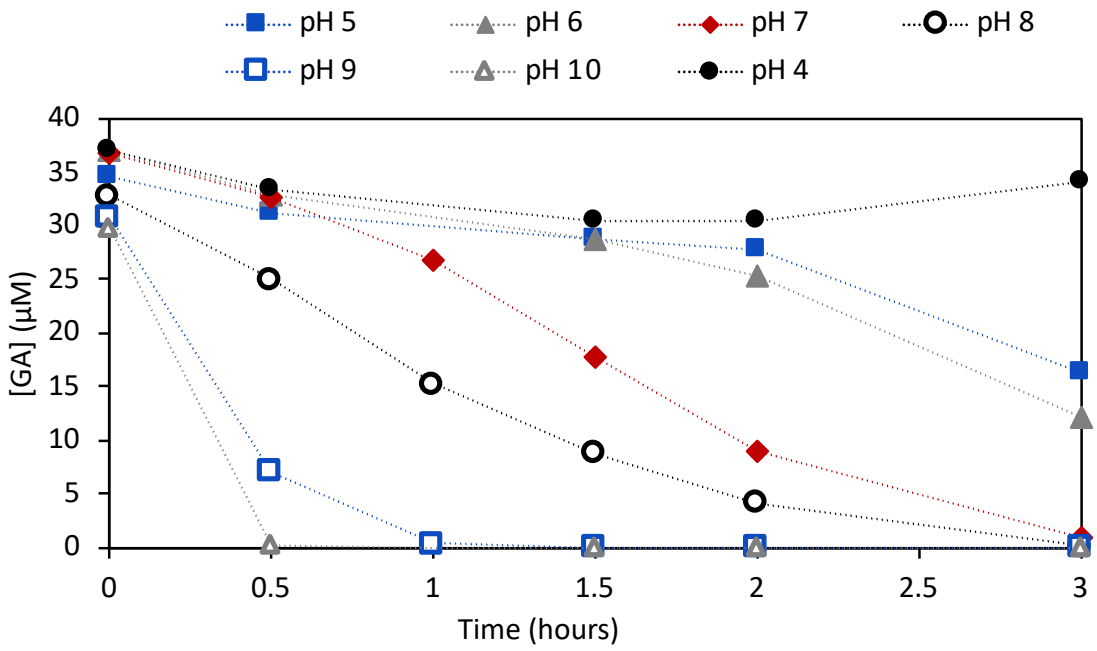

Figure D.5 Oxidation of GA over the pH range of 4-10 over three hours.

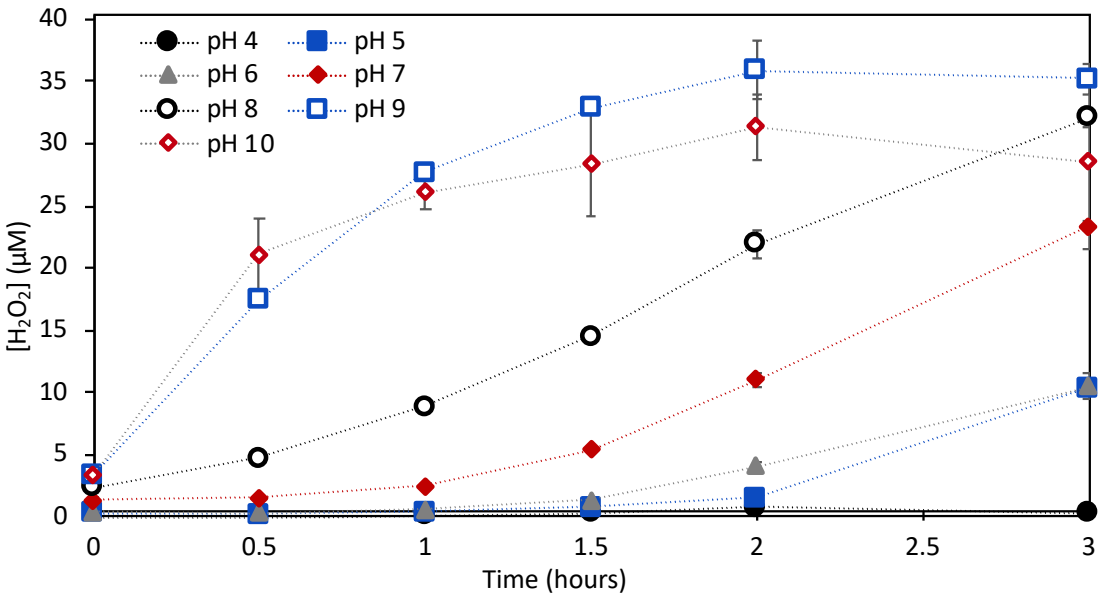

Figure D.6 Production of hydrogen peroxide over the pH range of 4-10 over three hours.

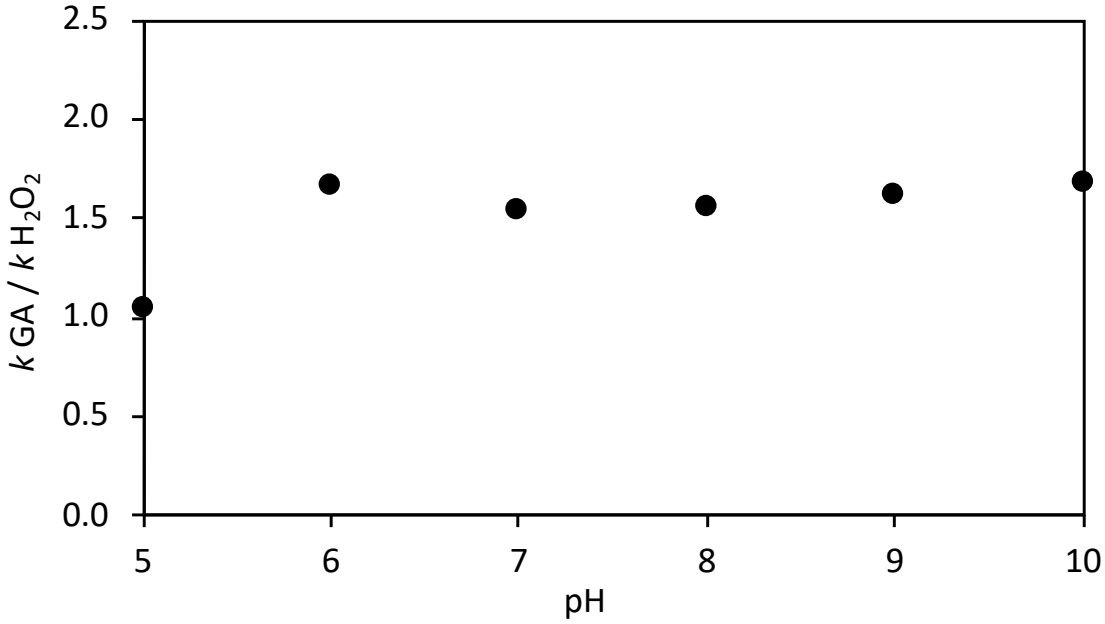

Figure D.7 The ratio of the rate of gallic acid oxidation and hydrogen peroxide production over the pH range 5-10.

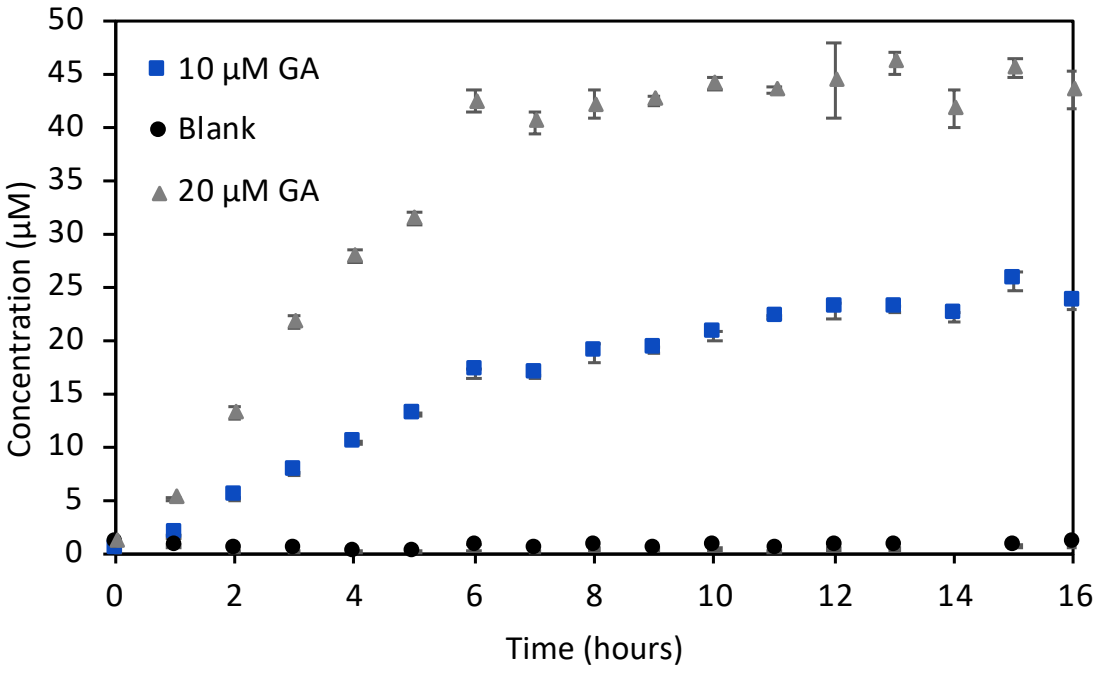

Figure D.8 Production of hydrogen peroxide during the oxidation of 10 µM and 20 µM gallic acid.

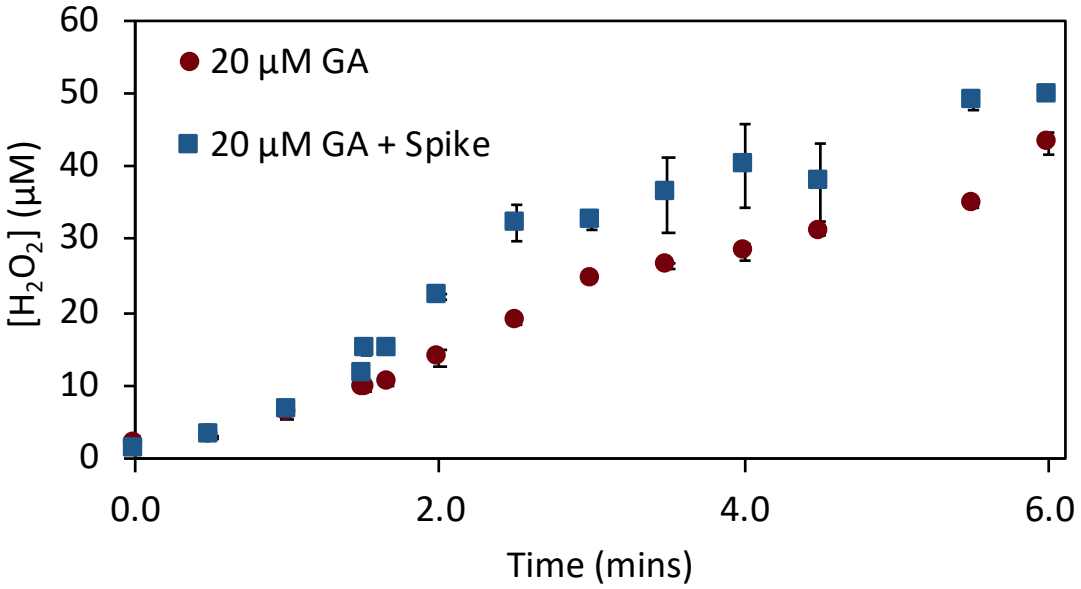

Figure D.9 Concentration of hydrogen peroxide from GA oxidation during an added 5 µm spike of hydrogen peroxide

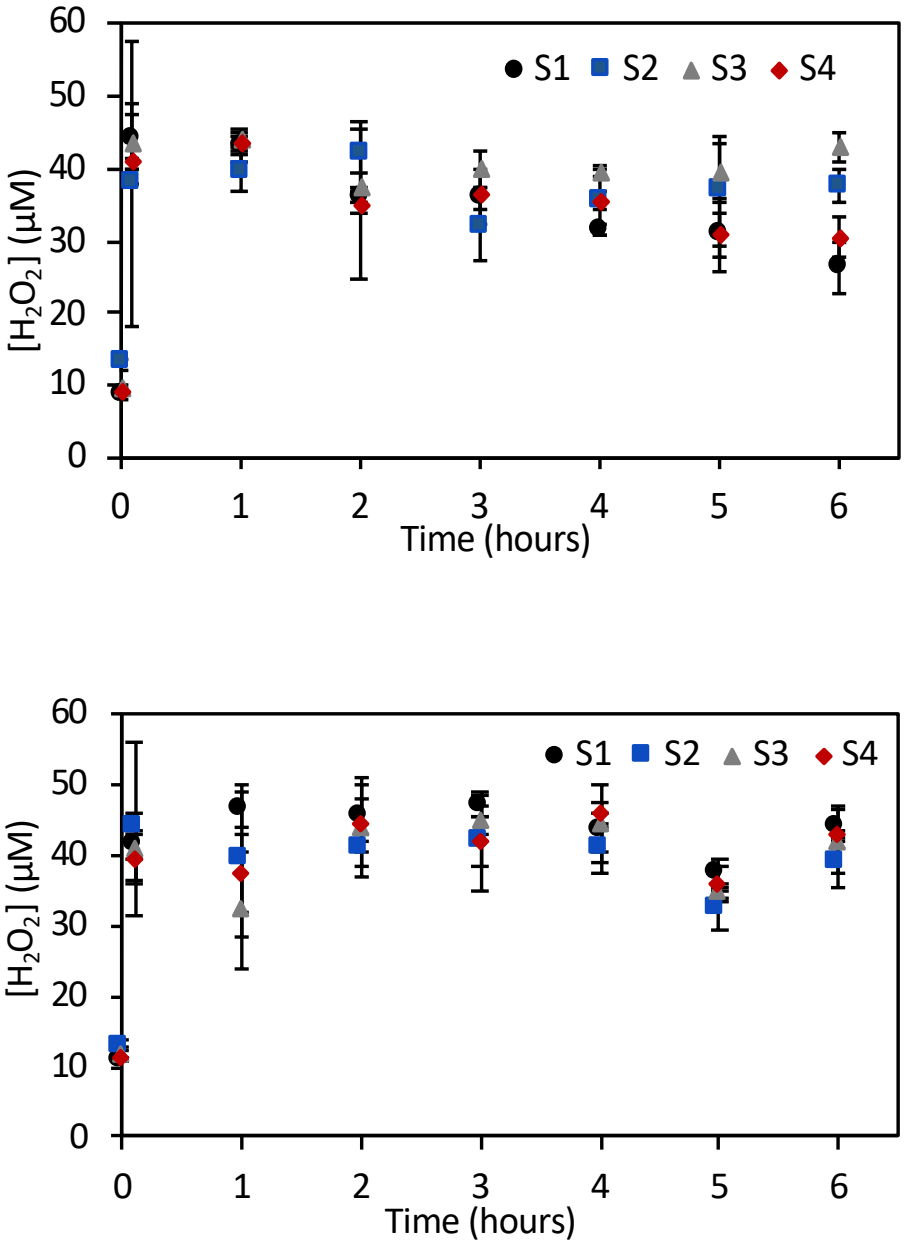

Figure D.10 Hydrogen peroxide stability in the four natural water samples, unfiltered (top) and filtered (bottom).

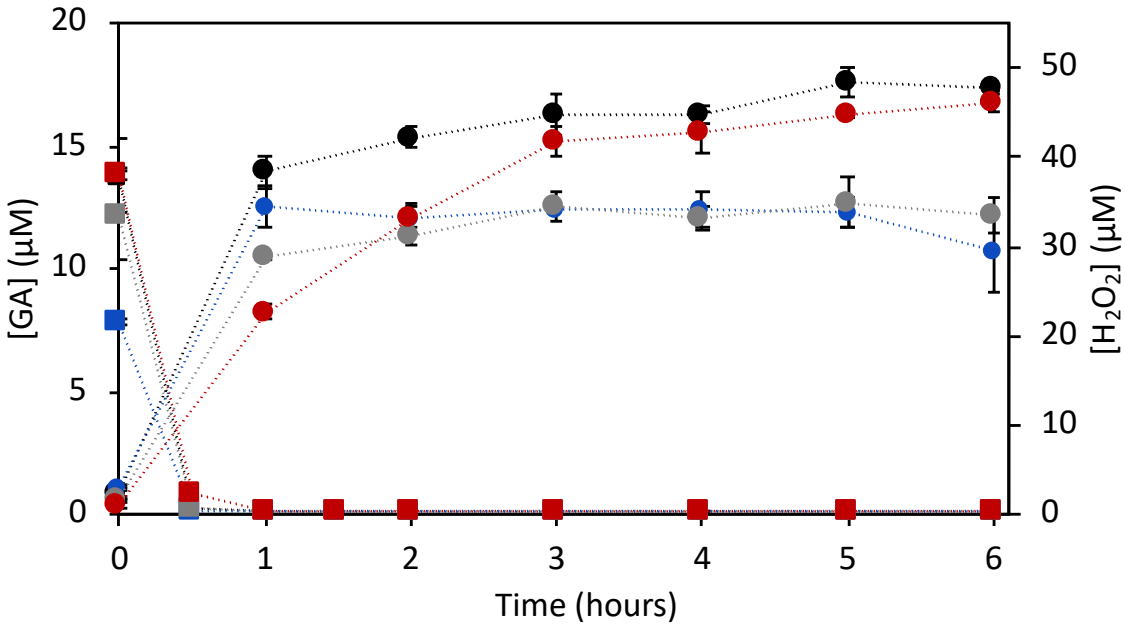

Figure D.11 Oxidation of GA (squares) and production of hydrogen peroxide (circles) in the four natural water samples.

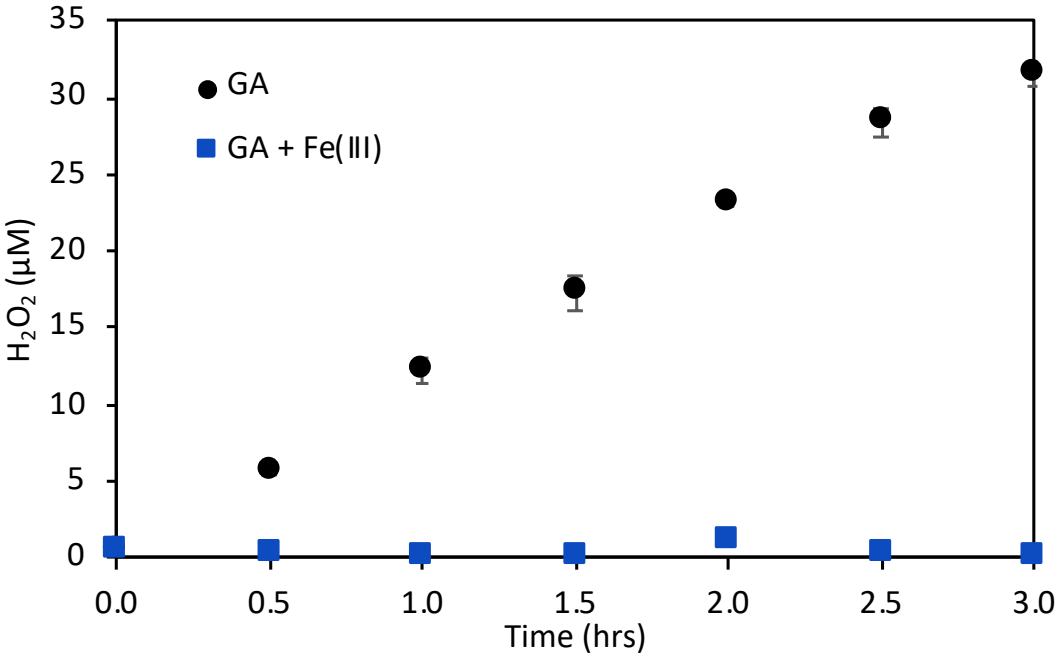

Figure D.12 Hydrogen peroxide production from the autoxidation of gallic acid in the presence and absence of 50 µM Fe(III).

$$\frac{-\mathrm{d}[O_2^{\cdot-}]}{\mathrm{dt}} = \mathrm{k_{obs}}[O_2^{\cdot-}]^2 \qquad \text{[S1]}$$

$$\sqrt{\frac{4.9\mathrm{x}10^{-10}\mathrm{M/s}}{15849\mathrm{M^{-1}s^{-1}}}} = [O_2^{\cdot-}] \qquad \text{[S2]}$$

$$[O_2^{\cdot-}] = 1.76\mathrm{x}10^{-7} \qquad \text{[S3]}$$

Figure D.13 The calculation for superoxide in our system derived from the superoxide steady state in aqueous solutions. The steady state of superoxide is shown in Equation S1, where K_{obs} at pH of 8.3 is 15849 M^{-1} s^{-1} (Bielski 1978) and the term ($\frac{-d[O_2^{\cdot-}]}{dt}$) was calculated from two times the hydrogen peroxide production rate from GA oxidation in the presence of SOD ($4.9\mathrm{x}10^{-10}$ M/s). Rearranging to solve for $[O_2^{\cdot-}]$ gives Equation S2 and solving for $[O_2^{\cdot-}]$ 0.176 μM of superoxide is generated from dismutation. Since dismutation only accounts for 8% of the hydrogen peroxide generated, we multiplied the superoxide concentration by 12 to come up with a superoxide concentration in our system of 2.11 μM.